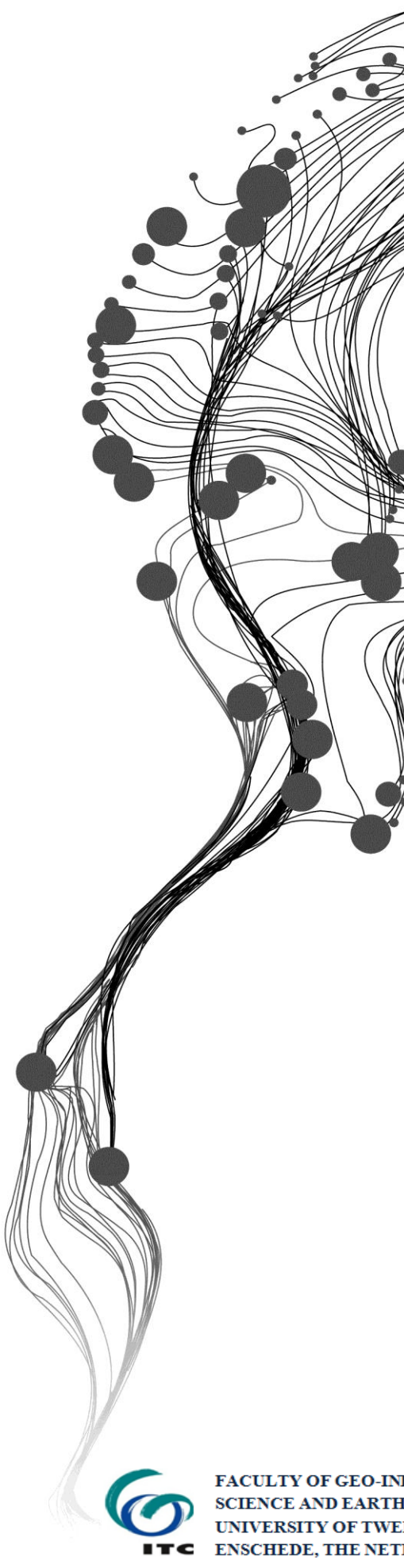


Development of Vulnerability Indices for Flood Damage Estimation using Remote Sensing data in part of Bhagalpur, Bihar

Surendar Mohan
April, 2014

IIRS SUPERVISOR
Dr. Bhaskar R. Nikam

ITC SUPERVISOR
Drs. Nanette C. Kingma



Development of Vulnerability Indices for Flood Damage Estimation using Remote Sensing data in part of Bhagalpur, Bihar

Surendar Mohan

Enschede, The Netherlands [April, 2014]

Thesis submitted to the Faculty of Geo-information Science and Earth Observation (ITC) of the University of Twente in partial fulfilment of the requirements for the degree of Master of Science in Geo-information Science and Earth Observation.

Specialization: Natural Hazards and Disaster Risk Management

THESIS ASSESSMENT BOARD:

Chairperson	:
External Examiner	:
Supervisors	: Dr. Bhaskar R. Nikam, IIRS Drs. Nanette C. Kingma, ITC

OBSERVERS:

ITC Observer	:
IIRS Observer	:



FACULTY OF GEO-INFORMATION
SCIENCE AND EARTH OBSERVATION,
UNIVERSITY OF TWENTE,
ENSCHEDE, THE NETHERLANDS



INDIAN INSTITUTE OF REMOTE SENSING
Indian Space Research Organisation
Department of Space, Government of India

DISCLAIMER

This document describes work undertaken as part of a programme of study at the Faculty of Geo-information Science and Earth Observation (ITC), University of Twente, The Netherlands. All views and opinions expressed therein remain the sole responsibility of the author, and do not necessarily represent those of the institute.

Dedicated to

my family

ABSTRACT

Estimation of damage to structures and agriculture during floods by physical examination is time consuming and human resource intensive. Often, this approach is operationally not feasible.

This study aims at developing vulnerability indices for estimating damage to structures and agriculture using remote sensing data. The study area was located along River Ganga in Bhagalpur district, Bihar, India for development of Vulnerability Indices for estimation of damage to structures and agriculture. However, the SAR data acquired for part of Madhepura district along River Kosi, just 30 km north to the above mentioned study area, was used for determining optimal speckle reduction filter for RISAT-I data.

The research used multi-temporal dataset comprising of eleven Synthetic Aperture Radar images from RISAT-I and a stereo ortho-kit from CARTOSAT-1. The research can be visualised in the form of five sequential steps viz. Evaluating of filters for speckle reduction in RISAT-I (SAR) data, Generation of flood duration and depth map, Determining exposure of habitat and agriculture to varying flood depths and duration, Development of vulnerability indices, Estimation of flood damage for entire study area.

An adaptive filter was used to reduce speckle in RISAT data. The optimal filter was determined by evaluating performance assessment measures such as Mean Square Error, Signal to Noise Ratio, Speckle Suppression Index, Speckle Mean Preservation Index and changes in mean and standard deviation. A single pass of Frost (7×7) filter was found to be most suited filter for flood mapping by RISAT-I data as it reduced speckle effectively yet preserved features. Flood extent was estimated from filtered SAR images by radiometric thresholding. The fuzziness between maximum and minimum thresholding values was reduced by examining flood connectivity in pixels. The accuracy of flood extent estimation was 4-5 pixels. Flood duration map was derived from multi-temporal dataset. The Digital Elevation Model was generated from a stereo ortho-kit using Rational Polynomial Coefficients and GCPs obtained by DGPS survey. Flood depth was estimated by density slicing of DEM. The RMSE of elevation was 2.72 m and the horizontal accuracy was 2.48 m and 2.35 m in X and Y direction respectively. The study area was exposed to floods for up to 105 days while the maximum depth exposure to structures was 2.66 m. A depth-duration map comprising nine classes was generated from depth map and duration map. The class boundaries were determined to ensure adequate variability. Habitat map was prepared by digitisation while agriculture map was generated by supervised classification of Landsat 8 data. Census data relating to structures was integrated with spatial data of habitat. The exposure to elements to varying depth and duration was analysed. It was observed that total 26,331 structures were affected by flood and out of 189.2 km² agricultural area, 170 km² was affected by flood. In order to develop vulnerability indices, a survey comprising of 203 samples well distributed throughout the study area and in each depth-duration class was carried out. Damage was measured by examination of structure while the depth was measured from flood depth indicator marks on the walls. Duration was estimated by interviewing occupants of respective structures. The costs to repair the structures and investments in case of agriculture were also estimated from survey data. Based on census data on construction materials used for floor, wall and roof, eight different of structures were identified (A to H). These structures were classified into three types (Type-I to III) by evaluating their damage response obtained from survey data. The average ratio of cost of repairs to the cost of total re-construction yielded vulnerability indices. Damage equations were also generated from vulnerability curves for each type of structure. Using the degree of flood exposure to various elements, vulnerability indices/damage equations and costs, the damage was estimated for the entire area. The total damage to all structures was valued at ₹ 212.66 million with the damage to Type-I, II, and III structures was ₹ 18.1 million, ₹ 41.1 million and ₹ 153.5 million respectively. The total estimated damage to agriculture was estimated as ₹ 389 million.

It also emerged that people living in Type-III structures suffered the maximum losses in absolute as well as relative terms. The optimal protection from flood at minimal cost was provided by structure type 'B' i.e. a house made of burnt bricks joined with cement and the roof made of tiles instead of concrete. The agriculture in study area comprised of vegetables. It was observed that there was 100% damage in all flood intensities.

The desired accuracy of vulnerability indices could not be achieved due to poor sample size of 203 samples against the requirement of 4553 samples. However, the methodology was well defined.

KEYWORDS : RISAT-I, Speckle, SAR, Flood Mapping, Damage Estimation, Vulnerability Indices

ACKNOWLEDGEMENTS

It's after so many years I have enjoyed every moment of pushing myself so hard academically and wish for more. None of this would have been possible if it was not for many of my well-wishers who cared to make their valued contributions along the way.

Foremost, I am thankful to Indian Army for permitting me to proceed on study leave. I am also thankful to IIRS, Dehradun for affording me an opportunity to undergo this course.

I am indebted to Lt Col Ashish Masih who not only initiated me into the current course (and another Masters just prior to this) but has also encouraged me all along.

I am thankful to my guide Dr. Bhaskar R. Nikam, Scientist 'SD', Water Resources Department, Indian Institute of Remote Sensing, Dehradun, who always had time available for me regardless of his pressing commitments. His enthusiasm was infectious and exhorted me to work harder. His guidance has been invaluable. I am thankful to Drs. Nanette C. Kingma, my guide at ITC, Netherlands who has always been so lively and approachable. She provided me with a deeper insight into the subject and then helped lay the firm foundations of my research. Her continued guidance during my research gave me the much needed direction to work.

I am indebted to S.P. Aggarwal, Head Water Resources Department, IIRS for extending the material resources and technical support during the course of research. I am also thankful to Dr Champati ray, Head Geosciences Division, IIRS for providing the necessary guidance for the entire duration of the course. I am thankful to Dr Praveen Thakur for providing clear understanding of the subject which enabled a fulfilling research.

I am thankful to Prof. Dr. V.G. Jetten and Dr D. Alkema, ITC, who provided key inputs in framing my research while at Netherlands. I am thankful to Dr. Luc Boerboom, who provided a wonderful insight into collaborative planning. I thank Dr Nicolas Hamm for providing his invaluable assistance in processing my case for time extension.

I am thankful to Col Sanjay Mohan for providing me assistance in post-processing of DGPS survey data especially for 'bringing back' all the data lost from the DGPS system memory.

I am thankful to Prof. Dr. Bruno Merz, Germany Research Centre for Geosciences, Potsdam, Germany for his sharing his research publications.

I am thankful to Mr Guru Pradhan and Mr Piyush who always gave a patient hearing whenever my research went off track. Most often, I found a solution as a result of the brainstorming that followed.

I am thankful to Mr Vipin Kumar Rai, OSD, Disaster Management Department, Bihar and Mr Sanjay Mathur, Flood Management System Centre, Bihar for providing research related data. I am also thankful to Dr Anand Bijeta, BSDMA, Bihar for his valuable advice.

I am thankful to Mr Girish Peter of Caritas (India), Patna and Mr Karlus Besra and Mr Sunil of Caritas (India), Bhagalpur who provided me with tremendous support in conduct of survey during my field visit to Bhagalpur, Bihar.

Finally and most importantly, I would have never been able to cross this milestone if it was not for the support from my wife Mrs Nita who took on all the responsibilities at home while I gave all my time for my academic pursuits. I am also thankful to her for quietly bearing the brunt of having to share my academic excitement so very often, which I am afraid, is not likely to end very soon.

TABLE OF CONTENTS

List of Figures	iv
List of Tables	v
1. Introduction	1
1.1. Background	1
1.2. Problem Statement.....	2
1.3. Aim of the research	2
1.4. Research Objectives	2
1.5. Research Questions.....	2
1.6. Limitations	3
1.7. Outline of Thesis	3
2. Literature Review	1
2.1. Speckle Reduction in RISAT-I Data	1
2.1.1. Radar Imaging	1
2.1.2. Radar Image Speckle	1
2.1.3. Speckle Reduction Techniques	2
2.1.4. Speckle Reduction Filters	2
2.1.5. Measuring Performance Efficiency of SAR Filters.....	4
2.2. Flood Intensity and Exposure Analysis.....	6
2.2.1. Estimation of Flood Extent.....	6
2.2.2. Digital Elevation Model	7
2.2.3. Generating an Accurate DEM.....	8
2.2.4. Accuracy in Flood Extent Mapping and Water Depth Estimation	8
2.3. Development of Vulnerability Indices and Damage Estimation	8
2.3.1. Defining Vulnerability.....	8
2.3.2. Survey	9
2.3.3. Definitions - Survey	9
2.3.4. Steps in a Survey	9
2.3.5. Formulation of Goals and Objectives	9
2.3.6. Survey Methods.....	9
2.3.7. Sampling Methods.....	9
2.3.8. Estimating Sample Size.....	10
2.3.9. Designing an Interview Schedule	12
3. Study Area	13
3.1. Study Area 1.....	13
3.1.1. Location and Extent.....	13
3.1.2. Geomorphology	13
3.2. Study Area 2.....	14
3.2.1. Location and Extent.....	14
3.2.2. Geomorphology	15
3.2.3. Rainfall.....	16
3.2.4. Agriculture	16
3.2.5. Human Development.....	16
4. Research Methodology	17

4.1.	An Outline of Research Methodology	17
4.2.	Speckle Reduction in RISAT-I Data	19
4.2.1.	Data used for evaluation	19
4.2.2.	Evaluation Process	20
4.2.3.	Generation of backscatter image	20
4.2.4.	Application of filters	20
4.2.5.	Evaluation of performance of filters	20
4.3.	Flood Intensity and Exposure Analysis.....	21
4.3.1.	Data	21
4.3.2.	Estimation of Flood Extent.....	21
4.3.3.	Generation of Flood Duration Map.....	22
4.3.4.	DGPS Survey.....	23
4.3.5.	Generation of Accurate DEM.....	23
4.3.6.	Estimation of Flood Depth.....	24
4.3.7.	Generation of Depth-Duration Map	24
4.3.8.	Exposure Analysis	24
4.4.	Development of Vulnerability Indices and Damage Estimation	25
4.4.1.	Pre-Field Work	26
4.4.2.	Field Work.....	29
4.4.3.	Post-Field Work	31
5.	Results and Discussion.....	33
5.1.	Speckle Reduction in RISAT-I Data	33
5.1.1.	Evaluation of SLC processing software for backscatter generation.....	33
5.1.2.	Evaluation of filters.....	34
5.2.	Flood Intensity and Exposure Analysis.....	38
5.2.1.	Estimation of Flood Extents	38
5.2.2.	Generation of Accurate DEM.....	42
5.2.3.	Flood Depth	44
5.2.4.	Flood Depth-Duration Map.....	45
5.2.5.	Exposure Analysis	46
5.3.	Development of Vulnerability Indices and Damage Estimation	49
5.3.1.	Statistical Analysis of Survey Database.....	49
5.3.2.	Classification of flood depth and duration	49
5.3.3.	Classification of Structures	50
5.3.4.	Population and Sample Size.....	53
5.3.5.	Development of Vulnerability Indices – Village Level	53
5.3.6.	Development of Vulnerability Indices – Single Structure	56
5.3.7.	Damage Estimation – Study Area.....	58
5.3.8.	Method I : Estimation of Damage using Damage Equation and Depth.....	58
5.3.9.	Method II : Estimation of Damage using Vulnerability Indices	63
5.3.10.	Damage Estimation – Single Structure.....	64
5.3.11.	Development of Vulnerability Indices for Agriculture	64
6.	Conclusions and Recommendations	65
6.1.	Conclusions	65
6.1.1.	Objective 1: Speckle Reduction in RISAT-I Data.....	65
6.1.2.	Objective 2: Flood Intensity and Exposure Analysis	65
6.1.3.	Objective 3: Development of Vulnerability Indices and Damage Estimation	66
6.2.	Recommendations.....	67

References69
Annexure75

LIST OF FIGURES

Figure 2.1 The boundaries of T_{min} and T_{max} on backscatter histogram.....	7
Figure 2.2 Sample Size and Population	11
Figure 3.1 Location and extent of study area 1	13
Figure 3.2 Location and extent of study area 2	14
Figure 3.3 Natural water drainage system in study area	15
Figure 3.4 Mean basin discharge, mid basin - River Ganga.....	16
Figure 4.1 Research Methodology Flow. Number refer to Research Questions.....	18
Figure 4.2 RISAT-I image dated 04 Aug 2013 used for evaluation of speckle filters.....	19
Figure 4.3 River extracted from RISAT-I image dated 04 Aug 2013 for evaluation of water bodies.....	19
Figure 4.4 Thresholding workflow	22
Figure 4.5 Masking of flood in village Rattipur due to high backscatter by structures	22
Figure 4.6 Village boundaries and habitat structures in study area	25
Figure 4.7 Habitat locations selected for survey.....	28
Figure 4.8 Flood level marks on the wall	29
Figure 4.9 Flood depth measurement	30
Figure 5.1 Positional accuracy of PAN, SARscape and PolSDP in terms of distances in m.....	33
Figure 5.2 SAR images processed using Left – ENVI (manual), Middle –SARscape, Right-PolSDP ...	33
Figure 5.3 Percentage change in mean and standard deviation due to each filter	36
Figure 5.4 Graph - Percentage change in mean and standard deviation due to each filter.....	36
Figure 5.5 Fuzzy region and threshold for Medium Resolution SAR (MRS) images	39
Figure 5.6 Date wise flood extents	40
Figure 5.7 Area flooded.....	41
Figure 5.8 Flood extent mapped using RISAT-I (07 Sep 13) image and overlaid on LANDSAT8 image (08 Sep 13)	41
Figure 5.9 Classified flood duration map	42
Figure 5.10 Control (Δ) and check points (o) for DEM generation	43
Figure 5.11 DEM generated from CARTOSAT Stereo Ortho kit dated 16 th March 2008.....	43
Figure 5.12 Classified flood depth map	45
Figure 5.13 Flood depth-duration classified map	45
Figure 5.14 Village boundaries and habitat structures	46
Figure 5.15 Exposure of habitat to varying flood depth and duration classes	46
Figure 5.16 Large scale map of exposure of habitat to different depth-duration classes.....	47
Figure 5.17 Exposure of agriculture to varying flood depth and duration	49
Figure 5.18 Distribution of samples - Flood duration	49
Figure 5.19 Distribution of samples - Flood depth.....	49
Figure 5.20 Comparative damage - wall and roof derived from survey data	51
Figure 5.21 Damage response of different types of walls to different flood depths	52
Figure 5.22 Different types of walls	52
Figure 5.23 Vulnerability response of Type I structure (BBC)	53

Figure 5.24 Vulnerability response of Type II structure (BBM)	54
Figure 5.25 Vulnerability response of Type III structure (Thatch).....	54
Figure 5.26 Monetary Loss for varying flood depths.	55
Figure 5.27 Vulnerability response for structures (i.e. A to H)	57
Figure 5.28 Average loss per house hold.....	60
Figure 5.29 Percentage of habitat structures damaged	60
Figure 5.30 Village habitat damage map.....	61
Figure 5.31 Damage contribution by different structures.....	62
Figure 5.32 Damage ratio for different Structures	62
Figure 5.33 Cost of new construction.....	62

LIST OF TABLES

Table 5.1	Positional accuracy of PAN, SARscape	33
Table 5.2	Mean Square Error and relative ranks of different speckle filter combinations	34
Table 5.3	Signal-to-Noise Ratio and relative ranks of different speckle filter combinations.....	34
Table 5.4	Speckle Suppression Index.....	35
Table 5.5	Speckle Mean Preservation Index.....	35
Table 5.6	Mean and standard deviation changes on application of filters	36
Table 5.7	Mean and standard deviation changes on water bodies only.	37
Table 5.8	Mean and standard deviation changes on second pass.....	37
Table 5.9	Radiometric threshold values used for flood mapping of SAR images	38
Table 5.10	RMSE of GCP photo coordinates.....	44
Table 5.11	Summary of RMSEs of control and check points	44
Table 5.12	Number of structures in flood zone.....	47
Table 5.13	Flood exposure to different type of habitat structures.....	48
Table 5.14	Exposure of agricultural area.....	48
Table 5.15	Number of samples – Depth and duration.....	50
Table 5.16	Variations in structures based on construction materials.....	50
Table 5.17	Types of walls and roof materials	51
Table 5.18	State of survey samples	53
Table 5.19	Damage equations for different structure types.....	54
Table 5.20	Evaluation of Vulnerability Indices	56
Table 5.21	Vulnerability Indices (Complete data).....	56
Table 5.22	Damage equations for structures A to H.....	57
Table 5.23	Vulnerability Indices for structures A to H.....	58
Table 5.24	Damage equation coefficients and constant values	59
Table 5.25	Monetary Damage in ₹ (Crores/10 Millions).....	59
Table 5.26	Monetary damage in ₹ (Crores/10 Millions)	63

1. INTRODUCTION

1.1. Background

An area of 498 thousand km² in India, equivalent to 15.1% of its total geographical area is prone to floods. On an average, each year flood affects 3.2 million people and 1612 lives are lost. Since 1951 to 2011, the total estimated damages have been 137 trillion USD. During the same period 20.6 trillion USD have been spent in flood prevention efforts (2011).

Bihar accounts for 17.2% of flood prone area in India. About 68,800 km² out of total geographical area of 94,160 km² comprising 73.06 percent is flood affected (FMIS, Bihar). It's 76% per cent of population in North Bihar comprising 104 million people, are affected by recurring floods.

River Ganges, called as Ganga in India, is for most of its course a wide and sluggish river flowing through one of the most fertile and densely populated regions in the world (Enc. Britannica). It is the third largest river by discharge in the world preceded only by Amazon and Congo rivers (Wiki). Some of its tributaries include Saryu (Ghaghra), Gandak, Budhi Gandak, Bagmati, Kamla-Balan and Mahananda. Other rivers of the state that join the Ganges or its associate rivers after flowing towards north include Sone, Uttari Koyal, Punpun, Panchane and Karmnasha (UNDP, Bihar). The volume of the Ganges increases markedly as it receives more tributaries and enters a region of heavier rainfall. From April to June the melting Himalayan snows feed the river, while in the rainy season from July to September the rain-bearing monsoons cause floods (Enc. Britannica).

The river systems in Bihar makes it one of the most fertile regions in India and yet has lowest per capita income(2012). It has a poverty rate of 54.4% (UNDP, Bihar). The economy of the region is primarily agriculture based. Of the total damage during floods, 76% is attributable to crop loss. As per the annual damage statistics released by the Government of Bihar (BSDMA, Bihar) in the last 20 years commencing 1992, Bihar has lost 4839 lives, crops valued at ₹ 7,960 million and habitat structures valued at ₹ 300 million i.e. an average of 783 human lives, ₹ 398 million worth of crops and habitat structures values at ₹ 15 million are lost each year. In terms of absolute numbers of habitat structures, an average of 160 thousand habitat structures are damaged by floods each year.

The Planning Commission of India's working group on flood management in its report of Oct 2011(2011) had highlighted the need to adopt remote sensing technology and tools as part of strategy in fighting against the menace of floods. In an effort in this direction, Bihar Government prepared its first Flood Hazard Atlas in June 2013. The hazard assessment is based on radar based satellite images. Annual flood layers for 13 years were integrated representing the flood inundated areas with different frequencies. The flood hazard was classified based on the frequency of inundation (2013). However in the document, flood intensity considerations of depth, duration, velocity etc. have not been taken into account.

In absence of flood depth and duration maps, optimal commitment of mitigation resources for villages can't be guaranteed.

1.2. Problem Statement

Poverty also makes the population more vulnerable to floods. Majority of the people in Bihar are marginal farmers having 2-3 acres of land. Since the land is riverine plain, large areas get flooded each year. They construct their houses using local expertise with bricks, mud, thatch and other low cost materials which are damaged even in low flood intensity. With very large flood plains getting flooded every year, farmers spend considerable amount of their already poor earnings in repairing their houses. In case of floods the farmers not only tend to lose their agricultural income, they also have to spend large sums of money to repair their house.

Government of Bihar has a policy of compensating farmers for loss of crop and damage to housing structures due to floods. An extract of Government policy document giving compensation rates for housing structures and agricultural loss is given in Annexure 1. To implement this policy, there must be a reliable mechanism to estimate damage; both, at the micro level i.e. a single household for payment of compensations and at a macro level i.e. village level and above for Government planning purposes.

The Government makes broad estimates of agricultural damage at macro level by using remote sensing technology. Damage to residential housing structures is based on physical examination of each structure.

Physical examination of each damage structure is human resource intensive and sometimes operationally not feasible within the time frame available. In such cases, estimates are based on comparing known history of flood damages in the past and flood intensity in the year under estimation. This limitation may not only deny legitimate compensations but may also generate unreliable Government records thus impacting planning decisions.

1.3. Aim of the research

The aim of this research is to develop vulnerability indices, for estimation of damage to rural residential structures and agriculture caused by river floods, as a tool for planners and Government authorities to make more accurate and timely damage estimates.

1.4. Research Objectives

Main objective of the research is development of vulnerability indices to estimate damage to residential structures and agriculture due to river floods in part of Bhagalpur district, Bihar.

The sub-objectives are

1. Process Single Look Complex RISAT-I data for flood mapping.
2. Estimate the exposure of habitat and agriculture to varying flood intensity levels in study area.
3. Develop vulnerability indices to estimate monetary damage to habitat structures and agriculture due to floods in study area in the year 2013.

1.5. Research Questions

1. Which filter has an optimal performance in reducing speckle in RISAT-I data for application in flood studies?
2. How to estimate varying flood depth and duration?
3. How to determine exposure of habitat structures and agriculture to varying flood intensities?
4. How do different structures and agriculture respond to different flood depth and duration?

5. How can the vulnerability indices be applied to estimate monetary damage at village level in the entire study area?

1.6. Limitations

The research had the following limitations; each one of them influenced the accuracy.

- The research was limited by the total time available. The resulting impact has been on limiting the number of respondents during the survey and hence the accuracy of vulnerability indices.
- The desired accuracy of elevation model can be achieved by LiDAR data. Since LiDAR data was not available, DEM was generated using stereo pair of CARTOSAT-I and GCPs which still has comparatively lower vertical accuracy.
- The RMSE of horizontal accuracy of RISAT-I data was 46.2 m assuming geo-referenced PAN image of the CARTOSAT-I as the benchmark. Since both the datasets were used to estimate flood depth and duration, the inaccuracies would be transferred.
- The flood duration was estimated using the multi date flood maps derived from RISAT-I data. The temporal resolution of RISAT-I data was of the order of 2 to 20 days, the dynamic behavior of flood extent between the actual dates of coverage goes unnoticed in this study. Hence the flood duration map generated may not have high absolute accuracy.

1.7. Outline of Thesis

The research has six chapters which are outlines as follows

Chapter 1: Introduction: The chapter gives a background, statement of problem, aim and the research objectives and research questions. It also specifies the limitation of research and gives an outline of thesis.

Chapter 2: Literature Review: The chapter provides a literature review on speckle reduction in SAR data, characterisation of flood intensity, exposure analysis and development of vulnerability indices and damage estimation.

Chapter 3: Methodology: The chapter commences by a outlining the methodology by research questions followed by detailed methodology for each of the five research questions organised into three groups corresponding to research objectives *viz.* Speckle reduction in RISAT-I data, flood intensity and exposure analysis and development of vulnerability indices and damage estimation.

Chapter 4: Study Area: The chapter gives a description of study area covering its location, extent, geomorphology and demography. Since there are two study areas i.e. a study area for objective 1 and another study area for objectives 2 and 3, both the study area descriptions have been given.

Chapter 5: Results and Discussion: This chapter gives out the results of the research and discusses them to draw inferences. This chapter too is organised into three groups corresponding to research objectives.

Chapter 6: Conclusion and Recommendations: Chapter concluded the research by systematically examining the research outcome of each of the research questions and ends in making recommendations.

2. LITERATURE REVIEW

2.1. Speckle Reduction in RISAT-I Data

2.1.1. Radar Imaging

Microwave part of the spectrum includes wavelengths within the approximate range of 1 mm to 1 m. Depending upon the specific wavelength, microwaves are capable of penetrating haze, light rain, snow, cloud and smoke. This makes radar imaging suitable during cloud and haze conditions when optical data is not useful.

The resolution of a side-looking radar system in the azimuth direction is determined by angular beam-width. As the distance increases, the beam-width “fans-out” resulting in deterioration of azimuth resolution. The effective antenna beam width can be controlled by one of the two different means: 1) by controlling the physical length of the antenna or 2) by synthesizing a virtual antenna length. Synthetic Aperture Radar (SAR) employs a short physical antenna, but through modified data recording and processing techniques, they synthesize the effect of a very long antenna (Lillesand et al., 2004).

Radar imaging process entails transmitting short bursts, or pulses, of microwave energy in the direction of interest and recording the strength and origin of ‘echoes’ or ‘reflections’ received from objects within the system’s field of view. Radar systems measure the intensity of the radiation that is backscattered by the surface – that is, the fraction of the incident energy that is reflected directly backwards towards the sensor. The amount of energy that is backscattered is controlled by system parameters such as wave length, look angle and polarisation and terrain parameters such as surface roughness, slope, dielectric constant and feature orientation (Lillesand et al., 2004).

There are several ways of quantifying and representing strength of the returning pulse measured by radar antenna. One commonly used radio-metric representation is signal *power*, either directly or in a log-transformed version with units of *decibels (dB)*. The visual appearance of radar images is often improved by converting them to *magnitude* format, in which pixel values are scaled in direct proportion to the square root of power (Lillesand et al., 2004).

The radar antenna may be set to send or receive data in *horizontal (H)* or *vertical (V)* polarizations. This results in four typical polarization combinations – HH, VV, HV, VH, where the first letter indicated transmitted polarization while the second letter indicates received polarization (Lillesand et al., 2004).

RISAT-1 employs ‘C’ band which corresponds to the wavelength in the range of 3.75-7.5 cm. allowing imaging in cloudy and light rain conditions during rainy season. National Remote Sensing Centre, ISRO Hyderabad is operationally using RISAT-1 data for flood mapping through Disaster Management Support Programme.

2.1.2. Radar Image Speckle

All radar images contain some degree of speckle, a seemingly random pattern of brighter and darker pixels. Radar pulses are transmitted coherently, such that the transmitted waves are oscillating in phase with one another. However, the waves backscattered from within a single ground resolution cell (or pixel) on the earth’s surface will travel slightly different distances from the antenna to the surface and back. This

difference in distance means that the returning waves from within a single pixel may be in phase or out of phase by varying degrees when received by the sensor. This may cause constructive or destructive interference. These interferences produce a seemingly random pattern of brighter and darker pixels giving the radar images a distinctly grainy appearance known as speckle (Lillesand et al., 2004).

The presence of speckle in an image reduces the detectability of ground targets, obscures the spatial patterns of surface features, and decreases the accuracy of automated image classification (Sheng and Xia, 1996). It is therefore essential that speckle is reduced before any further processing is carried out. There are many filters that have been proposed each having its unique strengths and limitations. Thus, the choice of which filter to use is dependent on the requirements of the specific application and the characteristics of the dataset employed (Lee et al., 1994). Despeckle filters with good noise removal capabilities often tend to degrade the spatial and radiometric resolution of an original image and cause the loss of image detail (Qiu et al., 2004). The performance of noise suppression must be balanced with the filter's effectiveness in order to preserve fine detail (Xiao et al., 2003).

2.1.3. Speckle Reduction Techniques

There are two techniques in speckle reduction. The first approach involves techniques such as multiple-look processing, which averages together several independent images or "looks" of different portions of the available azimuth spectral bandwidth (synthetic aperture), or different polarization states of the same area during image formation (Lillesand et al., 2004). The second technique involves use of image processing techniques to smoothen the image after it has been formed as a result of pre-processing. Further, in the second technique, there are two major approaches which may be followed to reduce speckle. The first approach to digital filtering is achieved in the frequency domain by wavelet transformation (Gagnon and Jauan, 1997). The second approach is accomplished in the spatial domain, where noise is removed by averaging or statistically manipulating the values of neighboring pixels (Qiu et al., 2004). The instant research focuses on the second approach wherein some of the commonly used filters for SAR data, provided by commercial software ERDAS Imagine, have been used to reduce speckle.

Following the assumption of multiplicative characteristic of noise, many filters such as Lee filter, Frost filter, Gamma (MAP or Maximum A Posteriori) Lee-sigma filter have been devised. All these adaptive filters aim to effectively reduce speckle in radar images without eliminating the fine details (Jenson, 2000).

2.1.4. Speckle Reduction Filters

2.1.4.1. Mean Filter

Mean filter is a low-pass filter and simply averages the values in the moving window. It is the least satisfactory method of speckle noise reduction as it results in loss of detail and resolution (Mansourpour et al., 2006).

2.1.4.2. Median Filter

Low value and high value pixels correspond to destructive and constructive interference (Sheng and Xia, 1996). Median filter effectively suppresses these extreme values.

The mean and median filters meet with only limited success when applied to SAR data. One reason for this is the multiplicative nature of speckle noise, which relates the amount of noise to the signal intensity. The other reason is that they are not adaptive filters in the sense that they do not account for the particular speckle properties of the image (Qiu et al., 2004).

2.1.4.3. Lee Filter

Lee filter, is based on the assumption that the mean and variance of the pixel of interest are equal to the local mean and variance of all pixels within the user-selected moving window (Lee, 1981). The filter removes the noise by minimizing either the mean square error or the weighted least square estimation (Qiu et al., 2004).

The calculation of Lee filter is (Lee, 1981)

$$DN_{out} = [Mean] + K[DN_{in} - Mean]$$

Where,

Mean = Average of pixels in moving window.

$$K = \frac{Var(x)}{[Mean]^2 \sigma^2 + Var(x)}$$

The Variance of x is defined as

$$Var(x) = \frac{[Variance\ within\ window] + [Mean\ within\ window]^2}{[Sigma]^2 + 1} - [Mean\ within\ window]^2$$

Lee filter, due to the use of a fixed sigma computed for the entire scene, blurs some of the low-contrast edges and linear features (Eliason and McEwen, 1990). A refined version of this filter is the Lee-Sigma filter.

2.1.4.4. Lee-Sigma Filter

The Lee-sigma filter is an effective alternative to the Lee filter and other sophisticated adaptive filters (Lee, 1983). It is based on the sigma probability of the Gaussian distribution. It first computes the sigma (standard deviation) of the entire scene, and then replaces each central pixel in a moving window with the average of only those neighboring pixels that have an intensity value within a fixed sigma range of the central pixel (Qiu et al., 2004).

Based on an assumption that speckle has a Gaussian distribution, 95.5% of random samples would be within 2 standard deviation range. The Standard Deviation of a 1,2,3,4 looks would yield standard deviation values of 0.52, 0.37, 0.30, 0.26 respectively. The filter averages the values within the moving window of only such pixels that are within a range corresponding to its number of looks. The coefficient of variance is calculated for the entire image and is used as an input parameter.

2.1.4.5. Local Region Filter

The filter divides the kernel window into eight regions based on angular positions. For each of the region variance is calculated. The pixel of interest is replaced by the mean of region with least variance.

2.1.4.6. Frost Filter

The Frost filter replaces the pixels of interest with a weighted sum of the values within the moving window (Frost et al., 1982). The weighting factors decrease with distance from the pixel of interest and increase for the central pixels as variance within the window increases. This filter assumes multiplicative noise and stationary noise statistics (Qiu et al., 2004). It follows the following formula:

$$DN = \sum_{n \times n} k \alpha e^{-\alpha |t|}$$

Where $\alpha = \left(\frac{4}{n \bar{\sigma}^2} \right) \left(\frac{\sigma^2}{\bar{I}^2} \right)$

k = normalized constant

\bar{I} = local mean

σ = local variance

$\bar{\sigma}$ = image coefficient of variation value

$|t| = |X - X_0| + |Y - Y_0|$, and

n = moving kernel size

Frost filter needs to consider the influence of damping factor. Larger damping values preserve edges better but smooth less, and smaller values smooth more. A damping value of 0 results in the same output as a low pass filter. After application of the Frost filter, the filtered images show better sharpness at the edges.

2.1.4.7. Gamma-MAP Filter

The Gamma-MAP (Maximum A Posteriori) filter was developed by Lopes et al., (1990). Prior knowledge of the probability density function of the scene is required before this filter can be applied.

The filter tends to maximise the posteriori probability of the original signal from the speckled signal. The scene reflectivity is assumed to be a Gamma distribution instead of a Gaussian distribution. It is based on a multiplicative noise model with non-stationary mean and variance parameters. However, the Gamma-MAP filter, like the Frost filter, will blur the edges. (Qiu et al., 2004)

The Gamma-Map algorithm follows the following cubic equation (Frost et al., 1982)

$$\tilde{I}^3 - \bar{I} \tilde{I}^2 + \sigma (\tilde{I} - DN) = 0$$

Where \tilde{I} = sought value
 \bar{I} = local mean
 DN = input value
 σ = original image variance

2.1.5. Measuring Performance Efficiency of SAR Filters

There are several methods to assess the filtered image quantitatively according to different aspects such as noise reduction, edge preservation, feature preservation (Sheng and Xia, 1996). The results of these different measurements can be contradictory. Hence, different assessment methods should be used to find the optimum trade off among the different aspects of image quality assessment (Qiu et al., 2004).

Although quantitative measures are often employed to compare different speckle suppression filters, visual inspection probably provides the best assessment of the performance of the speckle filter (Raouf and Lichtenegger, 1997).

Some of commonly used measures to assess performance of filters are as under:

- Mean Square Error (MSE)
- Signal to Noise Ratio (SNR)
- Speckle Suppression Index (SSI)
- Speckle Mean Preservation Index (SMPI)
- Edge-Enhancing Index (EEI)
- Equivalent Number of Looks (ENL)
- Speckle Image Statistical Analysis (SISA)
- Feature-Preserving Index (FPI)
- Image Detail-Preserving Coefficient (IDPC)

Since the purpose of filtering SAR data in present study is flood delineation, speckle reduction in a water bodies, preservation of edges and linear structures were essential requirements. Thus the filters have been evaluated based on specific measures - MSE, SNR, SSI, and SMPI. These measures are further examined hereafter.

2.1.5.1. Mean Square Error (MSE)

MSE is the measure of the extent to which the output image differs from the input image. This helps indirectly to assess the feature preservation (Senthilnath et al., 2013).

$$MSE = \frac{1}{K} \sum_{i=1}^K (I_o - I_f)$$

Where I_f = Filtered Image
 I_o = Original Image

2.1.5.2. Signal to Noise Ratio (SNR)

The standard signal-to-noise ratio (SNR) is not adequate to evaluate the noise suppression in the case of multiplicative noise. Instead, a common way to achieve this in coherent imaging is to calculate the signal-to-noise (I_o /MSE) ratio, defined as (Andrews and Hunt, 1977; Starck et al., 1998)

$$SNR = 10 \log_{10} \left(\frac{\sum_{i=1}^K I_{f_i}^2}{\sum_{i=1}^K I_{o_i} - I_{f_i}} \right)$$

Where K = Total number of pixels
 I_f = Filtered Image
 I_o = Original Image

2.1.5.3. Speckle Suppression Index (SSI)

One of the measurements for speckle strength is the coefficient of variance, or the ratio of the standard deviation to the mean (Lee et al., 1994). It remains constant over homogeneous areas, where it is fully determined by the amount of speckle in the image (Hagg and Sties, 1996). The speckle suppression index

(SSI) is the coefficient of variance of the filtered image normalized by that of the original image, which is defined as:

$$SSI = \frac{\sqrt{\text{var}(R_f)}}{\text{mean}(R_f)} \times \frac{\text{mean}(R_o)}{\sqrt{\text{var}(R_o)}}$$

Where R_f = Filtered image value
 R_o = Original noisy image value

As a result of filtering the resultant image has lower variance because speckle is suppressed. SSI smaller than 1.0 indicates efficient speckle suppression (Sheng and Xia, 1996).

2.1.5.4. Speckle Mean Preservation Index (SMPI)

SSI is not reliable when sometimes mean value overestimated. Therefore, apart from SSI, SMPI (Speckle Suppression and Mean Preservation Index) must also be used to assess the performance of filters (Wang et al., 2012). Lower values of SMPI indicate better performance of the filter in terms of mean preservation and noise reduction. The equation of the index is as follows (Shamsoddini and Trinder, 2010):

$$SMPI = Q \times \frac{\sqrt{\text{var}(I_f)}}{\sqrt{\text{var}(I_o)}}$$

Where I_f = Filtered Image
 I_o = Original Image

Q is calculated as under:

$$Q = 1 + |\text{mean}(I_o) - \text{mean}(I_f)|$$

2.2. Flood Intensity and Exposure Analysis

In the current research the scope of flood intensity is limited to flood depth and duration. The exposure considered in the research pertains to residential structures and agriculture in the defined study area. Flood intensity and exposure analysis was aimed at extending the application of vulnerability indices to estimate damage in the entire study area.

2.2.1. Estimation of Flood Extent

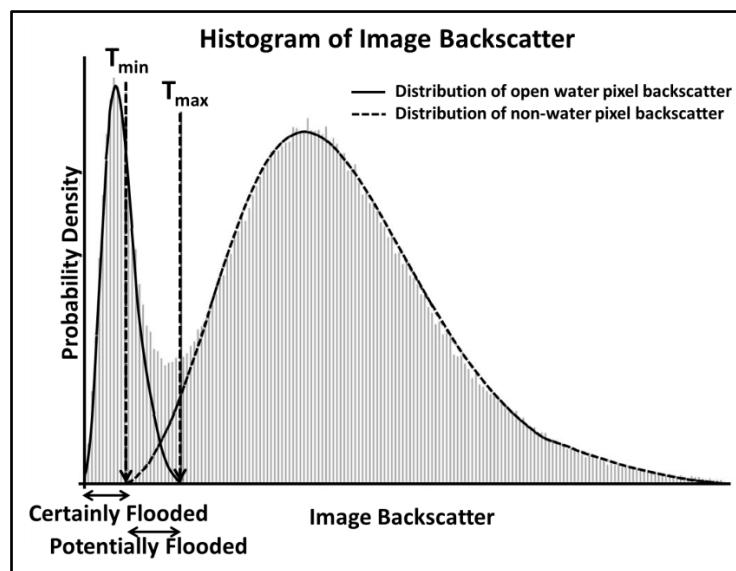
RISAT-1 employs microwave 'C' band which corresponds to the wavelength in the range of 3.75-7.5 cm allowing imaging in cloudy and light rain conditions during rainy season. Because of their all-weather image acquisition capability, synthetic aperture radar (SAR) satellites are very suitable for the spatial characterization of floods (Oberstadler et al., 1997).

In SAR datasets, moist areas due to its dielectric properties appear bright. But water bodies, even though, they have very high dielectric constant (dry areas have dielectric constant in the range of 3 to 8 when dry while water has dielectric constant of approximately 80) appear dark because of smooth surface. Smooth

water surfaces act as specular reflectors of radar waves and yield no or minimal returns to the antenna, but rough water surfaces return radar signals of varying strengths. Because the dielectric constant for water is at least 10 times that for dry soil, the presence of water in the top few centimetres of bare (un-vegetated) soil can be detected in radar imagery. The greater moisture content of the irrigated crops also increases the dielectric constant, which in turn increases the reflectivity of the crop surface (Lillesand et al., 2004).

Flood extent mapping using SAR images is widely applied because water appears dark with very low backscatter compared to other objects (Smith, 1997). Radiometric thresholding is a robust and reliable way to detect flooded areas on SAR images (Henry, 2004). On the image, the radiometric distributions of water bodies and other land use types are not totally separated and do thus overlay (Hostache et al., 2009).

Hostache et al. (2009) have designed a method of extraction of flood extent in SAR datasets wherein the uncertainty due to overlay, has been reduced by adopting thresholds – T_{min} and T_{max} . T_{min} represents the minimum radiometric value of non-flooded pixels while the T_{max} is the maximum radiometric value of water bodies outside the flooded area. The Intensity (I) values of SAR image pixels will provide the degree of likelihood of flooded area wherein $I > T_{max}$ = non-flooded, $I < T_{min}$ = certainly flooded, $T_{min} \leq I \leq T_{max}$ = potentially flooded. The fuzziness of ‘potentially flooded’ areas takes into account the radiometric uncertainty. Figure 2.1 shows the distribution of flooded and non-flooded pixel backscatter on a histogram. The location of T_{min} and T_{max} are indicated. The gap between them is the fuzzy area.



Hostache et al., 2009

Figure 2.1 The boundaries of T_{min} and T_{max} on backscatter histogram

2.2.2. Digital Elevation Model

Accurate estimation of flood depth is dependent upon several factors such as accuracy in flood extent delineation, methodology used to determine depth and the most important of all, the horizontal and vertical accuracy of DEM used to determine depth.

In their evaluation of various open source DEMs, Mukherjee et. al., 2013 have estimated the RMS error for the ASTER and SRTM as 6.08 m and 9.2 m with mean error of -2.58 m and -2.94 m, respectively. In both cases, the error is less than the error specification given by the nodal agency (8.86 m for ASTER and

16 m for SRTM)(Mukherjee et al., 2013). Horizontal accuracy of 2.08 m and 1.74 m and vertical accuracy of 3.72 m can be achieved in a DEM generated from CARTOSAT-I stereo image using GCPs acquired from DGPS (Bhardwaj, 2013).

The vertical accuracies of open source DEMs such as SRTM, ASTER and CARTOSAT would not be sufficiently accurate for development of vulnerability indices. The accuracy of the coordinates and hence the DEM depends on the source of RPC's. If GCP's are available one can refine the RPC's using polynomial functions (Bhardwaj, 2013).

2.2.3. Generating an Accurate DEM

GCPs acquired through a DGPS survey require to be corrected by utilising precise satellite ephemerides satellite clock corrections. Regional GNSS reference networks allows the approach of modelling the errors over a region, followed by correction parameters made available to the user (Kjorsvik et al., 2005). The approach uses known precise coordinates of IGS reference sites to determine errors. Alternatively, the same processing can be done using an online web based application over the internet (<http://webapp.geod.nrcan.gc.ca/geod/tools-outils/ppp.php>). CSRS-PPP (Canadian Spatial Reference System (CSRS) Precise Point Positioning (PPP)) uses the precise GNSS satellite orbit ephemerides to produce corrected coordinates of a constant "absolute" accuracy no matter where you are on the globe, regardless of proximity to known base station (Canada Geodetic Survey). While the 'final' GNSS orbit ephemerides which are available after 20 days, have an accuracy of ± 2 cm, the 'Rapid' ephemerides are available the very next day but have comparatively lower accuracy of ± 5 cm.

The global positioning system (GPS) computes the height relative to WGS84 (Kaplan and Hegarty, 2006). The elevation of a point on Earth surface computed from Mean Sea Level (MSL) can thus vary from GPS derived elevation because of the variation between WGS84 ellipsoid and Geoid (local MSL) (Mukherjee et al., 2013). However, EGM96 model is a very close approximation of Indian MSL (Sun et al., 2003).

2.2.4. Accuracy in Flood Extent Mapping and Water Depth Estimation

Over and above the fuzziness between the two thresholds and radiometric uncertainties mentioned earlier, the accuracy of the geo-referencing of a SAR image induces additional uncertainties on these fuzzy limits (Hostache et al., 2009). Also, due to high backscatter, both buildings and high vegetation may mask water on a SAR image (Horrit et al., 2001). During the merging between the flood extension fuzzy limits and the DEM, this uncertainty is transferred to the water level estimates (Brakenridge et al., 1998; Schumann et al., 2008). Consequently, the steeper the terrain underlying a flood extent fuzzy limit, the more important the uncertainty of derived water level estimates (Hostache et al., 2009).

2.3. Development of Vulnerability Indices and Damage Estimation

2.3.1. Defining Vulnerability

Multiple definitions and different conceptual frameworks of vulnerability exist, because distinct groups have different views on vulnerability (Van Westen and Kingma, 2009). Based on factors influencing vulnerability, it can be categorised into Physical, economic, social and environmental vulnerabilities (UN-ISDR, 2004).

Physical Vulnerability is the potential for physical impact on the built environment and population. It is the 'degree of loss' to a given 'element at risk' resulting from the occurrence of a natural phenomenon of a given magnitude and is expressed on a scale from 0 (no damage) to 1 (total damage) (UNDRO, 1991).

Vulnerability is analyzed per group of constructions (i.e. structural types) having similar damage performance. It is an intrinsic quality of a structure and it does not depend on location (Westen and Nanette, 2009).

2.3.2. Survey

The flood intensity can be determined using remote sensing techniques. However, estimating quantum of physical damage to structures and agriculture would require obtaining ground truth by means of a physical survey.

A common goal of survey research is to collect data representative of a population. The researcher uses information gathered from the survey to generalize findings from a drawn sample back to a population, within the limits of random error (Bartlett et al., 2001).

2.3.3. Definitions - Survey

The term '*Population*' is defined as the total membership or population or 'universe' of a defined class of people, objects, or events (UN Statistical Division). Each member of the population is termed an '*element*'.

A '*Sampling Frame*' is that portion of the population from which the sample will be selected, i.e. which might be observed. The '*Sample*' is that portion of the population that we have observed (Rossiter, 2013).

2.3.4. Steps in a Survey

The steps in a survey are as follows (Fellegi, 2003)

- Formulation of Objectives
- Selection of a survey frame
- Determination of the sample design
- Questionnaire design
- Data collection
- Data capture and coding
- Editing and imputation
- Estimation
- Data analysis
- Data dissemination
- Documentation

2.3.5. Formulation of Goals and Objectives

Survey's objectives must be clearly defined during the planning phase considering the information required, how the data would be used and analysed, required precision and operational constraints (Fellegi, 2003).

2.3.6. Survey Methods

There are many methods to collect data in a survey such as in-person interview, telephone interviews, mailed questionnaire, online surveys etc. Each one has certain advantages and disadvantages over the other.

2.3.7. Sampling Methods

Sampling frame provides the means of identifying and contacting the units of the survey population. This frame ultimately defines the survey population (Fellegi, 2003).

There are basically two types of sampling methods: probability sampling and non-probability sampling. In probability sampling, every unit of the population has a measurable chance of selection. In non-probability sampling, the chance of a unit's selection is not known (Cook, 1995).

Many probability sampling designs have been proposed such as simple random sampling, stratified random sampling, systematic and cluster sampling etc. The most basic type is random sampling. Simple random sampling is the selection of n units from a population of N units in a manner such that each of the n units has the same chance (probability) of being selected (Cochran, 1977). However, random sampling should be used only if the area of interest is homogeneous with respect to the elements and covariates of interest (Morrison, 2008).

In *stratified sampling*, the sampling frame is separated into different regions (*strata*) comprising the population to be surveyed and a sample of units within stratum are selected for study, usually by a random or systematic process (Morrison, 2008). Stratification may be used to increase the likelihood that the sampling effort will be spread over important subdivisions or strata of the study area, population. The primary objective of stratification is improved precision based on optimal allocation of sampling effort into more homogeneous strata (Morrison, 2008).

2.3.8. Estimating Sample Size

One of the real advantages of quantitative methods is their ability to use small groups of people to make inferences about larger groups that would be prohibitively expensive to study (Holton and Burnett, 1997). This leads to the question of how large should the sample size be to make inferences on the entire population?

The sample size is dependent upon the acceptable margin of error i.e. the accuracy desired from the survey. The smaller the acceptable margin of error, the larger the sample required. There is, however, an optimal size after which little appreciable gain in accuracy is made (Cook, 1995). The level of confidence required refers to a range above and below the estimated value which may be expected to contain the true value with a known probability. The greater the level of confidence required that the results fall into the range, the larger the sample size required (Cook, 1995).

There are two key factors for error estimation: (1) the risk the researcher is willing to accept in the study, commonly called the margin of error, or the error the researcher is willing to accept, and (2) the alpha level, the level of acceptable risk the researcher is willing to accept that the true margin of error exceeds the acceptable margin of error; (Cochran, 1977). The alpha level used in most educational research studies is either 0.05 or 0.01 (Cochran, 1977). For categorical data, 5% margin of error is acceptable, and, for continuous data, 3% margin of error is acceptable (Krejcie and Morgan, 1970).

There are many factors and approaches to determine the minimum sample size. Most commonly used formulae are given by Cochran for continuous and categorical data (Cochran, 1977) and Krejcie and Morgan (Krejcie and Morgan, 1970; NEA, 1960). Cochran has been critical of Krejcie and Morgan's formula since it assumes alpha of 0.05 and a degree of accuracy of 0.05. There may be instances when such an assumption may not hold true. However, in the current research, since the values are acceptable, any of the two formulas would be acceptable. The formulas given for estimating sample size (n_0) by both are as follows.

(Cochran, 1977), Continuous data

$$n_0 = \frac{t^2 \times s^2}{d^2}$$

where,

t = value of selected alpha level.

s = estimate of standard deviation in the population

d = acceptable margin of error

Categorical data

$$n_0 = \frac{t^2 \times (pq)}{d^2}$$

where,

t = value of selected alpha level.

pq = estimate of variance

(Krejcie and Morgan, 1970), For known population size

$$\text{Sample size} = \frac{X^2 NP (1 - P)}{d^2 (N - 1) + X^2 P (1 - P)}$$

where,

X^2 = table value of Chi-square @ degrees of freedom = 1 for desired confidence level

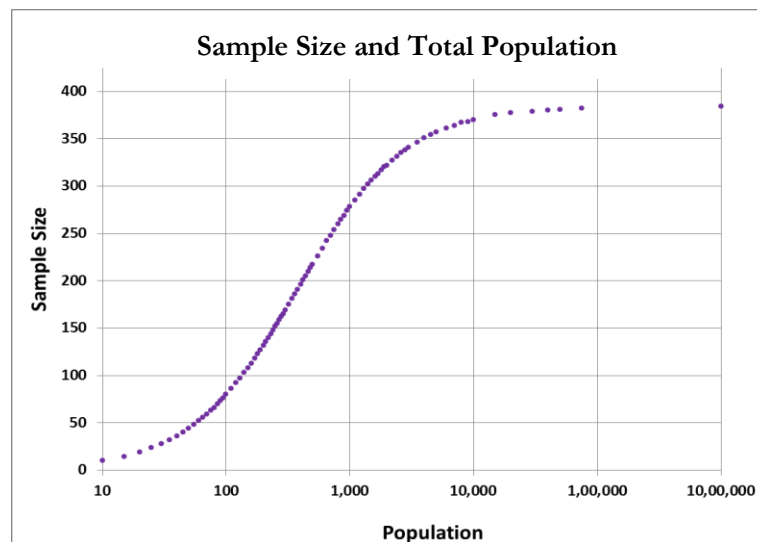
0.1 = 2.71 0.05 = 3.84 0.01 = 6.64 0.001 = 10.83

N = population size

P = population proportion (assumed to be 0.50)

d = degree of accuracy (expressed as a proportion)

For a certain level of accuracy, the proportionate requirement of samples reduces with increase in population size as shown at Figure 2.2.



Assumes Standard Error = 0.05

Krejcie and Morgan (1970)

Figure 2.2 Sample Size and Population

2.3.9. Designing an Interview Schedule

The tool used to conduct an interview is called '*Interview Schedule*'. Each interview schedule should have four sections *viz.* opening, transition, core survey and closing of interview.

Most of the data elements required in the current research relate to measurements. Offering respondents a set of closed quantity categories (e.g., less than 1 h, 1–3 h, more than 3 h) can produce error (Krosnick and Presser, 2010). One of the first decisions a researcher must make when designing a survey question is whether to make it open (permitting respondents to answer in their own words) or closed (requiring respondents to select an answer from a set of choices) (Krosnick and Presser, 2010). Open questions are usually preferable to closed items for measuring quantities (Allen, 1975).

Acquiescence is most common among respondents who have lower social status (Gove and Geerken, 1977), and less formally educated (Ayidiya and McClendon). A better approach of eliminating acquiescence is to avoid using agree/disagree, true/false, and yes/no questions altogether (Krosnick and Presser, 2010).

Two reservations sometimes expressed about measuring quantities with open questions are that some respondents will say they don't know or refuse to answer and others will round their answers. In order to minimize missing data, respondents who do not give an amount to the open question can be asked follow-up closed questions, such as "was it more or less than X? (Juster and Smith, 1997).

3. STUDY AREA

The study area for research objective 1 of the research is approximately 30 km North of the study area for objectives 2 and 3.

3.1. Study Area 1

3.1.1. Location and Extent

The Study Area-1 is located in Madhepura district in the state of Bihar. Madhepura district is surrounded by Araria and Supaul district in the north, Khagaria and Bhagalpur district in the south, Purnia district in the east and Saharsa district in the West. It comprises two of the nine administrative blocks of the district located in the southern extent of the district, namely, Chausa and Alamnagar. It lies between the coordinates Latitudes $25^{\circ} 26' 39''$ N to $25^{\circ} 38' 17''$ N and Longitudes $86^{\circ} 47' 51''$ E to $87^{\circ} 47' 51''$ E covering an area of 1788 km². River Kosi flows from West to East in the southern extent of the study area. Figure 3.1 shows the geographical location of study area.

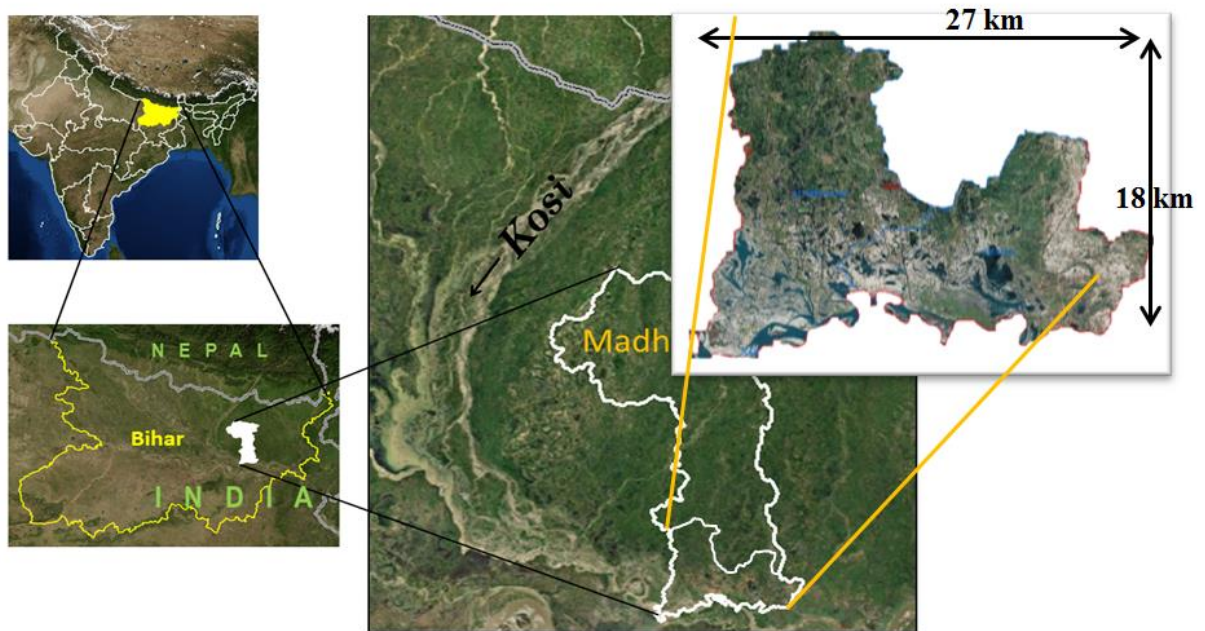


Figure 3.1 Location and extent of study area 1

3.1.2. Geomorphology

The area is flat riverine terrain with most of the area covered in agriculture interspersed with small villages comprising cluster of houses.

River Kosi flows to the south of Madhepura district. Ten km further south of Kosi is river Ganges. Both the rivers confluence approximately 20 km east of the study area. River Kosi originates in Nepal and has one of the largest fans in the world, measuring approximately 180 km long and 150 km wide. The channel

has shifted 120 km during the past 250 years (Regmi, 2013). Kosi river is a major tributary to Ganga River system and has long been considered as a problematic river due to recurrent and extensive flooding and frequent changes in its course (Sinha et al., 2008). The district is regularly affected by river floods especially the area under study is the worst affected. This area classified as highly flood prone area to monsoon floods of Kosi River.

Madhepura has a population of over two million and a decadal growth rate of 31.12%. Primary occupation is agriculture and nearly all the agricultural activity consists of rice cultivation.

3.2. Study Area 2

3.2.1. Location and Extent

The Study Area-2 is located in Bhagalpur district in the state of Bihar in India, partially overlapping two of the sixteen administrative blocks of Bhagalpur district. Specifically the study area comprises parts of Nathnagar and Sultanganj blocks of Bhagalpur district lying between the coordinates Latitudes $25^{\circ} 9' 50''$ N to $25^{\circ} 19' 7''$ N and Longitudes $86^{\circ} 45' 39''$ E to $86^{\circ} 58' 44''$ E, covering an area of 237 km². To the North of the study area is River Ganges which also forms the limit of the study area. Figure 3.2 shows the geographical location of study area.

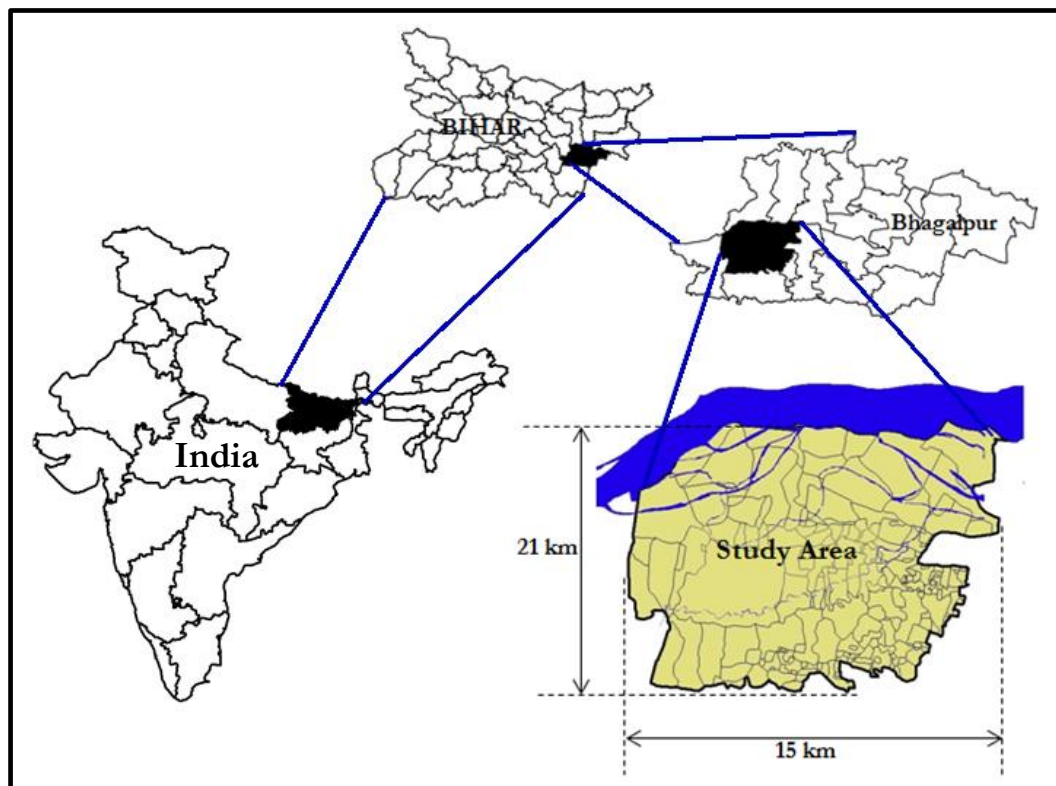


Figure 3.2 Location and extent of study area 2

3.2.2. Geomorphology

Bhagalpur district which is towards the south of the river Ganga falls in the Badua- Koa Sub-Basin while the area to north of Ganga falls in the Baghmata - Kosi sub-basin. These two sub-basins are parts of Mid-Ganga basin in Bihar.

The district is principally drained by the river Ganga, which enters the district at Sultanganj as shown in Figure 3.3. River Ganga has two major tributaries joining from south; Badua and Koa, the former is part of the study area. Gahra and Chanan are the two ephemeral streams that join the Ganga River, are located in the southern part of the study area.

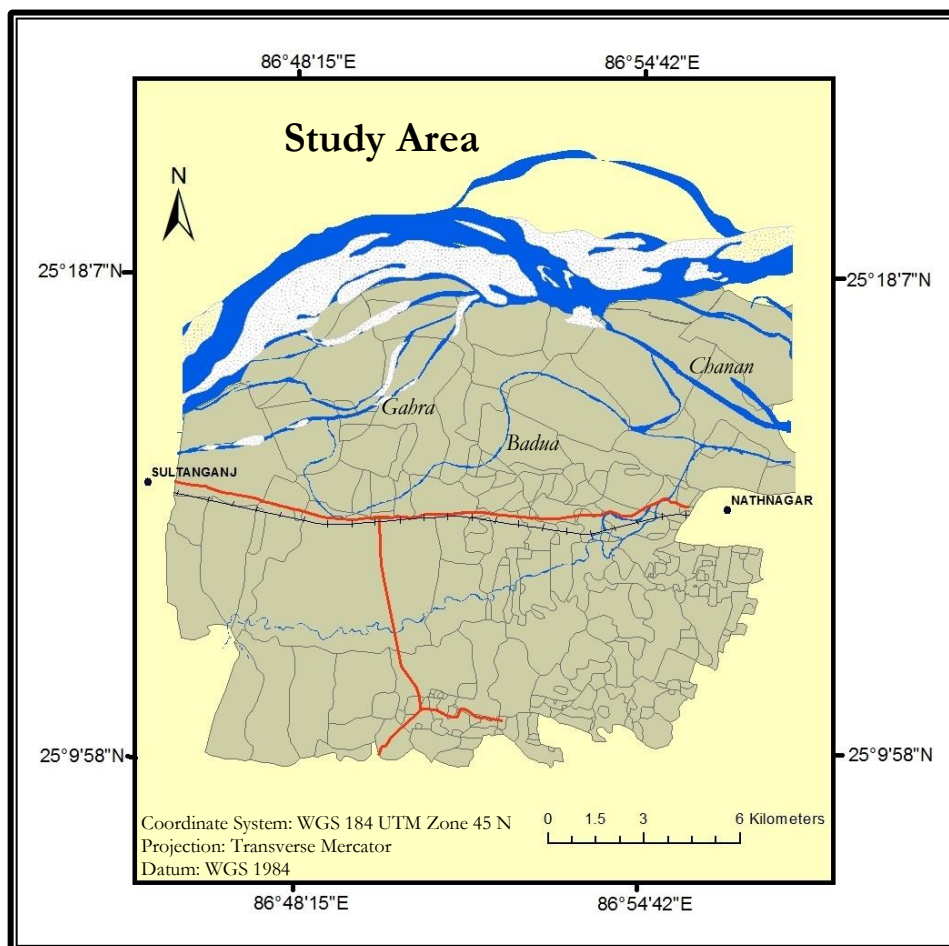


Figure 3.3 Natural water drainage system in study area

On the basis of distinctive valley morphology and channel characteristics, the (Ganga River valley) GRV has been divided into seven segments (Singh et al., 2007). The study area falls under GRV-V. In this segment, the river shows an extensive development of valley, almost 20 – 30 km wide with W – E orientation and an average slope of 6 cm/km (Singh et al., 2007).

The study area is divided into two clear segments by a National highway and a railway track, both running parallel with an approximate distance of 100-200 m from each other. In the Northern part of the study area there are many channels created by meandering of the river. Closer to river there are long sandbars which undergo considerable shifting during flood event. The geomorphology in the study area within a distance of 2-3 km of the river is undulating with crests rising approximately 3-4 m over a distance of 300-

400 m. Habitats are invariably constructed on the higher crests, but these crests undergo changes during floods. The study area comprises of 57,602 structures in 121 villages.

3.2.3. Rainfall

The study area is prone to monsoon floods every year. The onset of monsoon normally occurs in early June. By the end of July, the monsoon establishes itself over the entire basin. Heavy rainfall occurs everywhere during July, August, and September (Singh et al., 2007). Usually 70 – 80% of the total annual rainfall occurs during this period. Figure 3.4 shows the minimum basin discharge of river Ganga in the course of the year.

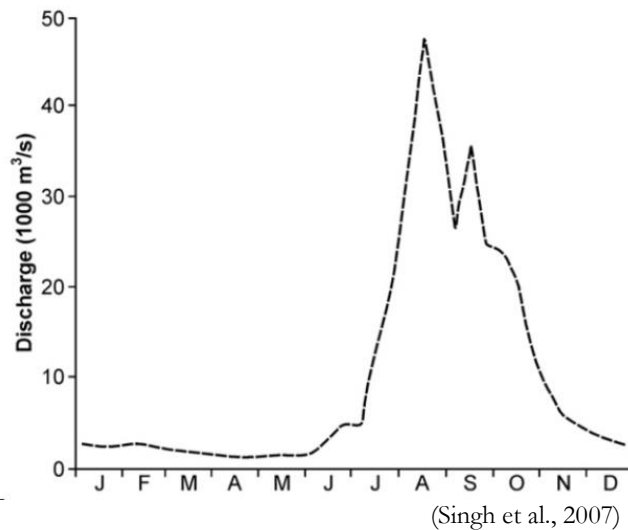


Figure 3.4 Mean basin discharge, mid basin - River Ganga

3.2.4. Agriculture

Agriculture is the prime occupation in the study area. The people are either land owners or work in the agriculture land as labourers.

3.2.5. Human Development

Bihar has the second largest percentage of rural population in the country. Out of the total population of 103 million, nearly 90 percent of the population lives in the rural areas.

Bihar has high levels of intra-state disparity with north Bihar lagging behind due to low agricultural productivity, poor irrigation facilities and high vulnerability to floods. According to the Tendulkar Committee Report 2009, nearly 54.4 percent of the population lives below the poverty line. Poverty in Bihar is a function of low per capita land holding, very low industrialization base and limited opportunities in the service sector (UNDP, Bihar).

4. RESEARCH METHODOLOGY

4.1. An Outline of Research Methodology

The research has three objectives and five research questions. The research methodology can be visualised as a sequence of six steps briefly given below and presented graphically in Figure 1.1.

The first step corresponds to research question 1 of objective 1. The research required identification of an optimal filter to reduce speckle in RISAT-I SAR data for flood studies. The process involved generating a dB images (pixel values are scaled in direct proportion to the square root of power to enhance visual appearance) from multi-temporal RISAT-I SLC dataset. The resulting image was filtered using an adaptive filter. The choice of optimal filter to reduce radar speckle was determined after evaluation of five filters which have been explained.

The second step corresponds to research question 2 of objective 2 *viz.* How to estimate varying flood depth and duration? To estimate flood depth, the filtered multi-temporal SAR images were used to estimate flood extent by thresholding method. A 'flood duration map' was prepared from resulting flood extent images. To estimate flood depth, it was pre-requisite to generate an accurate DEM. The DEM was generated using a CARTOSAT-I stereo pair and 21 GCPs obtained by DGPS survey. By density slicing of DEM, maximum flood depth map was generated. The slope of flood was estimated to enhance the accuracy of 'flood depth map'. Flood duration and depth map were classified into three classes each and then a 'flood depth-duration map' was prepared having nine classes.

The third step corresponds to research question 3 of objective 2 *viz.* How to determine exposure of habitat structures and agriculture to varying flood intensities? A 'habitat' implies a cluster of residential structures in a village. A habitat map was generated by digitising from Google Earth. The number of structures and their construction type was obtained from Census data and added to the Habitat Map database. Agriculture map was prepared by supervised classification of Landsat 8 image. The exposure of habitat and agriculture was determined using Habitat and Agricultural Maps and Flood Depth-Duration map.

The fourth step corresponds to research question 4 of objective 3 *viz.* Vulnerability Indices were determined by statistical analysis of data collected from 203 respondents from field. The analysis resulted in establishing a relationship between damage response of different structures to varying flood depth and durations. The monetary damage or the loss in percentage terms yielded the vulnerability indices and damage equations.

The fifth step corresponds to research question 5 of objective 3 *viz.* Using the flood classified depth-duration map, vulnerability indices, census data and cost of reconstruction, provided the total estimated damage in the entire study area. The agricultural damage was estimated based on agricultural area, estimated investments and depth-duration maps.

Figure 4.1 shows an overview of research methodology. The numbers refer to research questions.

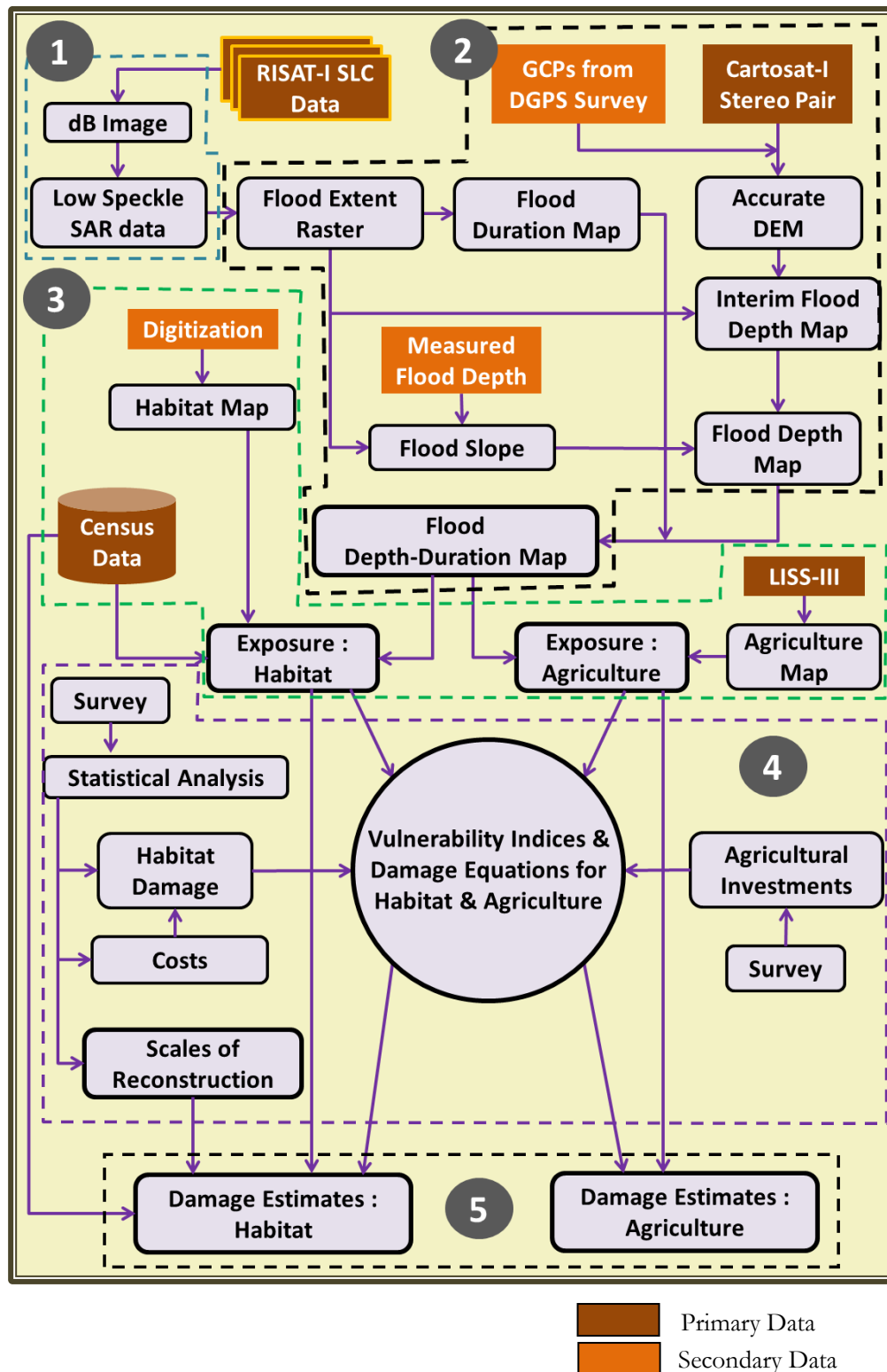


Figure 4.1 Research Methodology Flow. Number refer to Research Questions

4.2. Speckle Reduction in RISAT-I Data

4.2.1. Data used for evaluation

The RISAT-I data in C-band (5.35 GHz) was used for determining the optimal filter for speckle reduction for the purpose of flood delineation. The data was Medium Resolution SCANSAR (MRS) Single Look Complex (SLC) Level-1 in HH polarisation, incidence angle at 39.504° and nominal 8.33 m resolution. The image size used for evaluation was 5674 X 4437 pixels subset from RISAT-I scene number 7021_1_6 dated 04 Aug 2013 procured from National Remote Sensing Centre, Hyderabad, India. The image used is as shown in Figure 4.2.

Since, the ultimate purpose of the filtering is to accurately delineate flood, the complete evaluation was also carried out simultaneously on water bodies in order to make a comparison and determine if there is any benefit accrued by this approach. The extracted image of water bodies used for evaluation is as shown in Figure 4.3.

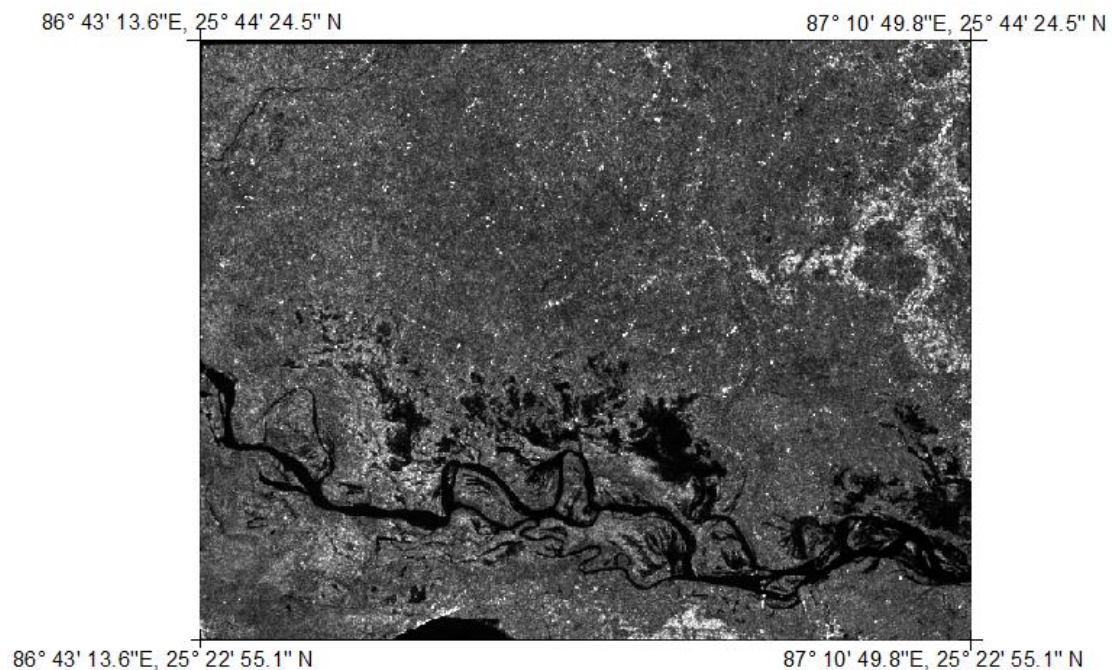


Figure 4.2 RISAT-I image dated 04 Aug 2013 used for evaluation of speckle filters.



Figure 4.3 River extracted from RISAT-I image dated 04 Aug 2013 for evaluation of water bodies.

4.2.2. Evaluation Process

The evaluation involved two steps. First, the SLC data was processed to generate backscatter image and as a second step, this image was used for evaluating performance of various filters.

4.2.3. Generation of backscatter image

The RISAT-1 was launched in April 26, 2012. As on date, only two commercial software applications are available to process RISAT-I data, namely, PolSDP developed by CSRE, IIT-Bombay and SARscape® which works as a plugin to ENVI. When using SARscape® multi-look image was generated using cartographic size of 10 m and 4th convolution cubic resampling. All other parameters were retained as default. Since no literature is available regarding performance evaluation of PolSDP and SARscape, the test data was processed thorough both the software. In addition, the test data was also processed manually using ENVI's band math tool. The manual processing using ENVI involved importing SLC data followed by conversion to Amplitude image. Amplitude image was converted to multi-look using open source tool, RAT. Slant range was then converted to ground range. An incidence angle image was generated. The multi-look image and the incidence angle image were then used to generate backscatter image.

Since topographic sheet was very old vintage, its co-relation with SAR image was not feasible. A Cartosat pan image was thus first geo-referenced using topographic sheet. The PAN image was then used as a reference to measure positional error of points identified in geocoded SAR images generated using SARscape and PolSDP. The coordinate system and datum of all the three datasets was GCS.

The three results were then evaluated to determine the best option for generating backscatter image.

4.2.4. Application of filters

The coefficient of variation of the image was measured and provided as a parameter in case of all filters except Local Region Filter since it does not consider global influences during the application of filter.

The image was subjected to following filters - Lee filter, Frost filter, Gamma (MAP or Maximum A Posteriori), Local Region filter and Lee-sigma filter. All the five filters were evaluated for three kernel sizes 3×3, 5×5 and 7×7 resulting in a total of fifteen images for evaluation. Henceforth each of this combination will be termed by name of filter window size i.e. Lee (3×3) or Lee (3×3). Similarly, the extracted river image shown at Figure 4.3 was similarly filtered resulting in another set of fifteen images.

4.2.5. Evaluation of performance of filters

Each of the resulting 15 × 2 images was tested for performance in speckle suppression, feature preservation and loss of meaningful data using several performance measures MSE, SNR, SSI, SMPI, examination of mean and standard deviation and also a close visual assessment. Models for each of the four measures i.e., MSE, SNR, SSI, SMPI were designed using model maker in ERDAS imagine. The original image and one of the thirty images to be evaluated was used one at a time as image variables in ERDAS Imagine model maker to obtain the result. The mean and standard deviation was obtained using ERDAS Imagine built-in functions. The results for each measure and image were recorded and a rank awarded to indicate a comparative performance.

4.3. Flood Intensity and Exposure Analysis

4.3.1. Data

The SAR data set used for flood intensity analysis was a subset of a RISAT-I dataset with Upper Left coordinates as Lon 86.749, Lat 25.306 and the lower right Lon as 86.961 and Lat as 25.163 degrees. Total of 11 images were used. All the images in the temporal datasets were processed using SARscape from Level 1 Single Look Complex to generate a dB image. A single pass of Frost (7X7) adaptive filter was applied to reduce speckle as elaborated in Chapter 3. The dates, scene number, sensor mode, polarisation and inclination angle of each image is as given in Annexure 2. The images are as given in Annexure 3.

An orthorectified LISS-III image from Resourcesat-I having spatial resolution of 23.5 m was downloaded from NRSC website 'Bhuvan' (Bhuvan, NRSC) and used to extract permanent water bodies in non-flood season. Image used was Path 106 Row 054.

The DEM was generated using a single Stereo Ortho Kit of Cartosat-I, Path-0579, Row-0281 and date of pass -16th March 2008.

Landsat 8 multi spectral data of 03rd May 2013 has been used to extract agricultural fields in the study area.

Census data used to carryout exposure analysis has been obtained from Department of census website and census data research facility at Jawaharlal Nehru University, New Delhi.

4.3.2. Estimation of Flood Extent

The thresholding method of flood extent mapping as discussed in Section 2.2.1 was applied in present study to generated flood maps using RISAT-I data. Using PAN and Google earth image and DEM, patches of vegetation were identified which because of higher elevation the area would certainly not be flooded and yet give the lowest backscatter values (other than flood). After digitising these patches, the minimum backscatter value of individual RISAT-I (SAR) image was picked up from each patch. The minimum value amongst these values was assigned to T_{min} . All backscatter values below these would certainly be flooded. Similarly T_{max} was determined by obtaining the maximum backscatter value from patches of river and permanent water bodies.

The correct threshold value between the range of fuzziness between T_{min} and T_{max} was obtained by close visual examination of pixels and fine adjustment of threshold value. The correct value was the maximum value in the fuzzy range that ensured continuity of flood water pixels. The workflow of thresholding method is shown in Figure 4.4.

The extent of flood was also validated from ground truth and is explained in Section 5.2.1.1.

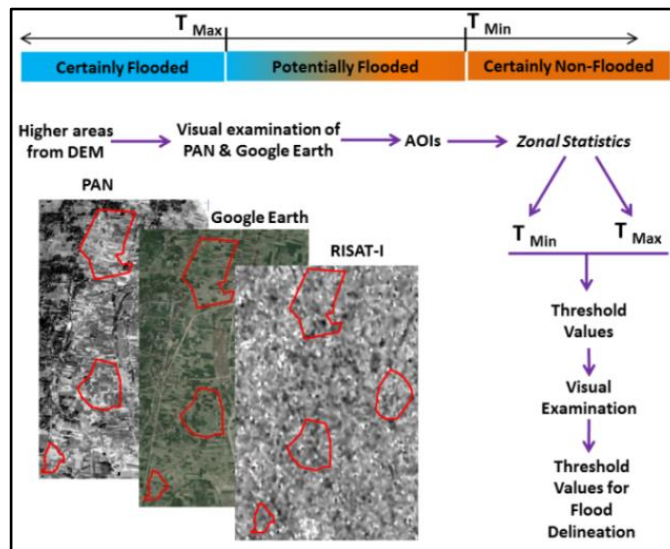


Figure 4.4 Thresholding workflow

4.3.3. Generation of Flood Duration Map

Due to high backscatter, both buildings and high vegetation mask water on a SAR image (Horrit et al., 2001). The masking was observed up to a distance of approximately 50-70 m i.e. 6 to 8 pixels from group of structures and trees. Figure 4.5 shows an example of masked flood around village structures due to high backscatter values. Field visit had confirmed that the area shown in the figure was flooded for over 60 days. In order to resolve the problem of masking of flood, a buffer of 150 m was created around the structures. Mean backscatter values of areas within this buffer, excluding the masked pixels, was applied to the masked areas.

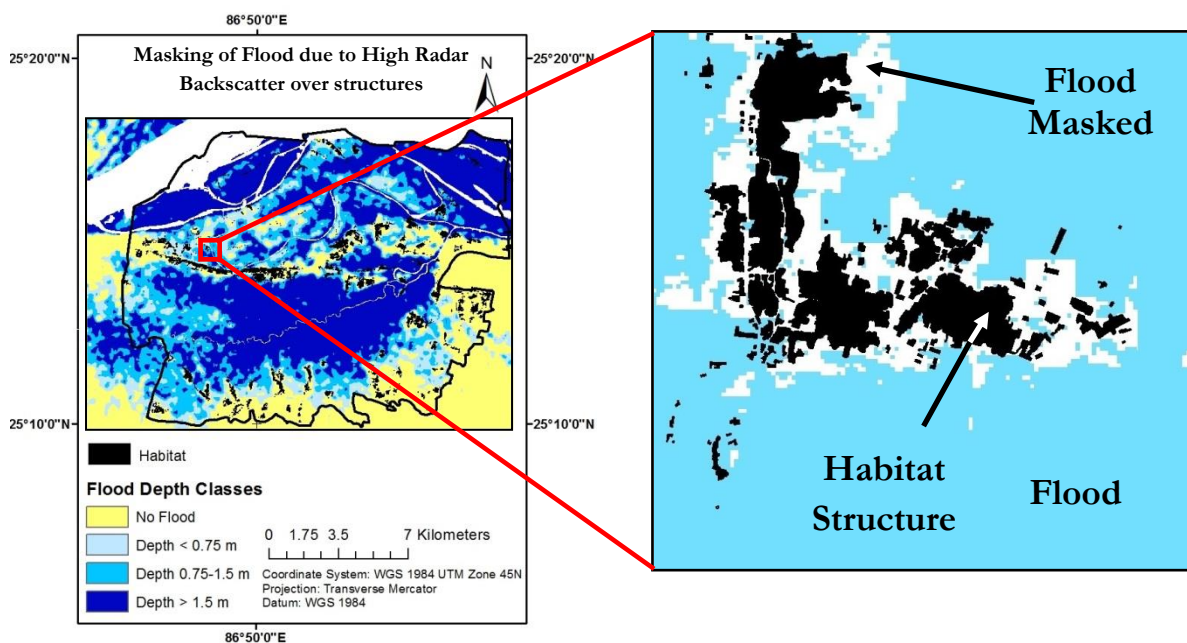


Figure 4.5 Masking of flood in village Rattipur due to high backscatter by structures

Using the threshold values, each image was classified into flood and non-flood areas and assigned values 1 and 0 respectively. Permanent water bodies were extracted from a LISS-III image of non-flood season and assigned as non-flood class in classified SAR image (flood maps).

Each flood extent raster was multiplied by a value equivalent to the difference between the date of SAR image and the date of preceding SAR image. The pixel values of all resulting flood extent raster data set were summed up to provide a flood duration raster where the pixel value represented the duration of flood. The temporal resolution of the 11 images (CRS and MRS) range from 2 to 20 days with an average of 9 days, there is likelihood that any variation within the span of two images may not get registered. In the present research it is assumed that there are no major variations within a span of two images.

4.3.4. DGPS Survey

Generation of accurate DEM was prerequisite to estimation of flood depth. DGPS survey was carried out during the field visit.

4.3.4.1. Selection of proposed Ground Control Points

The GCPs were identifiable points on ground as well as both, AFT and FORE, images, of Cartosat-I stereo pair from which DEM was to be prepared.

A total of 22 points were planned during pre-field visit stage of which 5 were planned to be used as check points for validation. The GCPs were also identified on the Google Earth image based on which field identification sheets were prepared for each GCP. All the GCPs were kept away from any obstructions such as buildings and trees etc.

4.3.4.2. Measurement of GCPs

The DGPS survey was conducted using a single frequency Differential GPS, Leica GPS 500. Base station was established on top of a building in Bhagalpur (25°15'1.99"N, 86°59'19.00"E) which provided a clear view of sky free from any intervening physical features in all directions. The base station was not moved during the entire survey since all the rover points were within a distance of 20 km from Base station. A total of 22 GCPs (21 Rover and a Base station) were collected as given in Annexure 11.

4.3.4.3. Post Processing of DGPS Survey Data

The raw GNSS observation data obtained from Leica 500 GPS System was first converted into RINEX (Receiver Independent Exchange Format) format to enable post processing using Trimble Business Centre 2.2 application software. The data format conversion was carried out by Leica Geo-Office software.

CSRS-PPP web based online application was used to compute higher accuracy positions from raw data using 'Rapid' ephemerides. The EGM96 geoid model was chosen to convert ellipsoidal heights to MSL. Baselines were processed and accurate horizontal and vertical coordinates of all the 22 GCPs (one base station and 21 GCPs) obtained.

4.3.5. Generation of Accurate DEM

Aerial triangulation was carried out using Leica Photogrammetry Suite (LPS). A stereo image pair from Cartosat-I was used to perform aerial triangulation. The cloud free stereo image acquired on 08 Jan 2010 was used. The processing was carried out using RPCs provided along with the Stereo Orthokit. Interior and exterior orientations were carried out automatically using the RPCs. In addition to 17 GCPs used as

control points, 1466 automatically generated tie points were also used to enhance accuracy. The accuracy of DEM was validated using 4 checkpoints.

4.3.6. Estimation of Flood Depth

Flood depth was estimated by using maximum flood extent map and an accurate DEM. There was a clear demarcation of flood due to elevated road passing through the study area in East-West direction. Elevation along the flood edges was measured from DEM separately for each of these flood zones.

In order to account for slope in flood, the maximum flood map was converted to vector. The two large resulting polygons represented flood on either side of the road. The boundary of the polygons representing the highest elevation up to which the flood had reached in this event (in other words the boundary in terms of elevation between flooded and non-flooded area) was converted to point data 500m apart. A buffer of 50 m i.e. 6 pixels around each point was used to obtain mean and standard deviation of underlying DEM. The mean values of buffers having low standard deviations were recorded in the attributes of respective point data. Buffers having high standard deviation were ignored. A linear trend interpolation was carried out using the point data with mean elevation. The interpolation was validated using known flood depths in seven locations collected during field visit. The variation in the flood level obtained from interpolation and flood level obtained using DEM were compared.

4.3.7. Generation of Depth-Duration Map

Flood duration map and flood depth map were classified using three classes each. The classes were determined based on distribution of flood as discussed in Section 5.3.2. The classes were as under

Duration

- Duration Class 1: Less than 20 days
- Duration Class 2: 20 – 40 days
- Duration Class 3: More than 40 days

Depth

- Depth Class 1 : Less than 0.75 m
- Depth Class 2 : 0.75 m – 1.5 m
- Depth Class 3 : More than 1.5 m

The Depth-Duration map was generated using classified duration and depth maps. A unique number was assigned to each of the possible combinations of flood depth and flood duration. Using conditional raster operations in ERDAS model maker a flood Depth-Duration map was generated. Invalid classes 'such as a river getting flooded' resulting because of shifting of river were replaced with adjoining class.

4.3.8. Exposure Analysis

The habitat in the area was digitised using Google Earth and then imported into GIS application. The attribute tables of polygons were populated with census data for analysis later. Figure 4.6 shows the map showing habitat structures in the study area.

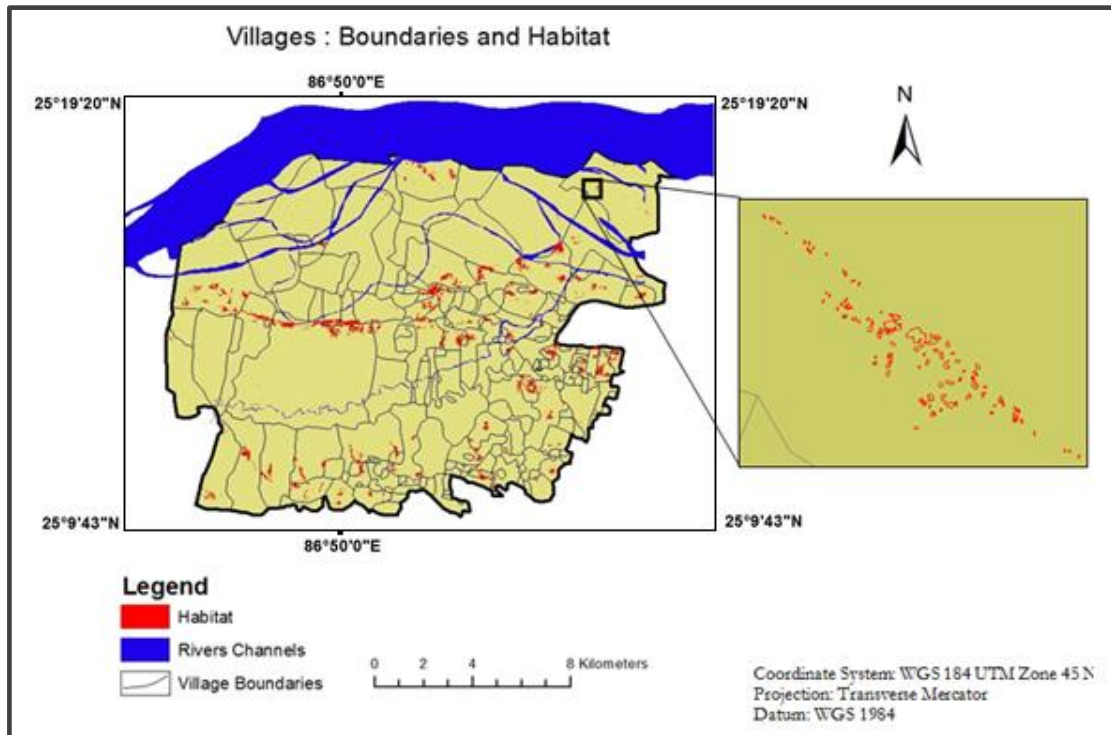


Figure 4.6 Village boundaries and habitat structures in study area

The classified Depth-Duration map was converted to vector and intersected with habitat vector map. The exposure of habitat to varying degrees of flood intensity was obtained.

The number of different type of structures in each village was obtained from census data. The area of the habitat of each village was obtained from vector data prepared by digitization. Based on these two data, the density of each type of structure in a village was obtained.

The Depth-Duration classified map and Habitat map was used to determine exposure to structures in 9 different depth-duration combinations. Village wise area of habitat exposed to the 9 combinations of depth-durations was determined. The density of different type of structures in each village and the habitat area exposed was used to estimate the number of different type of houses exposed to varying intensities of flood.

For determining exposure to agriculture fields, supervised classification of Landsat 8 Image of 03 May 13 was carried out. The agriculture fields were extracted and their exposure to varying flood intensities was determined.

4.4. Development of Vulnerability Indices and Damage Estimation

Development of vulnerability indices for flood is the main objective of this research. The damage to different houses (structural types) is mainly determined by the construction materials of the house, flood water depth and the flood duration (Thakur et al., 2012). The key requirement for achieving the objective is thus to establish a relationship between **flood intensity** and the **damage** caused by it to various **elements at risk**. In the current research, the intensity of flood implies flood *depth* and *duration* while the elements at risk were limited to the *residential structures* and *agriculture* in the study area. Only direct damage

was considered. The definition and the link between vulnerability and the damage too must be clearly established.

In the current research ‘degree of loss’ also called ‘damage’ is equal to the amount of financial expenditure that would have to be incurred in order to make good the loss to the ‘element at risk’ i.e. the cost of repairs in case of habitat structures or the value of lost investment in case of agricultural damage.

The study area had an intense flood event in 2013. Approximately 90% of the study area and 76% of the total number of structures were flooded. The vulnerability assessment was based on empirical method by analysing the observed damage in the study area. The damage has been measured by conducting a survey.

4.4.1. Pre-Field Work

Pre-field work involved collection and processing of data and survey design.

4.4.1.1. Data Collection and Processing

Flood duration and flood depth maps were prepared as already explained in Section 3.3. These maps formed the basis for determining different strata in the sampling process as explained in subsequent paragraphs.

Census Data was collected from Registrar General of Census. The data provides details of the study area at village and block level. Following census data was used in conjunction with the data collected during survey to achieve the research objectives.

- Village Name
- Number of house-holds in each village
- Number of census houses (residential structures) in each village
- Number of census houses using different construction material for each component i.e. wall, roof and floor
- Economic level indicators – number of households in possession of assets such as television, bicycle etc.

Village boundaries in study area were digitised using online map from Bhuvan (Bhuvan, NRSC).

Habitat comprising of residential structures was digitised using Google Earth.

4.4.1.2. Goal and Objectives of Survey

The goal of the field survey was to obtain representative samples for development of vulnerability indices for flood damage to structure and agriculture in the defined study area. The objectives of the survey were as follows:-

- Determine the flood depth and duration exposure for structures in study area.
- Determine the characteristics of damage to structures and its physical dimensions.
- Estimate the cost of re-construction part or complete structure after a flood event.
- Find out the loss of crop in varying flood depths and duration.
- Know about the investments made by a farmer in agriculture.

4.4.1.3. Target Accuracy

The survey should have ideally targeted to yield vulnerability indices for flood damage estimation within a confidence interval of 5% at 95% confidence level. However, with the limitations of time available for the research, the target accuracy was aimed at maximum achievable in a 12 day survey effort.

4.4.1.4. Survey Methodology

The census data indicates that the local populace is extremely poor and illiterate. The population comprises of marginal farmers dependent primarily on cultivation. Also since the survey requires taking physical measurements of the houses of subjects, the survey was based on personal interview method using a structured interview schedule.

4.4.1.5. Sampling Methodology

The population for survey comprises of all residential structures and agricultural crops within the study area. The study area consists of a total of 121 villages, comprising 31,732 households and having a total of 57,602 residential structures. The term '*residential structures*' is equivalent to the term '*census houses*' as used by the Department of Census.

The objectives of the survey require that all variations in flood intensity be covered in the survey. Since the flood intensity has a spatial dimension, stratified random sampling method was used to identify suitable areas for survey. Three strata were identified within which random sampling was carried out.

Three strata were identified by classification of 'Flood Duration Map' into three flood duration classes *viz.* less than 20 days, 20-40 days and greater than 40 days duration.

4.4.1.6. Estimating the number of different structures exposed to flood

The estimated number of structures of each type has been determined based on census data. It is assumed that the entire census population lives in the census specified village habitat only. Census data provides the number of census houses *viz.* structures and the total count of each type of structure in each village. It is assumed that different types of structures are uniformly distributed in the village. This assumption would imply that the number of structures exposed would be in the same ratio as the percentage of habitat area exposed. First, the overall density of structures was determined from census data and the area of habitat (obtained as a result of digitization of habitat area). Then, through use of GIS tools the area of habitat exposed to varying degrees of flood was determined. The structure density was then used to estimate the number of structures exposed in different flood classes.

Six villages were chosen from each stratum, totaling 18 villages. The villages were chosen ensuring a wide spatial spread over the entire study area. Some villages were chosen which were located well within the class while some were chosen which were located on the fringes. Figure 4.7 shows the village boundaries and habitat selected for selection of samples.

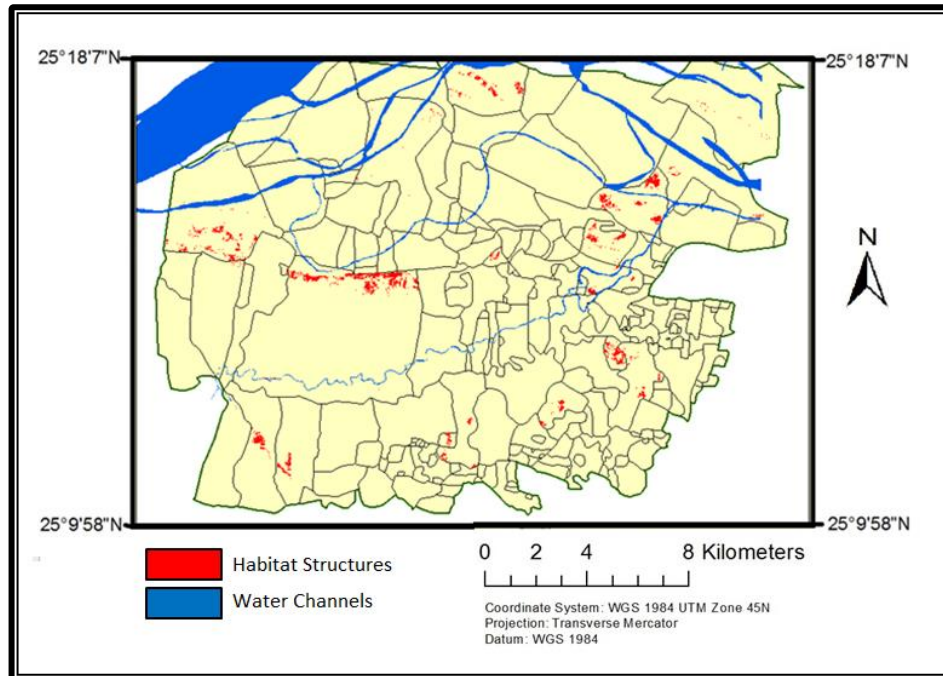


Figure 4.7 Habitat locations selected for survey

Within the selected villages, samples for survey were chosen based on random sampling. An electoral roll was used as a sampling frame. It is a public document published by the Election Commission of India. It consists of list of village wise lists of households in each village and the document is available on the internet (Electoral Roll, Bihar). The house numbers were used to generate a random list of house numbers using `RANDBETWEEN()` function in MS Excel. Duplicate numbers were removed and the list was then ordered in ascending order for easier access during survey.

4.4.1.7. Structured Interview Schedule

In the current research due to poor education levels amongst the population, in-person interview was the most appropriate. Based on the goals and objectives of the survey, a list of information required was prepared. The information requirement was transformed to specific questions and a structured interview schedule generated.

The detail of information required is as follows. The structured interview schedule is given in Annexure 4.

Information related to each residential structure

- What is the construction material used for floor, wall and roof?
- What was the flood depth exposure to the structure?
- For how long did the flood remain around the structure?
- How can the damage to a structure be quantified?
- What was the monetary loss to each structure as a result of damage due to flood?
- How can we optimally group the residential structures into classes on the basis of similarity in damage response to varying flood intensities?

Information related to agriculture

- What are the varieties of crop grown in the area and what is their extent in terms of area of cultivation?
- What was the intensity of flood in 2013 to which the crops were exposed to?
- What was the monetary loss due to varying flood intensities?

4.4.1.8. Database Design

Each piece of information requirement was broken down into specific data element. Data elements that would be calculated on completion of survey were also identified.

4.4.1.9. Data Recording Form

The list of data elements was organised into a logical flow of sequence and printed as a form. The data recording form is given in Annexure 5.

4.4.1.10. Testing of Interview Questionnaire

The questionnaire was tested on peer group before proceeding for field visit.

4.4.2. Field Work

Field visit was conducted from 30th Jan 14 to 16th Feb 14. The actual data collection lasted nine days. The process of collecting data is enumerated as follows.

The survey for structures was conducted by a team of three persons, which included an individual who interacted with the owner of the residential structure, a person who measured and recorded the data and a local mason.

4.4.2.1. Estimation of Flood Depth

Due to recent floods, almost all structures had flood level marks on the walls. The height of the flood was measured both inside and outside the structure. Figure 4.8 shows the typical wall marking indicating height of the flood.



Figure 4.8 Flood level marks on the wall

Flood was measured as shown in Figure 4.9. The difference between the flood depths inside and outside the structure was between 6-10 cm only.

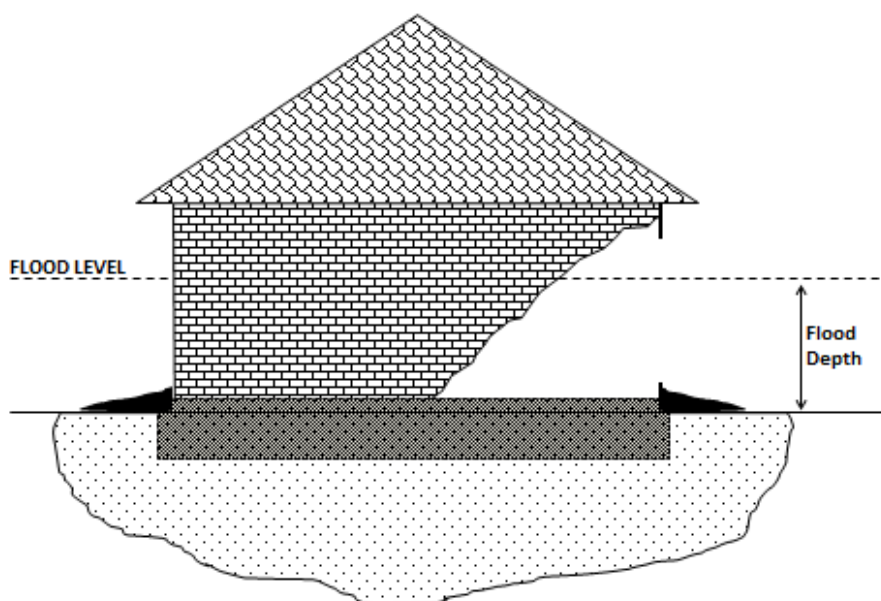


Figure 4.9 Flood depth measurement

4.4.2.2. Estimation of Flood duration

Flood duration was estimated based on responses of individuals and was suitably cross verified to ensure reliability.

4.4.2.3. Measurement of Physical Damage

'Physical damage' implied any part of wall, roof or floor requiring repairs as a consequence of flood impact. The decision, regarding the quantum and nature of repairs required was determined in consultation with the accompanying local masons.

The area of damage was measured and recorded separately for wall, floor and roof in terms of area damaged. The damage to structures made of burnt bricks, could be easily measured since the structure showed clear signs of loss of integrity and the boundaries of damage could be easily determined by visual inspection. However, in case of structures made of thatch, there was considerable ambiguity in measurement of dimensions of damage. The quantum of damage was thus estimated directly in terms money that would be required to repair the structure.

There were instances where the structures themselves were not damaged but the flood event had either deposited considerable mud around his house or removed it, sometimes to an extent of even exposing its foundation. In all such cases, the estimated cost of such maintenance too was recorded and incorporated as damage.

4.4.2.4. Estimation of Construction Costs

After having completed half the survey, it was estimated from the available surveyed data, that the average size of a residential structure is 41.7 m². The detailed breakdown of cost of construction for a structure measuring 41.7 m² was obtained from five local masons independently. The cost of materials that would

be re-used was reduced from the total construction cost. The *scales of re-construction* giving cost of repair per unit area for floor, wall and roof was then prepared for each type of material. The scales of repair were used to convert physical damage to total repair cost i.e. monetary loss for each damaged structure.

The detailed costing of different type of structures in study area is given in Annexure 6. The scales of re-construction per unit area are given in Annexure 7.

4.4.2.5. Field Survey - Agriculture

Field survey for agriculture was carried out by interacting with farmers in different villages. Since the area gets flooded between the months of July-August every year, the farmers have adapted their farming practices in such a way that they would make some profit even in the event of flood. The normal period of flood is Aug to Oct. Most farmers cultivate vegetables which have a short maturity period. Vegetables also allow continued harvesting till the plant reaches full maturity. Farmers are aware that the flood would destroy their crops but since the onset of flood is not known, they take a calculated risk by exploiting the small window of opportunity to cultivate crops that would be ready for harvesting before the area gets flooded. If the flood gets delayed by few weeks, they would make more profits than expected but in the event of an early flood, the farmers are likely to lose their entire investment.

Following crops are cultivated by farmers in the months of June-July, just prior to flood.

(Local Name/English/Scientific)

- Parval / Pointed Gourd / *Trichosanthes dioica*
- Bhindi / Lady Finger / *Abelmoschus esculentus*

The investment costs for the crops, yield, sale price and damage due to flood was determined based on field survey. The area under cultivation was determined by supervised classification of using Landsat 8 data.

4.4.3. Post-Field Work

Post field work involved organisation of data into a database, statistical analysis, development of vulnerability indices, validation and estimation of damage in entire study area.

4.4.3.1. Generation of Database

The data collected on survey forms was organised into a database using MS Excel. Based on data collected during field survey, several calculated data fields were added.

4.4.3.2. Classification of Structures

Classification of structures would be required if there is very large variations in types of structures and yet their damage response is similar. Ideally vulnerability indices should be developed for every type of structure; generalisation by classifying would introduce some inaccuracy. On the other hand classification would result in larger sample size for each class (the sample size requirement does not increase proportionately to total population size) thereby improving the accuracy in terms of confidence level and confidence interval of the vulnerability indices.

In the current research, both the methods have been followed i.e. the indices have been developed based on classification of structures as well without classification. Vulnerability indices based on classification can be applied at a village level to estimate damage for planning purposes. If sufficient samples are available for every type of structure, the vulnerability indices thus derived can be used for applications such as preliminary assessment of compensation, construction planning etc. The vulnerability indices

without classification have been developed primarily to bring out the methodology. They have not been applied to estimate damage due to insufficient sample size.

4.4.3.3. Vulnerability Indices and Validation

As per UNDRO (1991) definition of Vulnerability, it is a 'degree of loss'. 'Loss' has been defined in Section 2.3.1. In order to estimate the degree of loss of structures, the physical damage of wall and roof for each structure was measured and is given in Annexure 8. The cost of repairs i.e. the 'loss' is calculated by the costs of re-construction of wall, roof, and floor per unit area given at Annexure 7 and the physical damage from Annexure 8. Annexure 8 also gives the dimensions of the house which has been used in conjunction with repair scales given in Annexure 7 to calculate total cost of re-construction. The ratio of actual damage to the cost of re-construction the entire structure is the Vulnerability Index. A value of 1, implies total damage and value of 0 signifies no damage.

In order to validate the indices, the sample was randomly grouped into two groups 2/3rd and 1/3rd. Using RANDBETWEEN function in MS Excel, the database records were randomly assigned values of either 1, 2 or 3. All records with values 1, 2 were used for determining vulnerability indices while the remaining 1/3rd of records were used for validation.

The variation between vulnerability indices derived from 2/3rd and 1/3rd samples was compared.

4.4.3.4. Estimation of Accuracy

Based on Krejcie and Morgan(1970) formula on estimation of minimum number of samples required, the confidence level and the margin of error of the vulnerability indices were determined.

4.4.3.5. Damage Estimation of Structures for Entire Population

Following information was used to estimate village level damage in the entire study area

- Number of different type of structures estimated from census data.
- Depth and duration exposure to habitat from depth and duration map and habitat map.
- Damage equation developed as shown in Sections 5.3.5 to 5.3.7.

The damage to structures can be estimated based on all type of structures viz. A to H or based on three types of structures viz. Type-I, II and III. The choice would depend upon number of samples available and the accuracy desired. Finer classification would require higher number of samples and vice versa.

Structural damage is a function of type of structure, flood depth and damage exposure. If the damage has to be estimated for a single structure then the depth exposure of each structure must be estimated. In the present research depth has been estimated for the entire village as mean depth and not for each structure, hence damage cannot be calculated correctly at structure level.

The damage was estimated based on two methods. In the first method flood depth and the damage equation was used. The correlation of depth with duration has been established earlier, hence duration has not been considered. In the second method, the vulnerability indices for flood duration and depth have been used to estimate damage.

4.4.3.6. Damage estimation of agriculture

Vulnerability indices were computed based on survey data. Damage for the entire study area was determined based on area of agriculture estimated by supervised classification of Landsat 8 data and the yields and costs of different crops obtained during survey.

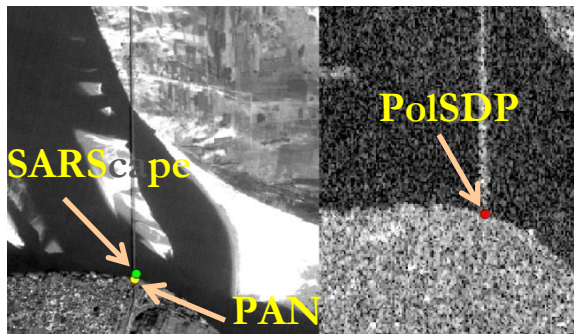
5. RESULTS AND DISCUSSION

5.1. Speckle Reduction in RISAT-I Data

5.1.1. Evaluation of SLC processing software for backscatter generation

The results of the approaches to generate a backscatter image viz. Using PolSDP, SARscape and manual using band math tool from ENVI are as shown Figure 5.1 and Table 5.1.

Table 5.1 Positional accuracy of PAN, SARscape



Reference Point	DISTANCES FROM PAN (m)		
	PAN	SARscape	PolSDP
1	0	158	2568
2	0	64	2615
3	0	59	2565
4	0	57	2421
5	0	44	2641

Figure 5.1 Positional accuracy of PAN, SARscape and PolSDP in terms of distances in m.

It is observed that the positional accuracy of images geocoded /processed using SARscape is increasing in the range direction, while the positional inaccuracies of PolSDP do not appear to be related to any direction. The positional accuracy of images geocoded/processed using PolSDP is around 2562 m.

By close visual examination, it was observed that there was least speckle in the image processed manually, while the image geocoded/processed using SARscape had moderate speckles. Images geocoded/processed using PolSDP had the most speckled image. Figure 5.2 shows the visual comparison of images.

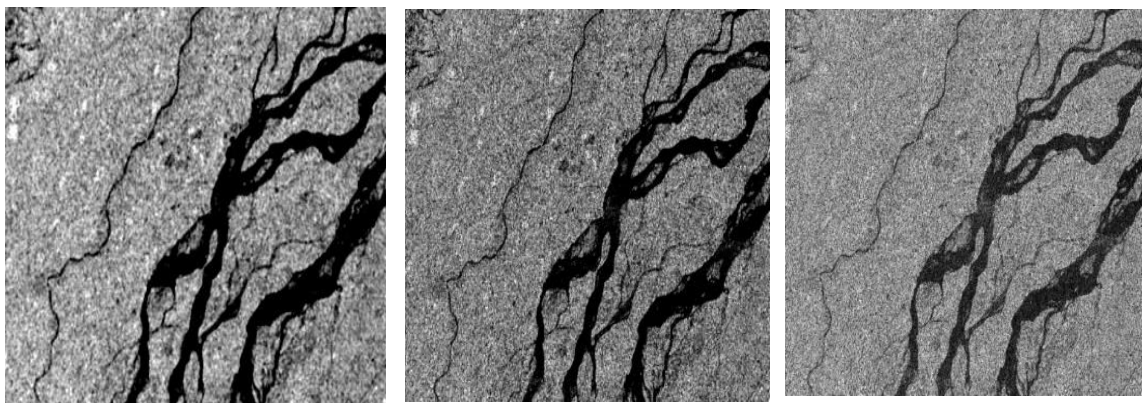


Figure 5.2 SAR images processed using Left – ENVI (manual), Middle –SARscape, Right-PolSDP

5.1.2. Evaluation of filters

The results of various performance measures for the entire image shown at Figure 4.2 are as follows.

5.1.2.1. Mean Square Error

Table 5.2 shows the MSE of different filters with varying moving window sizes and the relative ranks of each combination based MSE values. MSE value is an indicator to the extent of changes that the image has undergone as a result of application of speckle filter. It is observed that Lee (7×7) and Frost (7×7) filters have very low MSE, indicating their effectiveness in preservation of features. Local Region (7×7), Gamma Map (7×7) and Lee Sigma (7×7) have the highest values indicating the poor performance in preservation of features.

Table 5.2 Mean Square Error and relative ranks of different speckle filter combinations

	MSE			Rank		
	3×3	5×5	7×7			
Lee Sigma	0.0059	0.0110	0.0140	7	9	11
Lee	0.0021	0.0016	0.0009	4	3	1
Frost	0.0032	0.0025	0.0014	6	5	2
Local Region	0.0075	0.0186	0.0244	8	13	15
Gamma MAP	0.0113	0.0171	0.0209	10	12	14

5.1.2.2. Signal-to-Noise Ratio

Table 5.3 shows the SNR values. SNR gives the strength of the pure signal or image, as compared to the noise present which is removed by the filter (Senthilnath et al., 2013). Higher the values better is the reduction of noise. It is seen that Lee filter is performing well in all the moving window sizes. SNR is a global measure, thus it does not measure local variations.

Table 5.3 Signal-to-Noise Ratio and relative ranks of different speckle filter combinations

	SNR			Rank		
	3×3	5×5	7×7			
Lee Sigma	10.592	5.308	2.814	5	10	12
Lee	16.139	12.594	11.223	1	3	4
Frost	15.250	10.312	7.914	2	6	8
Local Region	7.072	2.021	-0.397	9	13	15
Gamma MAP	8.553	3.797	1.540	7	11	14

5.1.2.3. Speckle Suppression Index (SSI) and Speckle Mean Preservation Index (SMPI)

Table 5.4 and Table 5.5 show SSI and SMPI values respectively along with the relative ranking of each filter combination. A lower value of SSI or SMPI indicates higher proficiency in reduction of speckle. A value of 0, currently not achievable by any of the existing methods, indicates 100% removal of speckle. A SSI or SMPI value of 1 indicates that no speckle reduction has taken place where as a value higher than one, which in reality no filter would produce, indicates that speckle has been added.

When the filters were evaluated over the entire image, both SSI and SMPI gave consistent results. The speckle suppression index value reduces as the window size increases in case of all filters, indicating superior speckle suppression with increase in size of the moving window. The lowest SSI values as well as SMPI values correspond to Gamma-Map (7×7) and Lee Sigma (7×7) filters are indicative of the most effective speckle suppression. The comparative performance of these very filters at 3×3 moving window size is indicative of another perspective. While Gamma-MAP was found to be less efficient in 3×3 window size as compared to 7×7 window size, it was still the most efficient amongst all the filters in size 3×3, however, Lee Sigma is the least effective amongst all the filters in 3×3 window size.

When the effectiveness of the filters was evaluated only on the water surface, which is homogenous and smooth, the values varied but ranking was only marginally different as compared to the evaluation based on entire image. The Gamma-MAP (7×7) was still the most effective with Lee Sigma (7×7) nearly as effective.

Table 5.4 Speckle Suppression Index

	SSI			Rank		
	3 X 3	5 X 5	7 X 7			
Lee Sigma	0.828	0.685	<u>0.590</u>	12	4	1
Lee	0.894	0.821	0.781	13	11	7
Frost	0.904	0.810	0.752	14	9	6
Local Region	0.941	0.802	0.641	15	8	3
Gamma MAP	0.816	0.692	0.608	10	5	2

Table 5.5 Speckle Mean Preservation Index

	SMPI			Rank		
	3 × 3	5 × 5	7 × 7			
Lee Sigma	0.885	0.625	<u>0.524</u>	15	6	3
Lee	0.880	0.811	0.775	13	12	9
Frost	0.881	0.794	0.743	14	11	8
Local Region	0.790	0.621	0.517	10	5	2
Gamma MAP	0.743	0.597	<u>0.505</u>	7	4	1

5.1.2.4. Performance based on changes in Mean and Standard Deviation

For quantitative evaluation of filters, the application of filters should ideally not bring about any change in mean of target image while it should reduce the standard deviation (Mansourpour et al., 2006). Table 5.6 shows a comparison between changes in mean and standard deviations for various filters and window size combinations.

The filters, Gamma (7×7), Local Region (7×7) and Lee Sigma (7×7) were most effective in reducing the standard deviation but at a considerable cost of change in mean thereby implying that the filters have reduced speckle considerably but have also caused considerable loss meaningful data. On the contrary, Frost (7×7) filter made the least change in the mean while reducing the standard deviation moderately at 25.95%. Lee Sigma (5×5) provides a fair balance by reducing the standard deviation without seriously affecting the mean.

The comparison of change in mean and standard deviation is as shown graphically at Figure 5.3 and Figure 5.4.

Table 5.6 Mean and standard deviation changes on application of filters

	Filter	Mean	SD	Percent Change - Mean	Percent Change - SD
	Unfiltered Image	0.113	0.131		
1	Gamma MAP 7 X 7	0.092	0.065	18.58%	50.38%
2	Local Region 7 X 7	0.089	0.066	21.24%	49.62%
3	Lee Sigma 7 X 7	0.099	0.068	12.39%	48.09%
4	Gamma MAP 5 X 5	0.096	0.077	15.04%	41.22%
5	Lee Sigma 5 X 5	0.102	0.081	9.73%	38.17%
6	Local Region 5 X 5	0.095	0.088	15.93%	32.82%
7	Gamma MAP 3 X 3	0.102	0.096	9.73%	26.72%
8	Frost 7 X 7	0.112	0.097	0.88%	25.95%
9	Lee 7 X 7	0.112	0.101	0.88%	22.90%
10	Lee Sigma 3 X 3	0.107	0.103	5.31%	21.37%
11	Frost 5 X 5	0.111	0.104	1.77%	20.61%
12	Lee 5 X 5	0.112	0.106	0.88%	19.08%
14	Frost 3 X 3	0.110	0.115	2.65%	12.21%
13	Lee 3 X 3	0.111	0.115	1.77%	12.21%
15	Local Region 3 X 3	0.106	0.115	6.19%	12.21%

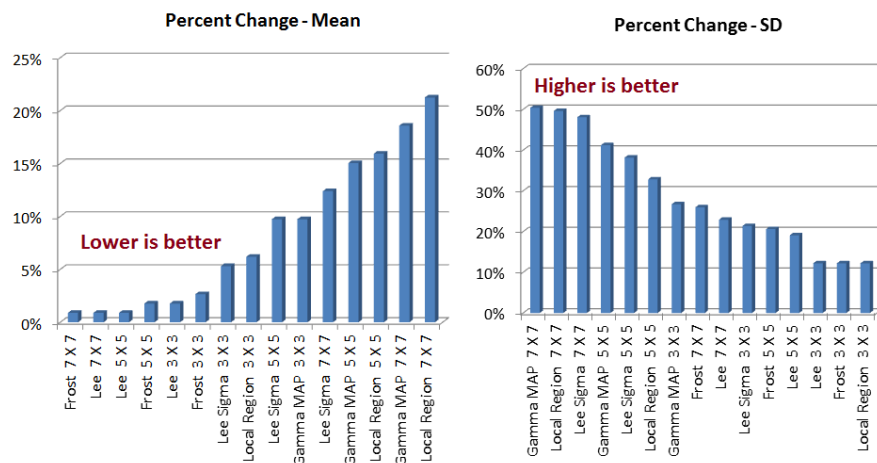


Figure 5.3 Percentage change in mean and standard deviation due to each filter

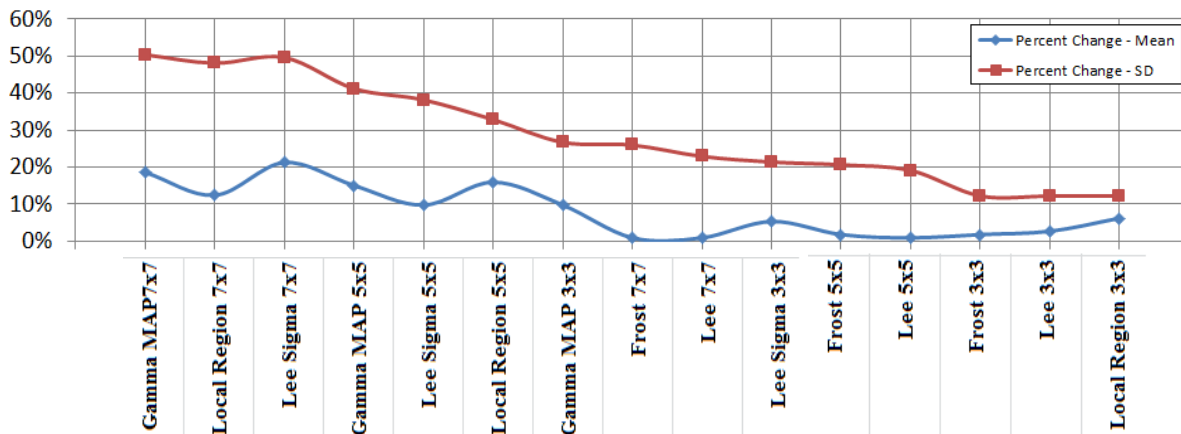


Figure 5.4 Graph - Percentage change in mean and standard deviation due to each filter

The performance of various filters was also measured for only water bodies. The method of measurement was exactly the same as that followed for the entire image. The values of different measure and the change in rankings between the entire image and the water bodies are given in Annexure 9.

From the table given in Annexure 9, it is observed that there is insignificant change in performance efficiency of filters when tested specifically for water bodies. This indicates the observations and deductions based on measures comprising MSE, SNR, SSI and SMPI will equally apply to water bodies as well.

A comparison of change in Mean and Standard Deviation was also carried out for water bodies. The results are as shown at Table 5.7. Frost (7×7) made no changes to mean at all while it reduced the standard deviation by 42.86%. Even when the entire image was considered, Frost (7×7) filter had resulted in a minimal change in mean at 0.88%, reduction in standard deviation by 25.95%.

Table 5.7 Mean and standard deviation changes on water bodies only.

	Filter	Mean	SD	Percent Change - Mean	Percent Change - SD
	Unfiltered Image	0.008	0.007		
1	Gamma MAP 7×7	0.006	0.003	25.00%	57.14%
2	Frost 7×7	0.008	0.004	0.00%	42.86%
3	Lee Sigma 5×5	0.007	0.004	12.50%	42.86%
4	Gamma MAP 5×5	0.007	0.004	12.50%	42.86%
5	Lee Sigma 7×7	0.007	0.004	12.50%	42.86%
6	Local Region 5×5	0.007	0.004	12.50%	42.86%
7	Local Region 7×7	0.006	0.004	25.00%	42.86%
8	Frost 5×5	0.008	0.005	0.00%	28.57%
9	Gamma MAP 3×3	0.007	0.005	12.50%	28.57%
10	Lee 5×5	0.008	0.005	0.00%	28.57%
11	Lee 7×7	0.008	0.005	0.00%	28.57%
12	Lee Sigma 3×3	0.007	0.005	12.50%	28.57%
13	Frost 3×3	0.008	0.006	0.00%	14.29%
14	Lee 3×3	0.008	0.006	0.00%	14.29%
15	Local Region 3×3	0.007	0.006	12.50%	14.29%

When the entire image, earlier filtered using Frost (7×7), was subjected to second iteration pass of the same filter, the change in mean as compared to original unfiltered image is shown in Table 5.8. The gain of reduced standard deviation is not commensurate with the loss of data as indicated by enhanced change in mean. Around 31.30% change in SD was achieved with only 5.31 % change in mean by applying Frost (7×7) in two successive iterations, where as to achieve the same or higher level of change in SD around 9 to 21 % change in mean has to be tolerated if any other combination of filter is applied. This proves the superiority of Frost (7×7) filter in terms of changes in mean and SD during speckle filtering process.

Table 5.8 Mean and standard deviation changes on second pass

	Percent change - Mean		Percent Change - SD	
	1 st Pass	2 nd Pass	1 st Pass	2 nd Pass
Frost 7×7	0.88%	5.31%	25.95%	31.30%

It can be reasonably inferred that using the yardstick of mean and standard deviation, Frost (7×7) filter reduces speckle with least loss of original data.

5.1.2.5. Visual examination

Visual examination was carried out by observation of chosen pixels with a view to ascertain removal of speckle, contamination due to alteration, loss of details and preservation of features.

Annexure 10 shows preview of different filters in window size 3×3 and 7×7 .

It is observed that regardless of which filter is used, 3×3 window size retains the edges much better than window size 7×7 . Larger window size results in loss of edges.

Lee, Lee Sigma and Frost retained edges as well as fine details. It was not possible to grade them visually since the variation was nor perceivable. Local Region and Gamma MAP clearly resulted in loss of edges and details.

Higher window size smoothed the image and reduced the speckle more effectively as compared to smaller window size. Local Region, Gamma MAP, Lee Sigma appeared to reduce filter most effectively. Other filters did reduce the speckle but not the extent of Local Region and Gamma MAP filters. The filters which reduced speckle effectively also resulted in considerable loss of meaningful data.

Frost (7×7) is a reasonable trade-off between degree of speckle reduction and data loss.

5.2. Flood Intensity and Exposure Analysis

5.2.1. Estimation of Flood Extents

The T_{\min} , T_{\max} and final radiometric threshold values used for flood mapping in the study area are as shown in Table 5.9. Figure 5.5 shows the fuzzy region between T_{\min} , T_{\max} and the threshold values of Medium Resolution SAR (MRS) images. The Coarse (CRS) images are not included since their backscatter range of values is different.

Table 5.9 Radiometric threshold values used for flood mapping of SAR images

ID	Date	Scene	Polarisation	T_{\min}	T_{\max}	Threshold Value for Flood Delineation
1	17 Jul 13	6742_1_14	HH	-44.201	-6.767	-14.23
2	31 Jul 13	6961_1_1	RH	1515	2989	2511.00
3	04 Aug 13	7021_1_6	HH	-42.657	-8.185	-16.62
4	11 Aug 13	7119_1_14	HH	-37.765	-15.616	-18.13
5	30 Aug 13	7413_1_4	RH	-40.119	-5.228	-12.25
6	05 Sep 13	7496_1_14	HH	-34.016	-10.439	-13.18
7	07 Sep 13	7534_1_1	RH	1436	3078	2583.00
8	22 Sep 13	7760_1_1	RH	-34.627	-4.737	-10.32
9	30 Sep 13	7873_1_14	HH	-38.341	-8.089	-12.50
10	05 Oct 13	7956_1_3	RH	1327	3061	2576.00
11	25 Oct 13	8250_1_14	HH	-28.243	-6.088	-13.01

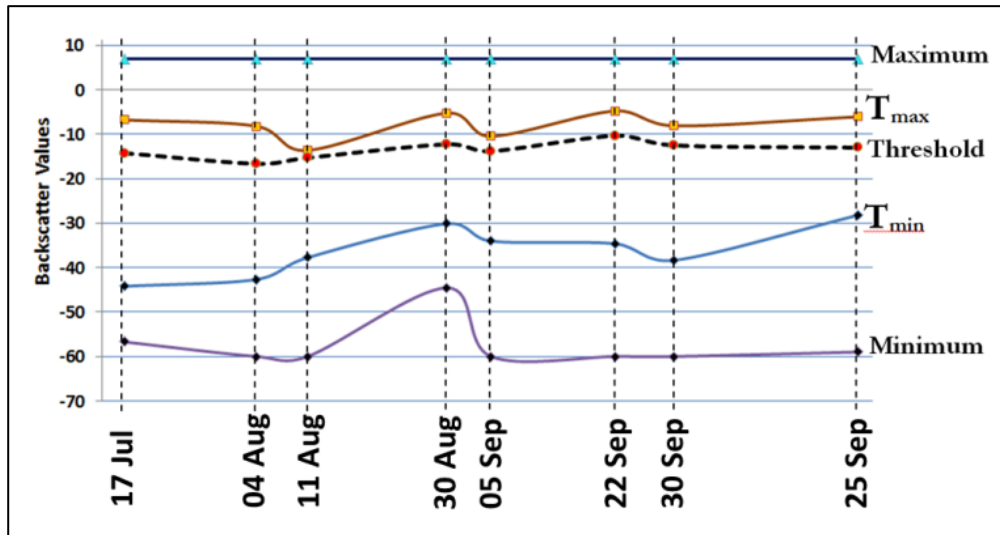


Figure 5.5 Fuzzy region and threshold for Medium Resolution SAR (MRS) images

It can be observed from the graph at Figure 5.5 that the fuzzy region is very wide and choice of threshold in these cases was primarily based on close visual examination and maintaining connectivity of flood pixels.

The flood extent, mapped using thresholds mentioned in Table 5.9, are shown in Figure 5.6 for each date.

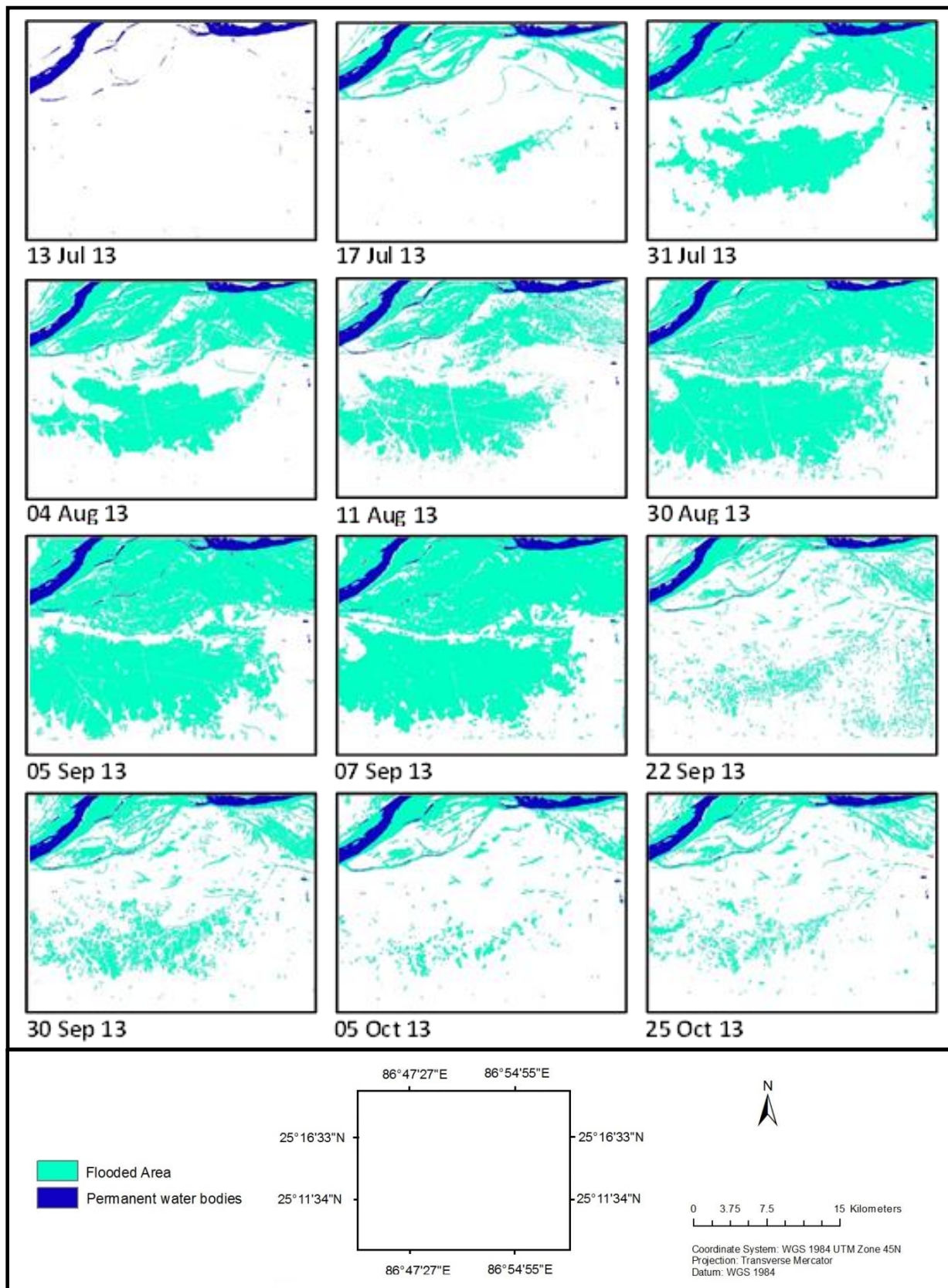


Figure 5.6 Date wise flood extents

Figure 5.7 shows the progressive flooding area. The inundation in the study area commenced between 13-17 Jul 2013. It increased gradually and peaked on 05 Sep 2013 i.e. 45 days of initial onset of flood. The flood recession continued till 22 Sep 2013 after which there was slight inundation once again.

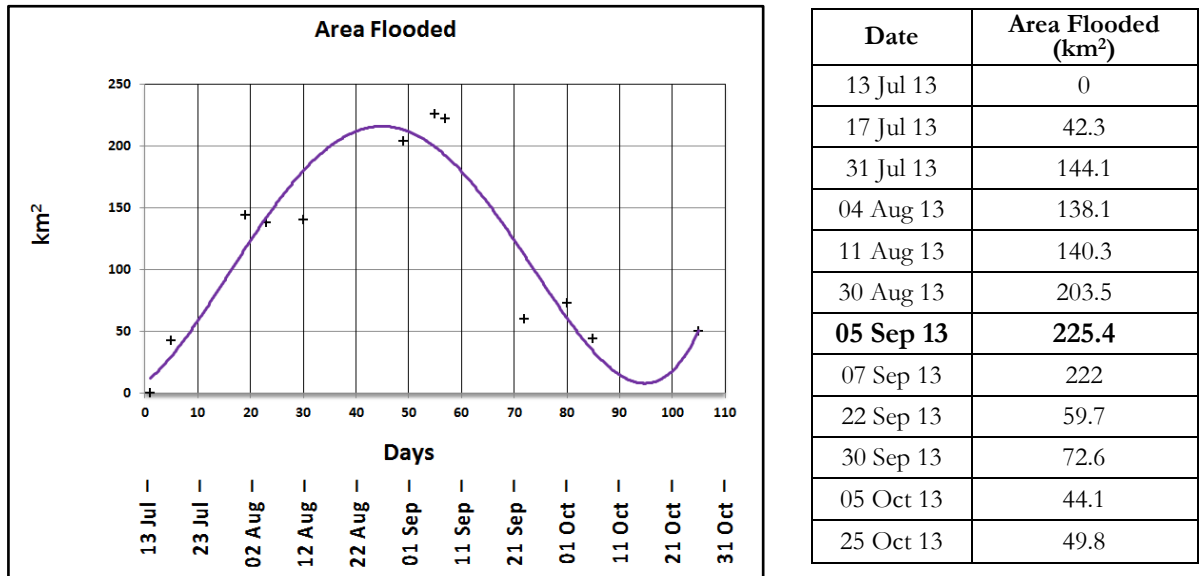


Figure 5.7 Area flooded

5.2.1.1. Validation of Flood Extent

Flood extent was validated using the exact location of maximum flood extent at six points obtained during field visit. At field, these points were identified on Google Earth and their coordinates obtained. Using the same coordinates the points were located on SAR data. The positional accuracy of Google Earth has been compared to 21 GCPs obtained using DGPS. The RMSE of horizontal position of Google Earth was found to be 1.09 m in X direction and 1.75 m in Y direction respectively. The error in flood extent identified during field and the obtained by radiometric thresholding was ~42 m i.e. 5 pixels. Since the ground has a very gradual slope this distance would not result in any major change in depth, hence the estimated flood extent was acceptable. Validation was also carried out comparing extents of LANDSAT 8 image of 08 Sep 13 and flood extent of 07 Sep 13. The comparison is as shown in Figure 5.8. There is a variation of 4-5 pixels which may be explained by the changes over a single day.

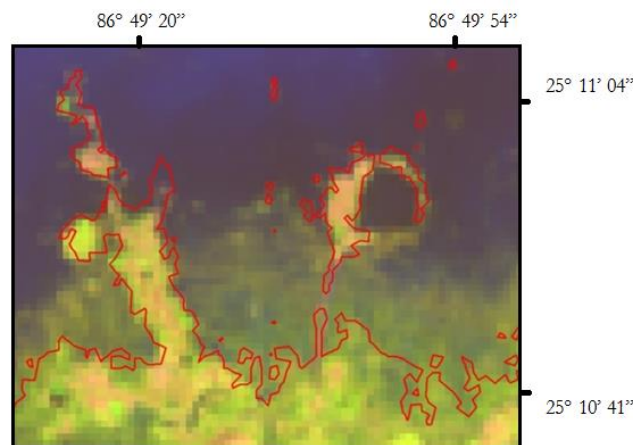


Figure 5.8 Flood extent mapped using RISAT-I (07 Sep 13) image and overlaid on LANDSAT8 image (08 Sep 13)

5.2.1.2. Flood Duration Map

The flood duration map classified according to the classes mentioned in Section 4.3.7 is shown at Figure 5.9.

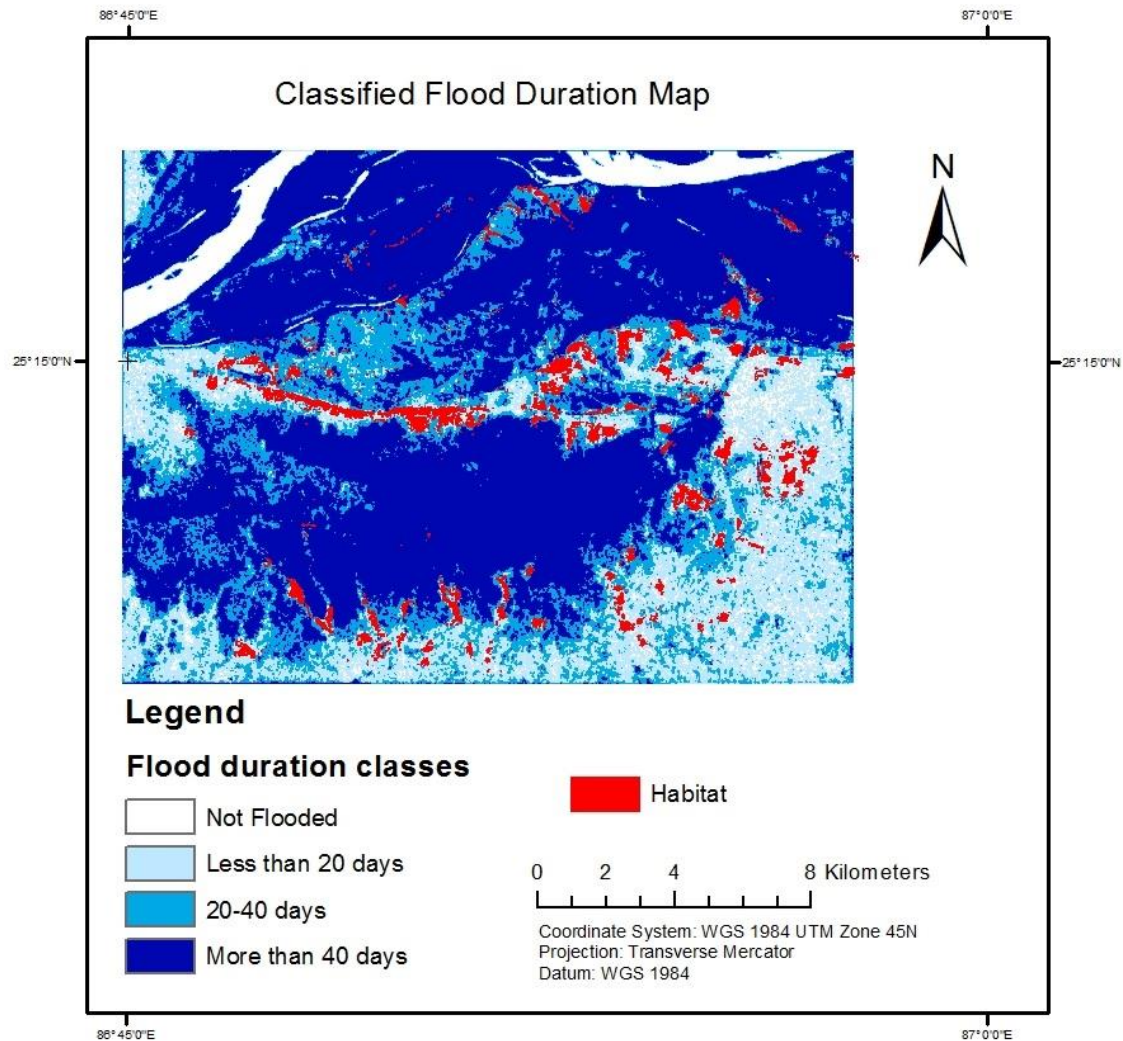


Figure 5.9 Classified flood duration map

5.2.2. Generation of Accurate DEM

Out of 22 GCPs processed, 21 GCPs had horizontal precision and vertical precision better than the acceptable specified limit of 10 cm and 20 cm respectively. The horizontal precision of one GCP was 13 cm and was thus rejected. In total 21 GCPs were used for further processing including the base station point. The processing summary is given in Annexure 11.

Out of total 21 GCPs, four GCPs resulted in high RMSE hence were not used. Of the remaining 17 GCPs, 13 GCPs were used as control points and 4 were used as check points for validation. The spatial distribution of checkpoints is shown at Figure 5.10.

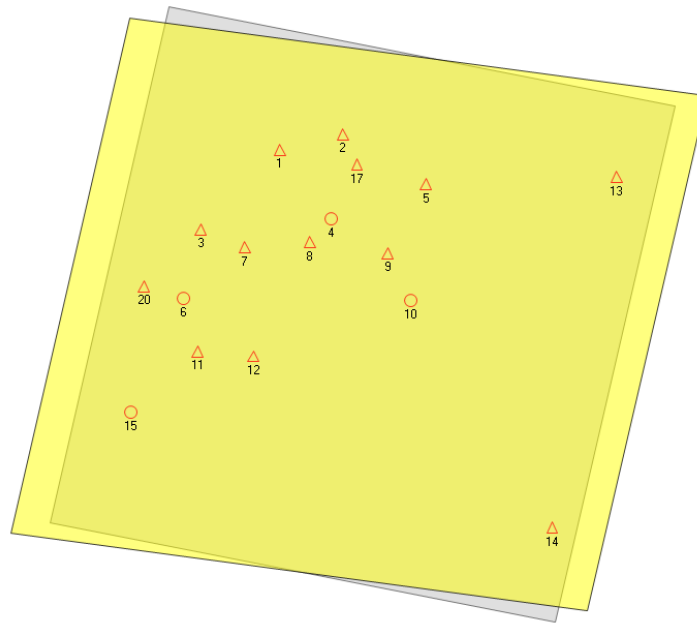


Figure 5.10 Control (Δ) and check points (o) for DEM generation

In addition to 13 GCPs, 1466 automatically generated tie points were also used to enhance accuracy. The resulting DEM and an orthorectified image of the area are shown at Figure 5.11.

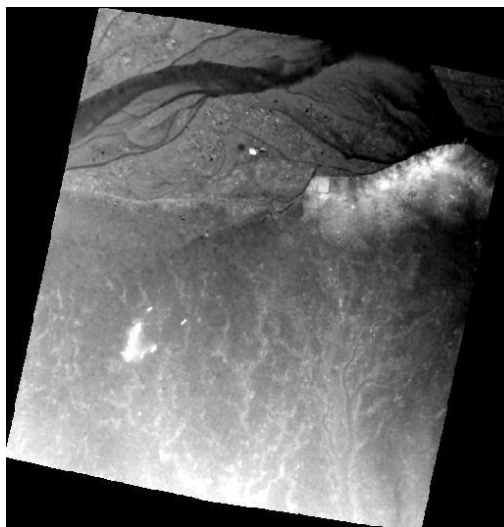


Figure 5.11 DEM generated from CARTOSAT Stereo Ortho kit dated 16th March 2008

5.2.2.1. Accuracy Assessment of DEM

Detailed report on accuracy assessment of GCPs is given in Annexure 12.

The RMSE of the GCP photo-coordinates are as shown in Table 5.10. Since all the values, are less than a pixel size, it implies that the unknown parameters have been computed accurately.

Table 5.10 RMSE of GCP photo coordinates

Image	rmseX	rmseY	rmseX	rmseY
AFT	0.366	0.0	0.412	0.0
FORE	0.414	0.557	0.489	1.218

Table 5.11 gives a summary of RMSEs of Control and Checkpoints. Number of observations is given in parenthesis.

Table 5.11 Summary of RMSEs of control and check points

	RMSE	
	Control Point	Check Point
Ground X	0 (13)	2.4832 (4)
Ground Y	0 (13)	2.3474 (4)
Ground Z	0 (13)	2.7174 (4)
Image X	0.4542 (26)	0.39008 (8)
Image Y	0.9469 (26)	0.00039 (8)
Total Image RMSE:		0.2506

The total Image RMSE was 0.251 m. This indicates that the residuals within the observations were adequately minimised. Since the RMSE is less than 2.5 m (1 pixel), the quality of aerial triangulation was acceptable.

The measured and computed elevation of control and check points is given in Annexure 13. The RMSE of elevation using four check points was 2.72 m and the horizontal accuracy was 2.48 m and 2.35 m in X and Y direction respectively. In an accuracy assessment by (Bhardwaj, 2013) using similar data and method, using 12 control GCPs and 6 check points, the vertical accuracy was assessed at 3.72 m while the horizontal accuracy was assessed at 2.08 m and 1.74 m in X and Y direction respectively. The variation of comparatively lower accuracy assessed by Bhardwaj, (2013) may be explained by the partial hilly terrain of his study area.

5.2.3. Flood Depth

Classified flood depth map is shown in Figure 5.12. The correction of flood water slope was not applied as the slope determined through interpolation was found to be insignificant as the flood depth was further generalisation by classification. It can be logically inferred that the flood water slope was low because the flood depth map was prepared based on maximum flood level on 05 Sep 13. The flood level on 07 Sep 13 clearly shows reduction in flood extents. This would therefore be the time when the slope in flood waters would be the lowest.

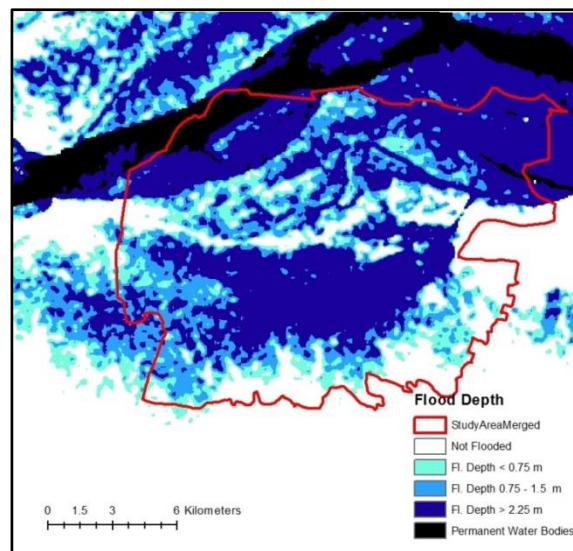


Figure 5.12 Classified flood depth map

5.2.3.1. Validation of Flood Depth

Flood depth was validated using ground truth. During field survey, marks of the recent flood were clearly observed most of the buildings indicating maximum flood level. Seven flood levels were measured using flood level marks on buildings. The reference benchmark was the DGPS. Since the DGPS was kept away from the building a water level was used to ensure the level is same. The exact flood heights were known after post-processing of DGPS data. These depths thus obtained, were compared to the depths obtained from DEM processed using GCPs. The RMSE was 1.71 m which was better than the acceptable accuracy of CARTOSAT-I DEM.

5.2.4. Flood Depth-Duration Map

The flood depth-duration map classified in all possible combinations of depth and durations i.e. nine classes as mentioned in Section 4.3.7 is shown in Figure 5.13. It is observed that the study area has all the three combinations of depth and duration. However the study area is dominated by depth class 2 and 3 and duration class 2 and 3. There are fewer areas where the depth is high yet the duration is low and vice versa. There is a clear co-relation between depth and duration.

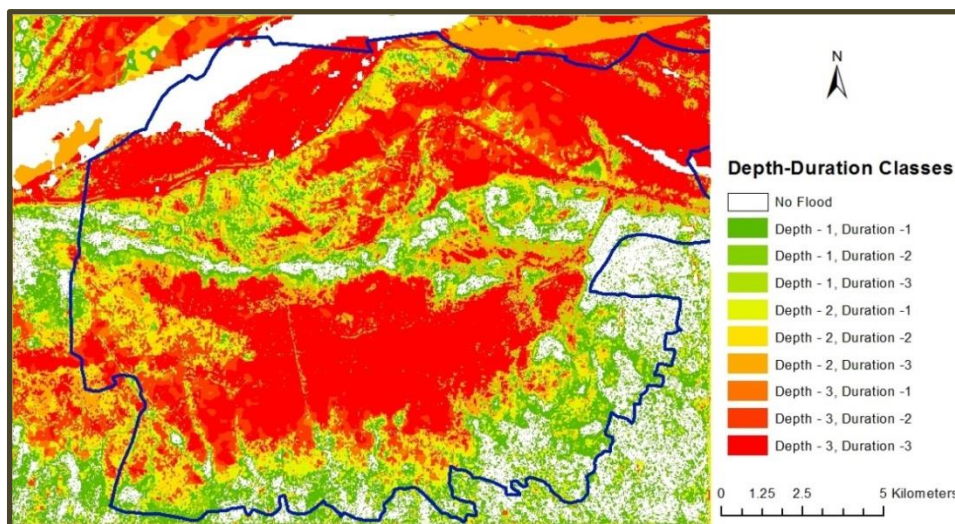


Figure 5.13 Flood depth-duration classified map

5.2.5. Exposure Analysis

5.2.5.1. Habitat Structures

Figure 5.14 shows the village boundaries and the habitat structures.

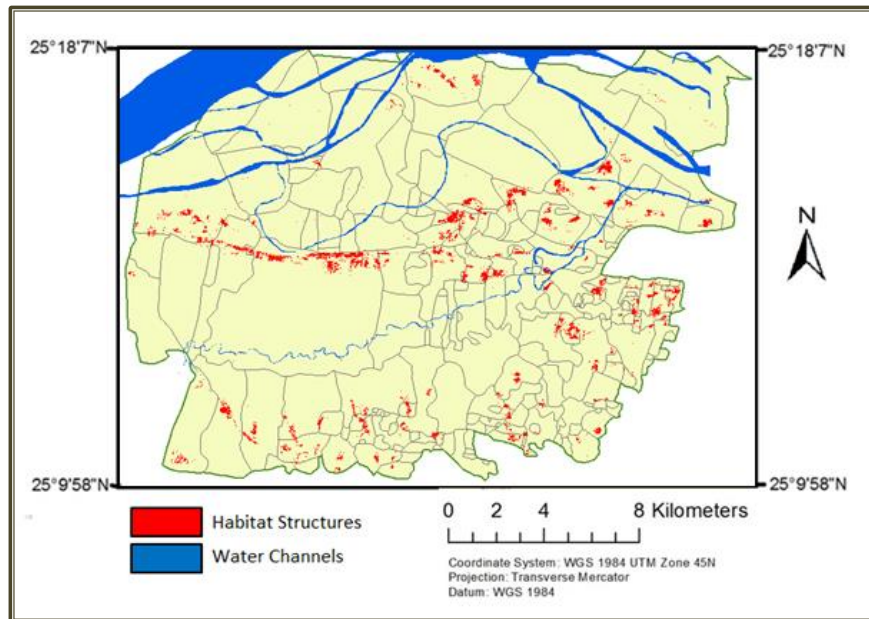


Figure 5.14 Village boundaries and habitat structures

Figure 5.15 shows the exposure of habitat structures to varying classes of flood depth and duration.

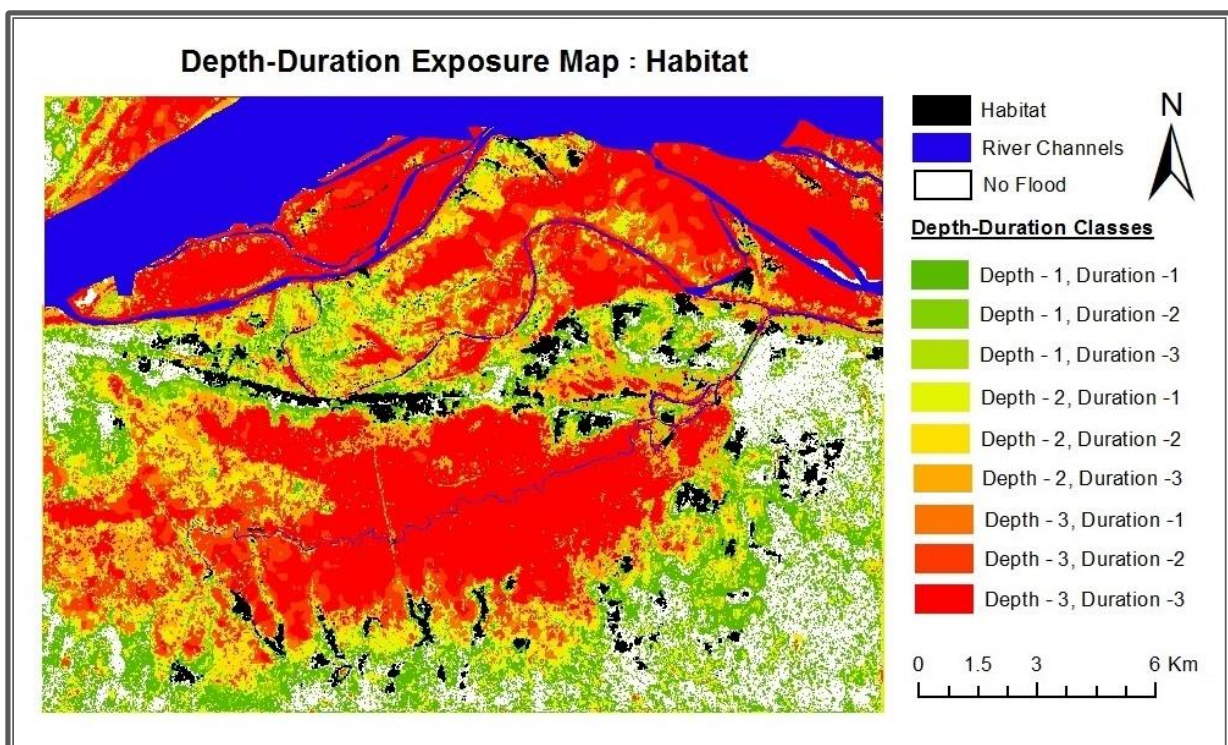


Figure 5.15 Exposure of habitat to varying flood depth and duration classes

Figure 5.16 shows the exposure of habitat to different depth and duration classes at a larger scale.

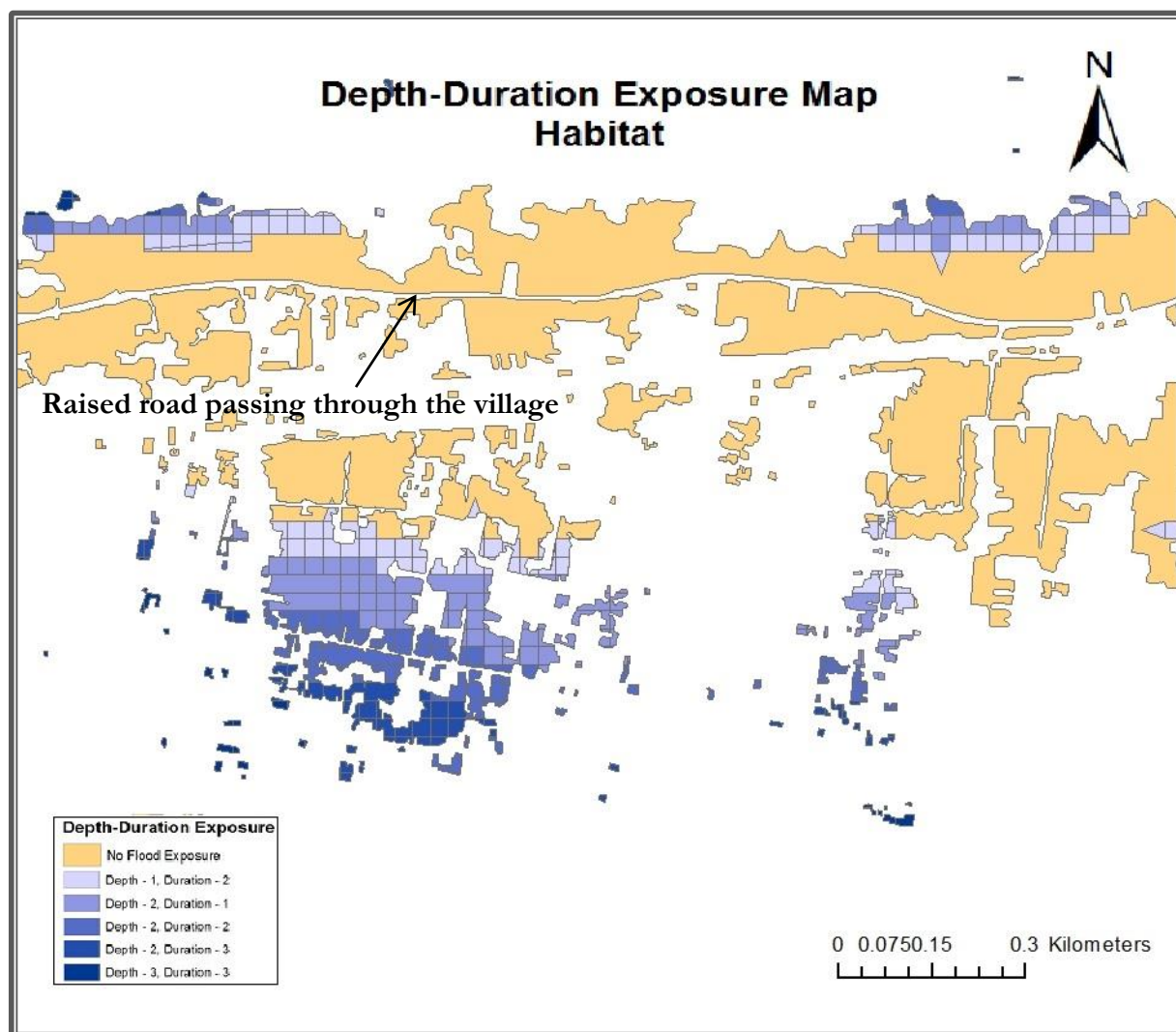


Figure 5.16 Large scale map of exposure of habitat to different depth-duration classes

As per census data which is in the form of figurative database, there are 57602 structures in the study area, out of which 43,849 habitat structures were in flood zone. Table 5.12 shows the number of structures in flood zone. Not all the structures in flood zone were exposed to flood.

Table 5.12 Number of structures in flood zone

Duration Class	% Area of Habitat Exposed	Estimated Number of Structures
Less than 20 days	20.65%	9,056
20 to 40 days	62.79%	27,533
More than 40 days	16.56%	7,260
Total		43,849

Census data classifies the structures into 8 categories based on construction material of roof, wall and floor. Similar classification has also been adopted in the current research. Based on number of each type of structures in a village and the total area of the village habitat, the density of each type of house was estimated. Based on this density and flood exposure the number of each type of house exposed to flood was as shown in Table 5.13.

Table 5.13 Flood exposure to different type of habitat structures

ID	Code	Wall	Roof	Floor	No of Structures exposed to flood
1	A	Burnt Brick – Cement Joined	Concrete	Mud	727
2	B	Burnt Brick – Cement Joined	Tiles	Mud	1,717
3	C	Burnt Brick – Mud Joined	Tiles	Mud	12,085
4	D	Burnt Brick – Mud Joined	Thatch	Mud	1,789
5	E	Thatch with mud plaster	Tiles	Mud	4,590
6	F	Thatch with mud plaster	Thatch	Mud	1,006
7	G	Thatch without mud plaster	Tiles	Mud	867
8	H	Thatch without mud plaster	Thatch	Mud	3,550
Total					26,331

The number of each type of structure and its exposure of different flood depth-duration classes is given in Annexure 14.

5.2.5.2. Agriculture Crops

The study area covers an extent of 237.2 km². Of this, 189.2 km² i.e. 80% was agriculture. A total of 170 km² of agriculture was flooded. Table 5.14 shows the distribution of agricultural land in different flood intensity classes.

Table 5.14 Exposure of agricultural area.
Left - km², Right - Percentage of total agricultural area

Depth Class	Duration Class		
	1	2	3
1	22.8	5.5	2.7
2	15.1	17.6	13.8
3	4.0	17.1	71.5

Area in km²

Depth Class	Duration Class		
	1	2	3
1	13.4%	3.2%	1.6%
2	8.9%	10.4%	8.1%
3	2.3%	10.0%	42.0%

The spatial distribution of exposure of agriculture to varying flood depths. And duration is given at Figure 5.17

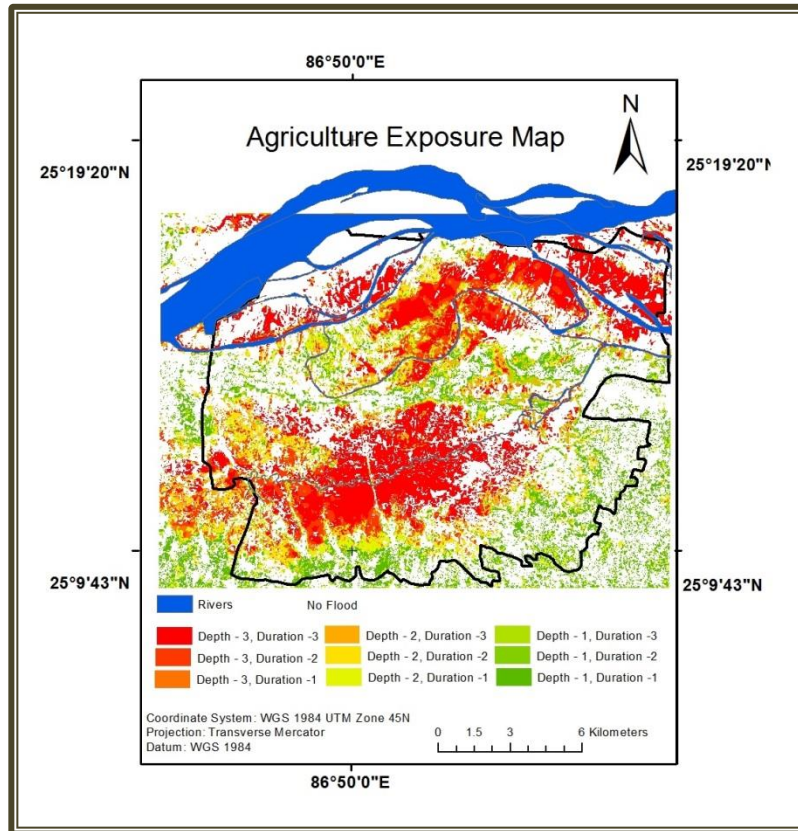


Figure 5.17 Exposure of agriculture to varying flood depth and duration

5.3. Development of Vulnerability Indices and Damage Estimation

5.3.1. Statistical Analysis of Survey Database

The data collected was organised into a database and its extract is given in Annexure 8. The statistical analysis performed to develop vulnerability indices for structures and agriculture is given in subsequent section.

5.3.2. Classification of flood depth and duration

The total number of responses collected was 203. The frequency distribution of depth and duration of samples is as shown at Figure 5.18 and Figure 5.19 respectively.

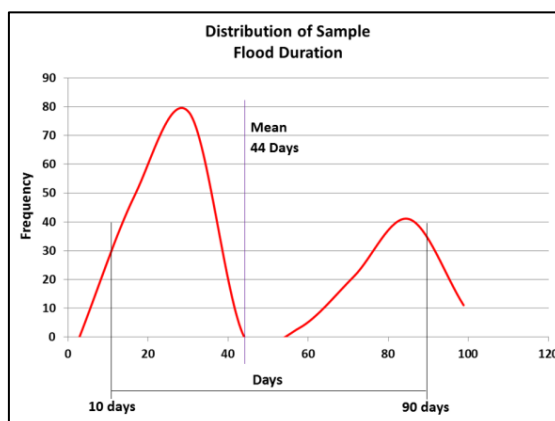


Figure 5.18 Distribution of samples - Flood duration

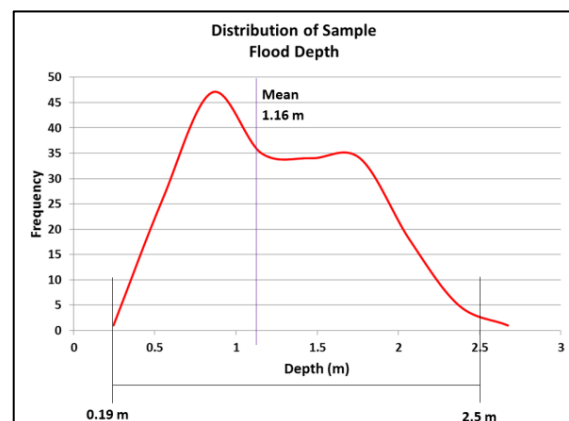


Figure 5.19 Distribution of samples - Flood depth

The distribution of duration at Figure 5.18 is not well distributed, primarily because to low sample size. Keeping in view that structures constructed from mud and straw show considerable vulnerability in durations less than 10 days (Thakur et al., 2012), the classification of flood duration has been made as under.

- Duration Class 1: Less than 20 days
- Duration Class 2: 20 – 40 days
- Duration Class 3: More than 40 days

The distribution of depth at Figure 5.19 has a right skew of 0.28. The distribution indicates fairly well representation of all depth ranges. A suitable classification of depth would thus be as under.

- Depth Class 1 : Less than 0.75 m
- Depth Class 2 : 0.75 m – 1.5 m
- Depth Class 3 : More than 1.5 m

Based on the aforesaid classification of depth and duration, the number of responses collected for each class is shown at Table 5.15.

Table 5.15 Number of samples – Depth and duration

Depth Class	Duration Class			Total
	1	2	3	
1	42	19		61
2	7	46	30	83
3		13	46	59
Total	49	78	76	203

It is observed that there were no samples for depth class 1 in duration class 3 and vice versa. There were only five samples in depth class 2 in duration class 1 which is too low for any meaningful analysis.

5.3.3. Classification of Structures

The floor in the structures in the study area is invariably made of mud. The walls are made up of burnt bricks or thatch. These burnt bricks may be either joined by cement or by mud. The thatch, which is made from split bamboo and sticks or dry grass, may be either plastered with mud or left without it. The roof is made up of concrete, tiles or thatch. The combination of these construction materials results in eight variations. The variations and the numbers of samples for each class based on construction material are given at Table 5.16.

Table 5.16 Variations in structures based on construction materials

ID	Code	Wall	Roof	Floor	No of Samples
1	A	Burnt Brick – Cement Joined	Concrete	Mud	12
2	B	Burnt Brick – Cement Joined	Tiles	Mud	17
3	C	Burnt Brick – Mud Joined	Tiles	Mud	79
4	D	Burnt Brick – Mud Joined	Thatch	Mud	11
5	E	Thatch with mud plaster	Tiles	Mud	32
6	F	Thatch with mud plaster	Thatch	Mud	23
7	G	Thatch without mud plaster	Tiles	Mud	14
8	H	Thatch without mud plaster	Thatch	Mud	15
Total					203

It is observed from Table 5.16 that every house surveyed, had a mud floor but the construction material for roof and wall had variations. Classification of houses is based on their response to flood. Since floor is same for all structures, it will not be the determining factor for vulnerability and hence has not been considered as the basis for classification. Ignoring the floor, there were four types of wall and three types of roof as shown in Table 5.17.

Table 5.17 Types of walls and roof materials

Wall		No of Houses	Roof	No of Houses
Burnt Brick – Cement Joined	BBC	29	Concrete	12
Burnt Brick – Mud Joined	BBM	90	Thatch	49
Thatch with mud plaster	MT	55	Tiles	142
Thatch without mud plaster	Thatch	29	Total	203
Total		203		

The percentage of damage to wall and damage to roof observed through survey data is plotted in Figure 5.20. The figure indicates that the integrity of the roof is maintained for as long as the wall is not damaged. In few structures the roof starts to lose its integrity, when wall is damaged beyond 10% but in most cases the roof starts disintegrating when the wall is damaged beyond 20%. When the wall damage reaches 62% the roof is unable to sustain and is 100% damaged i.e. the entire structure collapses.

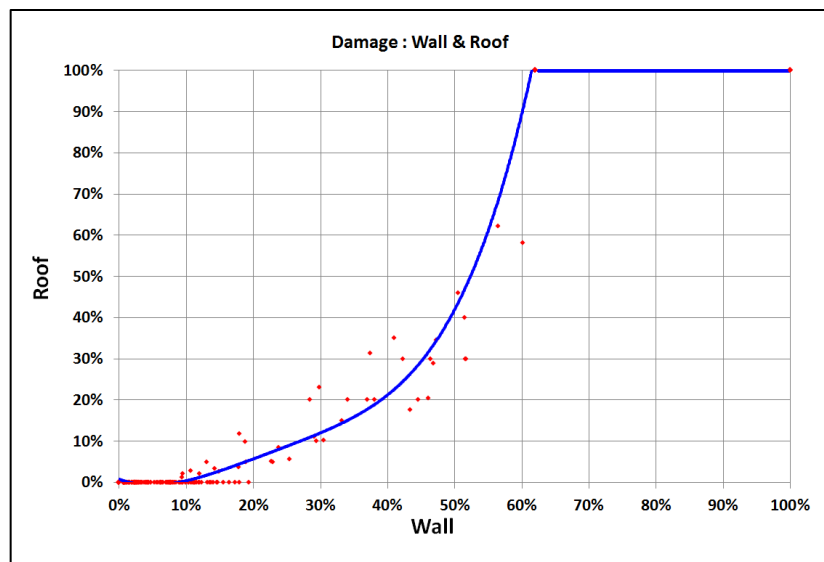


Figure 5.20 Comparative damage - wall and roof derived from survey data

Since at the maximum depth of 2.5m, no structures were fully submerged, it can be conclude that the vulnerability of roof and also the entire structure is directly dependent on the vulnerability of wall. The classification of the structure was therefore based only on damage response of the wall.

Figure 5.21 shows depth damage curve for four types of walls. For ease of comparison, all the four graphs have similar x and y axis scales. It is observed that only Thatch with mud plaster (MT) wall and Thatch without mud plaster (Thatch) wall share similarity in their damage response. Thus, based on the damage response, we can classify the structure types into following three classes for further analysis:-

- Type – I : BBC (Burnt Brick – Cement joined)
- Type – II : BBM (Burnt Brick – Mud joined)
- Type – III : MT & Thatch

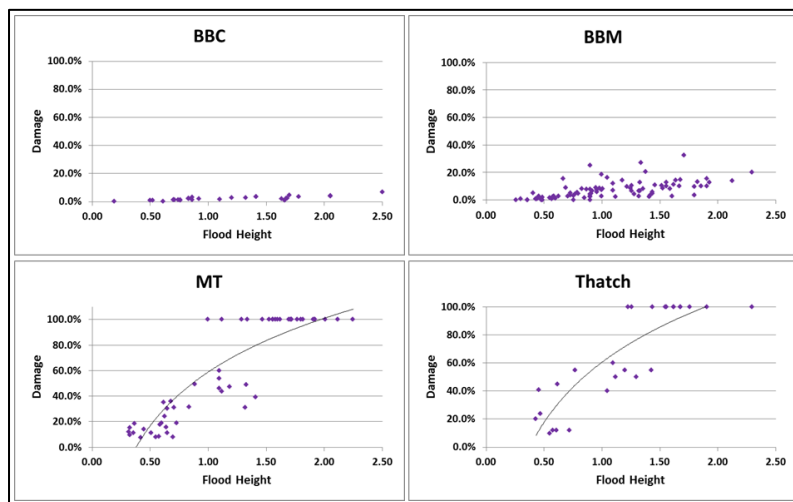


Figure 5.21 Damage response of different types of walls to different flood depths

Figure 5.22 shows different type of wall materials used in the study area for three types of structures.



Figure 5.22 Different types of walls

- Top Left : Type-I, Burnt Brick joined using cement (BBC)
- Top Right : Type-II, Burnt Brick joined using mud (BBM)
- Bottom Left : Type-III, Thatch with mud plaster (MT)
- Bottom Right : Type-III, Thatch without mud plaster (Thatch)

5.3.4. Population and Sample Size

As per census data there are 57,602 structures in the study area. Out of these, 43,849 structures were in flood zone and 26,331 structures were actually affected by flood and hence becomes the population for present study. The distribution of the population and the samples size required for 95 percent confidence level with 5 percent confidence interval and actual samples available in varying flood depth and duration classes for three different structure classes shown at Table 5.18.

Table 5.18 State of survey samples

	POPULATION SIZE [26331]				SAMPLES REQUIRED [4553]				SAMPLES TAKEN [203]			
	Depth Class	Duration Class			Depth Class	Duration Class			Depth Class	Duration Class		
		1	2	3		1	2	3		1	2	3
Type I	1	1559	282	5	1	310	165	5	1	5	3	
	2	153	224	22	2	113	144	19	2		8	4
	3	65	110	29	3	56	86	28	3		3	6
Type II	1	8835	1596	31	1	370	310	29	1	21	3	
	2	868	1268	125	2	267	297	97	2	7	21	17
	3	366	622	166	3	188	236	118	3		5	15
Type III	1	6371	1151	22	1	364	288	21	1	16	13	
	2	626	914	90	2	240	272	73	2		17	8
	3	264	448	119	3	158	207	92	3		5	25

95% Confidence Level

5% Confidence Interval

Even though different structures were classified to benefit from reduced requirement of samples, the samples available still fall short of the minimum requirement to achieve the desired accuracy levels.

5.3.5. Development of Vulnerability Indices – Village Level

As defined in Section and 2.3.1 and 4.4.3.3, the ratio of cost of repairs to the cost of re-construction defines the vulnerability of a structure in the current research. Figure 5.23 to Figure 5.25 show the vulnerability response of the three types of structure in varying flood depths.

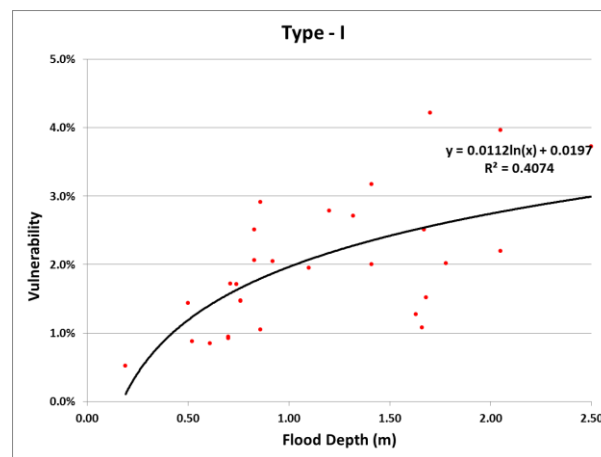


Figure 5.23 Vulnerability response of Type I structure (BBC)

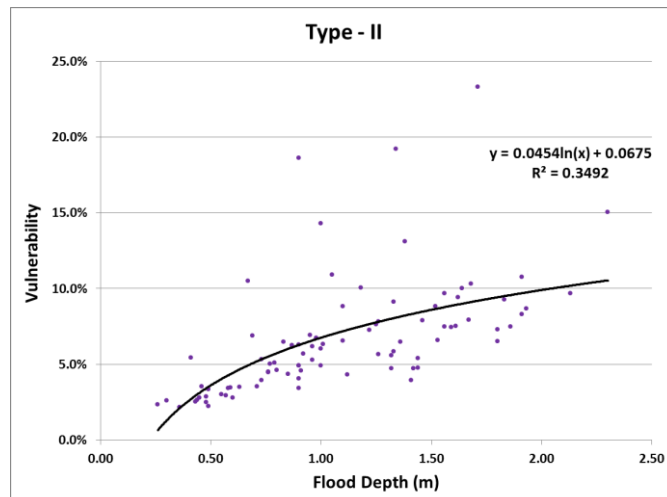


Figure 5.24 Vulnerability response of Type II structure (BBM)

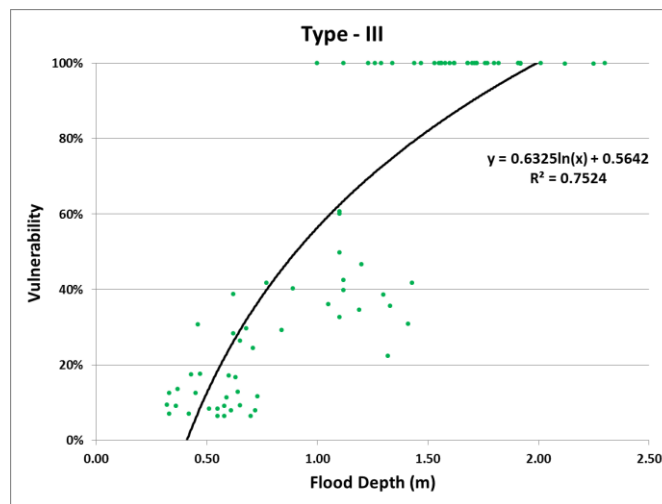


Figure 5.25 Vulnerability response of Type III structure (Thatch)

From the Figures it is observed that Type – I structures are least vulnerable while Type-II are most vulnerable. At maximum depth of 2.5 m, Type – I structure is likely to suffer damage of approximately 3% of its re-construction cost while in the same depth Type-II would suffer a damage of approximately 10%. Type-III structures would suffer 100% damage as a result of total collapse of structure even at 1.25 m of flood depth.

The damage equations for the three types of structures are as shown in Figure 5.19.

Table 5.19 Damage equations for different structure types

Type of Structure	Damage in % for depth = x
Type - I	$0.0112\ln(x) + 0.0197$
Type - II	$0.0454\ln(x) + 0.0675$
Type - III	$0.6325\ln(x) + 0.5642$

Figure 5.26 Monetary Loss for varying flood depths. shows the Monetary Loss suffered for three types of structures in varying flood depths. The flood depth for each sample structure is given in Annexure 8. The monetary loss has been calculated using the repair costs of roof and floor per unit area as given in Annexure 7 and the observed physical damage to roof and wall given in Annexure 8.

It is observed clearly that people who have Type –III structures suffer losses far more than those who own Type –I or Type – II structures.

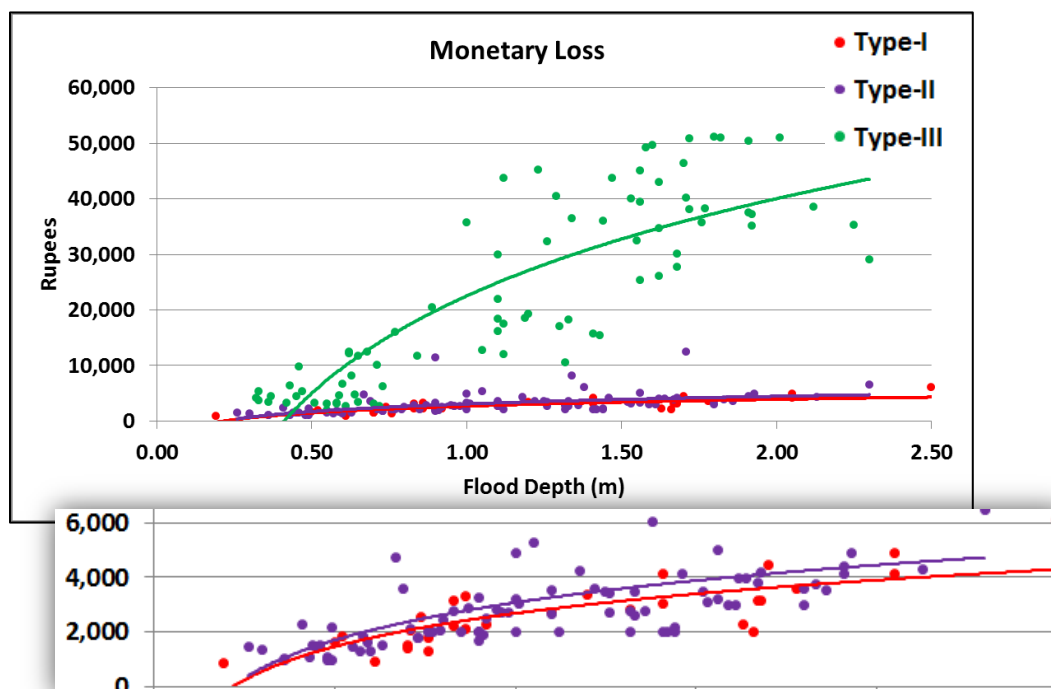


Figure 5.26 Monetary Loss for varying flood depths.

The vulnerability indices based on classification of flood depth and duration are given at Table 5.20..

Since with a small sample size there is high probability of having bias, the vulnerability indices were developed using Jack knife sampling technique (Quenouille, 1956). In this method, first the samples were randomly divided into two groups comprising of $2/3^{\text{rd}}$ and $1/3^{\text{rd}}$ of entire sample size. The randomness was achieved by using RANDBETWEEN function of MS Excel. For each group, a mean was calculated (for each type of structure and for each depth-duration class) after removing one sample. The process of taking mean was repeated, each time replacing the element left out earlier. Once the iterative cycle was complete, a mean of means was obtained as a final value. The process was repeated for each index and also for the $1/3^{\text{rd}}$ set of samples. Some indices have considerable variation. This is explained because of too few samples. The vulnerability indices were also computed using all samples as shown at Table 5.21.

It is observed that as the depth increases, the vulnerability too increases. Similarly, as the duration increases the vulnerability too increases.

Table 5.20 Evaluation of Vulnerability Indices

VULNERABILITY INDICES					VALIDATION OF INDICES				
2/3 rd Samples					1/3 rd Samples				
	Depth Class	Duration Class				Depth Class	Duration Class		
		1	2	3			1	2	3
Type I	1	1.07%	1.13%		Type I	1	1.14%	1.33%	
	2		1.91%	2.67%		2		1.96%	
	3		2.63%	2.42%		3		2.74%	2.42%
Type II	1	3.46%	4.60%		Type II	1	3.47%		
	2	4.72%	7.19%	7.45%		2	4.68%	7.24%	7.23%
	3		8.59%	9.97%		3		8.52%	9.85%
Type III	1	8.98%	21.56%		Type III	1	8.95%	21.54%	
	2		40.10%	100%		2		40.37%	100%
	3		100%	100%		3		100%	100%

Table 5.21 Vulnerability Indices (Complete data)

VULNERABILITY INDICES				
	Depth Class	Duration Class		
		1	2	3
Type - I	1	<u>1.08%</u>	<u>1.20%</u>	
	2		<u>1.93%</u>	<u>2.67%</u>
	3		<u>8.58%</u>	<u>2.42%</u>
Type - II	1	3.47%	<u>7.20%</u>	
	2	<u>4.71%</u>	7.20%	7.39%
	3		<u>8.58%</u>	9.92%
Type - III	1	8.97%	21.55%	
	2		40.16%	100%
	3		100%	100%

5.3.6. Development of Vulnerability Indices – Single Structure

The vulnerability response of different types of structures as defined in Table 5.16 are shown in Figure 5.27.

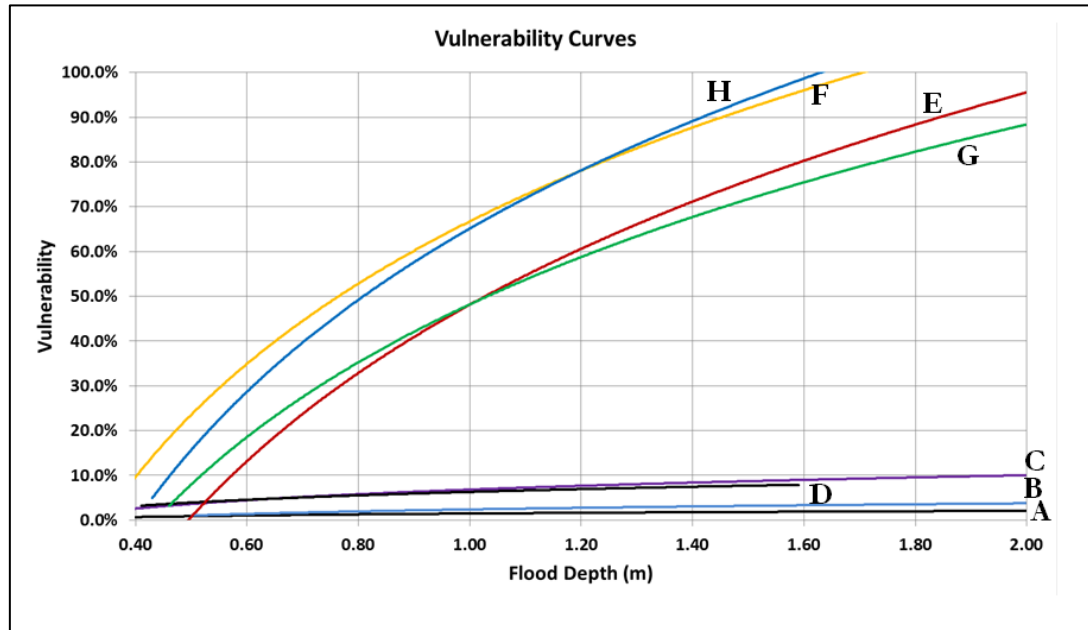


Figure 5.27 Vulnerability response for structures (i.e. A to H)

Table 5.22 Damage equations for structures A to H

Structure	Damage in % for depth = x	R ²
A	$0.0087\ln(x) + 0.0145$	0.5394
B	$0.0197\ln(x) + 0.0236$	0.7273
C	$0.0463\ln(x) + 0.0679$	0.3377
D	$0.0344\ln(x) + 0.0627$	0.6916
E	$0.6843\ln(x) + 0.4814$	0.7727
F	$0.6231\ln(x) + 0.6674$	0.8509
G	$0.5802\ln(x) + 0.4819$	0.5775
H	$0.7135\ln(x) + 0.6514$	0.9398

It is observed that structures A and B have similar vulnerability. Structures C and D too are similar but more vulnerable than A and B. The variation is explained by the joining material used. Structures C and D are more vulnerable than A and B because, C and D are joined by mud, which is easily removed by the flowing water causing damage to the structure. But even though the walls in case of C and D may collapse, the vulnerability variation as compared to A and B is not large because the re-construction cost is low as the bricks can be re-used and the cost of joining material i.e. mud is also low. Structures E, F, G and H are very vulnerable to flood depth. Structures F and H are the most vulnerable. Structures E and G, even though they are made of Thatch with tiled roof are less vulnerable because after the flood, the tiles would still be reusable thus reducing the cost of re-construction.

Vulnerability Indices for all type of structures based on varying flood depths and duration is as shown in Table 5.23.

Table 5.23 Vulnerability Indices for structures A to H

VULNERABILITY INDICES - SINGLE STRUCTURES							
Floor	Wall	Roof	Code	Depth Class	Duration Class		
					1	2	3
Mud	Burnt Brick - Cement Joined	Concrete	A	1	0.70%	0.93%	
				2		1.05%	2.00%
				3		1.27%	2.11%
Mud	Burnt Brick - Cement Joined	Tiles	B	1	1.33%	1.72%	
				2		2.06%	2.89%
				3		3.36%	3.96%
Mud	Burnt Brick - Mud Joined	Tiles	C	1	3.29%	5.42%	
				2	4.61%	7.18%	7%
				3		9%	10%
Mud	Burnt Brick - Mud Joined	Thatch	D	1	4.54%	2.95%	
				2	4.97%	7.64%	6.56%
				3		8.14%	
Mud	Thatch with Mud Plaster	Tiles	E	1	7.63%	20.28%	
				2		38.43%	
				3		100.00%	100.00%
Mud	Thatch with Mud Plaster	Thatch	F	1	10.76%	18.59%	
				2		29.18%	100%
				3		100%	100%
Mud	Thatch without Mud Plaster	Tiles	G	1	7.85%	30.74%	
				2		41.20%	100.00%
				3			100.00%
Mud	Thatch without Mud Plaster	Thatch	H	1	8.74%	24.57%	
				2		60.57%	100.00%
				3		100.00%	100.00%

5.3.7. Damage Estimation – Study Area

The damage was estimated based on two methods. In the first method flood depth and the damage equation was used. The correlation of depth with duration has been established in Section 5.2.4, hence duration has not been considered. In the second method, the vulnerability indices for flood duration and depth have been used to estimate damage.

5.3.8. Method I : Estimation of Damage using Damage Equation and Depth

The number and type of structures exposed to varying flood depths of exposure was determined earlier as elaborated in Chapter 3 and is given in Annexure 15. The depth exposure to structures in a village was taken as the mean depth of the habitat area that was exposed to flood in the village. The coefficients and constant values of damage equations for different structures as determined from damage curves at Figure 5.27 are as given at Table 5.24.

Table 5.24 Damage equation coefficients and constant values

Structure	Damage Equation		Structure	Damage Equation	
	Coefficient	Constant		Coefficient	Constant
A	0.0087	0.0145	Type – I	0.0112	0.0197
B	0.0197	0.0236			
C	0.0463	0.0679	Type – II	0.0454	0.0675
D	0.0344	0.0627			
E	0.6843	0.4814	Type – III	0.6325	0.5642
F	0.6231	0.6674			
G	0.5802	0.4819			
H	0.7135	0.6514			

The damage equation for total damage in Rupees to structures in the study area is given by

$$\sum_{v=1}^{v=N} \sum_{t=1}^{t=n} n_t A \alpha_t (k_t \ln(x_v) + c_t)$$

Where,

N = Number of villages exposed to flood in study area (from Annexure 15)

n = number of structures of each type in each village (from Annexure 15)

A = Average area of structure (41.7 m² for all villages in the current study area – Field Survey)

α = Cost of re-construction per m² (from Annexure 6)

k = Coefficient of damage equation (from Table 5.24)

c = Constant value of damage equation (from Table 5.24)

x = Average depth exposure of village (from column 3 of Annexure 15)

The total estimated monetary damage to the structures in study area was ₹ 17.865 Crore or ₹ 178.65 million. As given at Table 5.25. List of Villages along with the structure wise damage is given in Annexure 16.

Table 5.25 Monetary Damage in ₹ (Crores/10 Millions)

Structure	Damage
A	0.152
B	0.334
C	2.941
D	0.366
E	6.300
F	1.834
G	1.039
H	4.899
Total Damage	17.865

Figure 5.28 shows the average loss per house hold. In some villages there is no habitat at all (only agriculture fields exist) hence there is no structural damage. While calculating damage, households who did not suffer any damage at all were excluded. Figure 5.29 shows the percentage of habitat damaged.

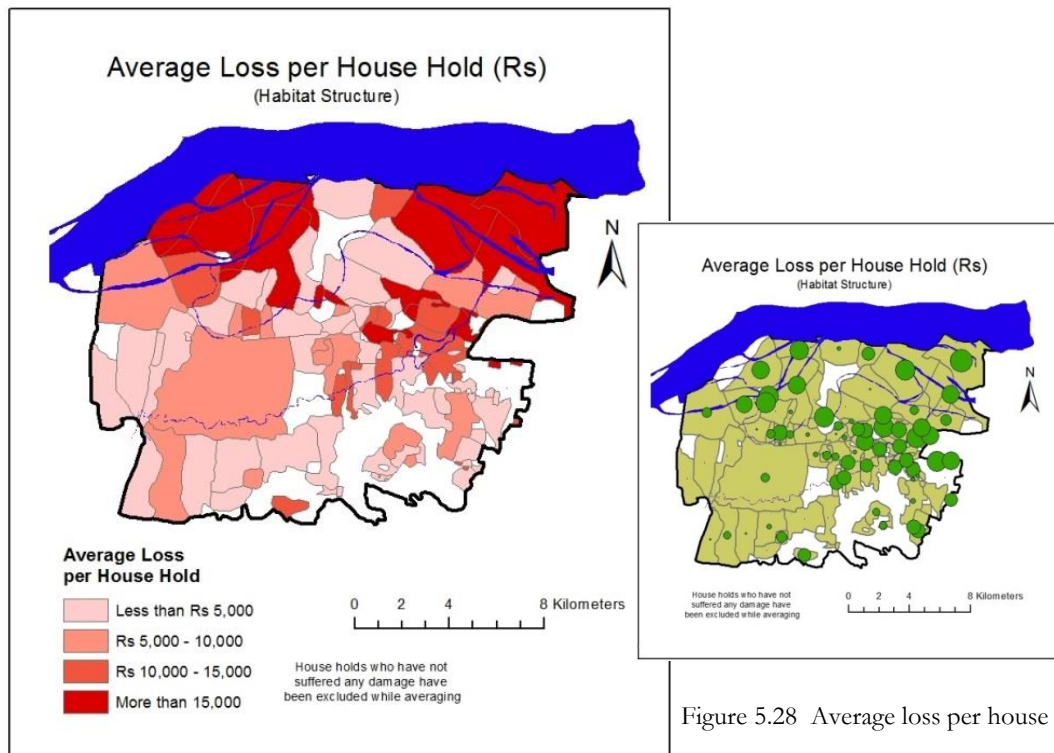


Figure 5.28 Average loss per house hold

Coordinate System: WGS 184 UTM Zone 45 N
Projection: Transverse Mercator
Datum: WGS 1984

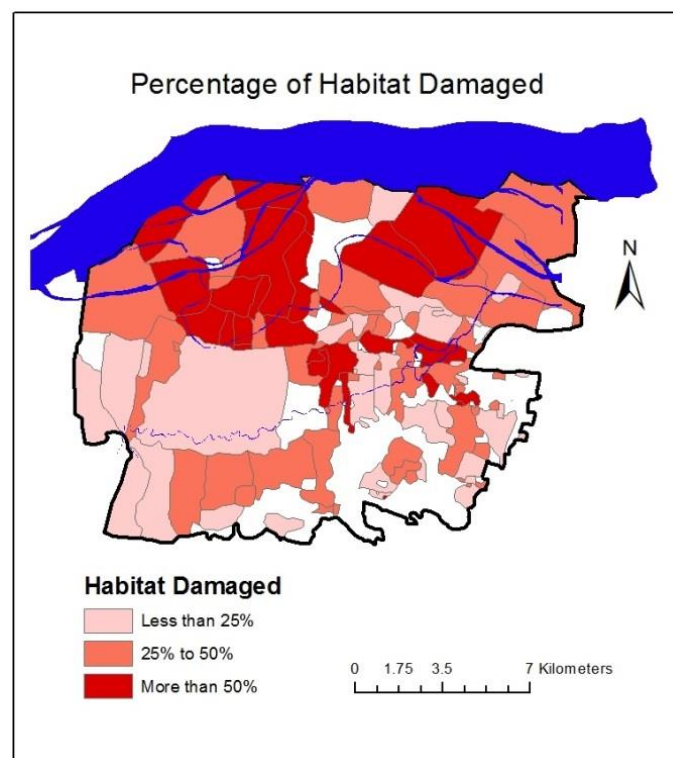


Figure 5.29 Percentage of habitat structures damaged

Coordinate System: WGS 184 UTM Zone 45 N
Projection: Transverse Mercator
Datum: WGS 1984

Figure 5.30 shows the village wise damage in three classes. Higher damages are at places with high density of structures along the national highway and the railway line. Both act as temporary barriers to water submerging structures in vicinity.

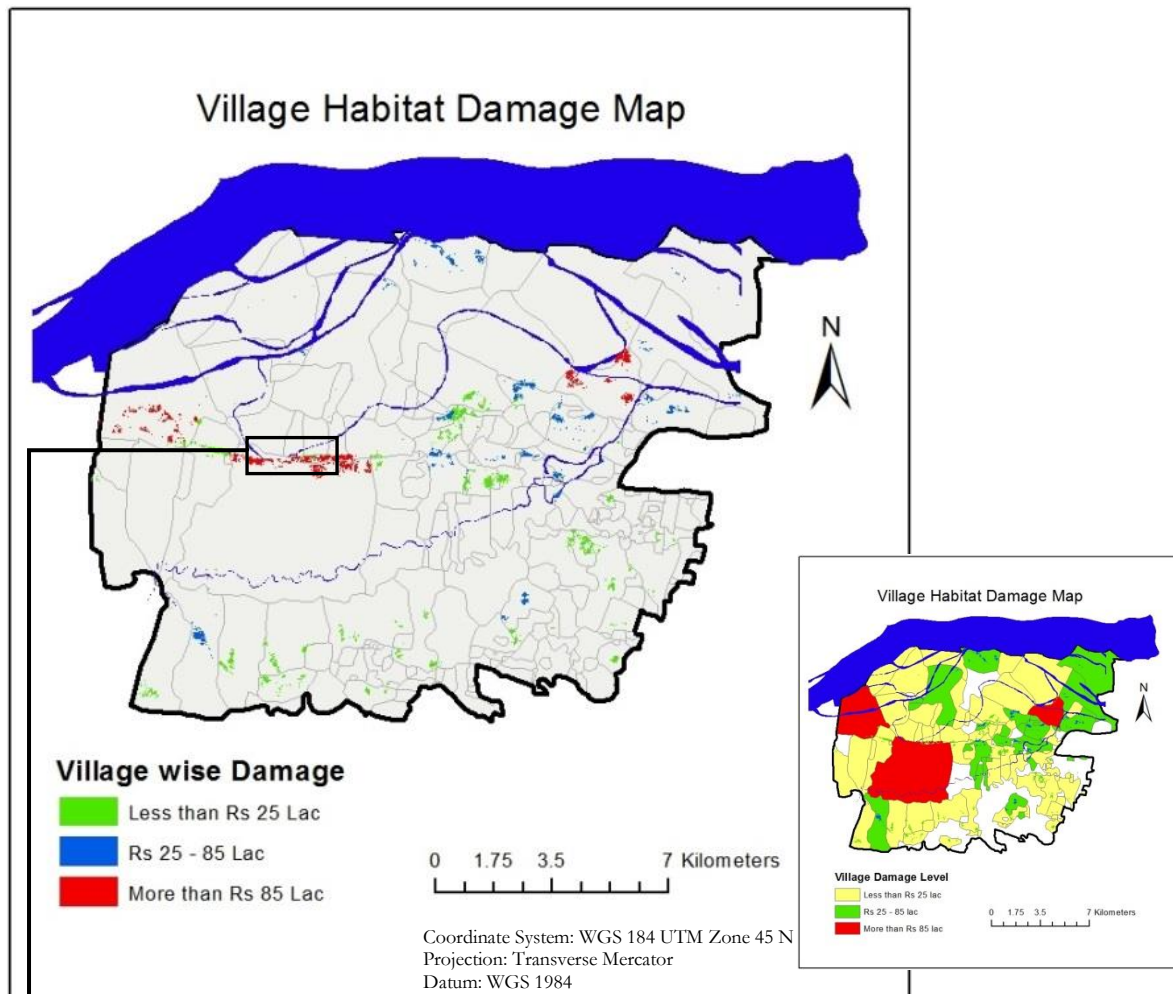


Figure 5.30 Village habitat damage map



Figure 5.31 shows the damage contribution of each type of structure. The number of structures and damage are in percentage of their respective totals. It is inferred that structures of Type E and H are the

major contributors to overall damage. The structure of Type C, even though contributes to damage substantially; its damage ratio is low as shown at Figure 5.21.

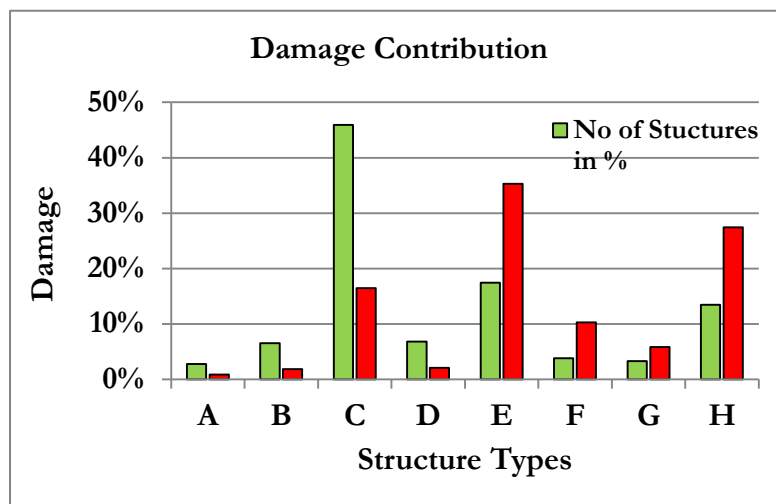


Figure 5.31 Damage contribution by different structures

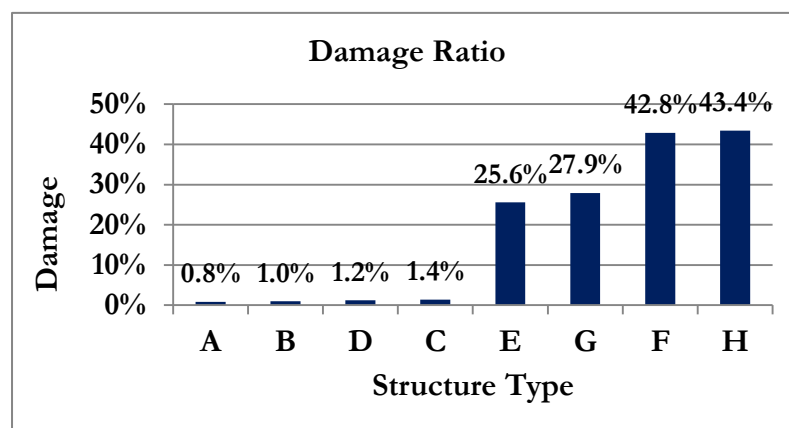


Figure 5.32 Damage ratio for different Structures

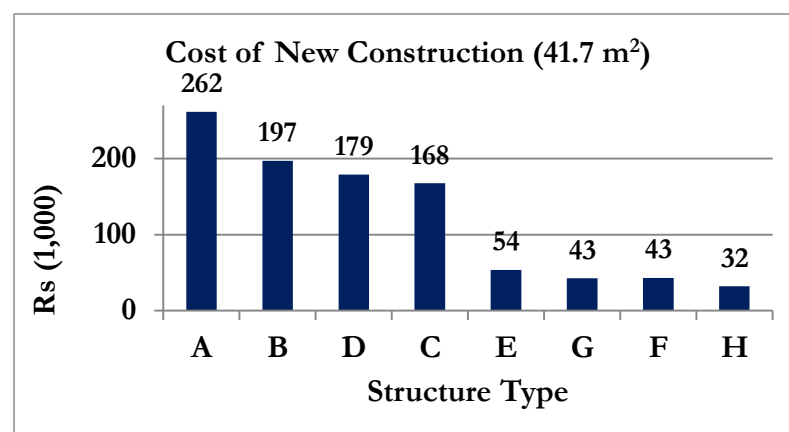


Figure 5.33 Cost of new construction

Figure 5.32 shows that structures E, F, G and H suffer marked percentage damage far beyond structures A, B, C and D. Figure 5.33 shows the cost of constructing a structure of mean size 41.7 m². It is observed from Figure 5.32 and Figure 5.33 that even though structure A costs substantially more than structures B, C, and D it does not provide protection commensurate to its additional cost. The difference between structure A and B is only in the roof with former having concrete roof while in the later it is tiles. It is also observed that the cost difference between type C, D and B is not substantial. It must be pointed out here that the damage to structures C and D which are made of burnt bricks joined with mud is low not because the physical damage is absent but because it's reconstruction cost is low as most of the material i.e. bricks can be reused again.

5.3.9. Method II : Estimation of Damage using Vulnerability Indices

The estimated damage based vulnerability index is given by

$$\sum_{v=1}^{v=N} \sum_{t=1}^{t=n} n_t A \alpha_t V$$

Where,

N = Number of villages exposed to flood in study area (from 15)

n = Number of structures of each type in each village (from Annexure 15)

d = Number of flood intensity classes.

A = Average area of structure (41.7 m² for all villages in the current study area – Field Survey)

α = Cost of re-construction per m² (from Annexure 6)

V = Vulnerability Index (from Table 5.21)

The damage was estimated based on three types of classes of structures. The estimated damage using vulnerability indices was ₹ 21.266 crore or ₹ 212.66 million as given at Table 5.26.

Table 5.26 Monetary damage in ₹ (Crores/10 Millions)

Structure	Damage
Type – I	1.811
Type – II	4.109
Type – III	15.346
Total	21.266

The variation between Methods-I and II is attributed to lack of accuracy in indices and vulnerability equations and due to classification of flood intensity and structure types.

5.3.10. Damage Estimation – Single Structure

Damage can be estimated for a single structure. However the depth exposure and area of the structure must be specific to the structure under examination. Determining specific depth was not carried out being out of scope of the research. However, if accurate depth is known, the damage to a single structure would be given by

$$\text{Damage (Rs)} = a \propto (k \ln(y) + c)$$

Where,

a = Area of structure in m² (41.7 m² for current study area – Field Survey)

\propto = Cost of re-construction per m² (from Annexure 6)

k = Coefficient of damage equation (from Table 5.24)

c = Constant value of damage equation (from Table 5.24)

y = specific depth exposure to the structure (from Annexure 15)

5.3.11. Development of Vulnerability Indices for Agriculture

The study area covers an extent of 237.2 km². Of this, 189.2 km² i.e. 80% was covered by agriculture. A total of 170 km² of agriculture was flooded. Based on field survey, all respondent claimed to have suffered 100% damage. No vulnerability indices could thus be developed for agriculture. It had emerged during the survey that the farmers grow vegetables since it allows partial harvesting prior to flood. If the flood is delayed, the profits are larger while on the contrary, in case the floods are early, they may lose all their investments. The flood in 2013 was exceptionally early flood, hence the total damage.

The average investment on agriculture by a farmer is ₹ 9,255 per acre or ₹ 2,28,6935 per km².

The total estimated damage in the study area is thus estimated to be ₹ 38.9 Crores i.e. Rs 389 million.

6. CONCLUSIONS AND RECOMMENDATIONS

6.1. Conclusions

6.1.1. Objective 1: Speckle Reduction in RISAT-I Data

Research Question 1. *Which filter has an optimal performance in reducing speckle in RISAT-I data for application in flood studies?*

An optimal performance of a filter implies that on application of a filter, there should be minimal loss of data that is essential for accurate flood delineation. For flood studies, it is essential that the features should be preserved while reducing speckle, especially in water bodies.

MSE values indicate that Frost (7×7) is amongst the best options for preservation of features. The reason for effective feature preservation is that Frost filter adapts to the local statistics by replacing the pixel of interest by a weighted factor which decreases with distance from the pixel of interest.

SNR, SSI and SMPI values indicate that the Frost (7×7) was more effective in noise reduction as compared to Frost (3×3). Lee Sigma and Gamma MAP filters reduced noise more effectively than Frost filter but also caused unacceptable loss of meaningful data. The comparison of Mean and Standard Deviation indicated similar results. With minimal loss of data and yet reducing speckle effectively, Frost (7×7) was found to be most optimal filter.

Although with increase in filter window size from 3×3 to 7×7 the speckle reduction is improved, the loss of actual data also increases, but the trade-off between speckle reduction and data loss is optimal at 7×7 window size.

The results of water bodies were too aligned to those of the entire image. For water bodies, the Frost (7×7) filter makes no change in mean while reducing standard deviation by approximately 43%. A second pass of Frost (7×7) filter did increase the percentage change in standard deviation but also resulted in considerable change in mean.

A single pass of Frost (7×7) is thus the most suited filter for flood delineation using RISAT-I dataset.

6.1.2. Objective 2: Flood Intensity and Exposure Analysis

Research Question 2. *How to estimate varying flood depth and duration?*

The estimation of flood extent using radiometric thresholding was accurate only up to a limit. The fuzziness between T_{\min} and T_{\max} was reduced by making a judgement based on flood water connectivity. The approach was found to be accurate since the accuracy of flood extent estimation was found to be 4-5 pixels. This level of accuracy was insignificant considering the objectives of the research. The study area was estimated to be flooded for varying periods from 1 to 105 days. The exposure of habitat and agricultural land in nine flood depth-duration classes was determined. It was found that 63% of the structures were exposed to flood between 20 to 40 days.

The RMSE of DEM was 2.72 m and the horizontal accuracy was 2.48 m and 2.35 m in X and Y direction respectively. The flood depth varied and reached a maximum of 2.66 m.

Research Question 3. *How to determine exposure of habitat structures and agriculture to varying flood intensities?*

Out of 57,602 structures in the study area, 43,849 (76.1%) habitat structures were in flood zone. Of these, 26,331 (60%) structures were exposed to one of the depth-duration intensity. Type C structures, i.e. structures made of burnt brick-joined with mud comprised 46% of the total structures exposed to flood intensity.

The study area covers an extent of 237.2 km². Of this, 189.2 km² i.e. 80% was agriculture. A total of 170 km² of agriculture was flooded.

6.1.3. Objective 3: Development of Vulnerability Indices and Damage Estimation**Research Question 4.** *How do different structures and agriculture respond to different flood depth and duration?*

The desired accuracy of vulnerability indices was 95% confidence with 5% confidence interval; the same could not be achieved due to limited sample size. As against 4553 samples required for a population size of 26331, only 203 samples could be collected.

It is clearly observed that people who have Type –III (Thatch packed or without mud packing) structures suffer losses far more than those who own Type –I (Burnt brick – Cement joined) or Type – II (Burnt brick – Mud joined) structures. Assuming that people staying in Type-III structures i.e. made of Thatch, are the poorest amongst others, the yearly loss may actually be a major factor in contributing to their continued poverty. However, this would need to be further researched before making any firm conclusion.

Even though structure A costs substantially more than structures B, C, and D it does not provide protection against flood commensurate to its additional cost. While the structure C and D are cheaper, the low cost of re-construction is due to reusability of most of the material after flood damage. The optimal protection from flood at minimal cost is thus provided by structure B i.e. a house made of burnt bricks joined with cement and the roof made of tiles instead of concrete.

Only vegetables are grown in the study area. The vulnerability indices for agricultural losses for varying flood depth and duration were not prepared as the agricultural vulnerability of agriculture was found to be 100%. Most likely, the reason for cropping only vegetables is precisely the damage caused by yearly flood as any delay in onset of flood would allow farmers to make at least 1-2 cycles of harvest giving them fair return of their investment.

Research Question 5. *How can the vulnerability indices be applied to estimate monetary damage at village level in the entire study area?*

The monetary damage at village level was estimated by determining mean depth exposure of the flood affected structures in each village, the proportionate number of different type of structures exposed in each village and the damage response equation for different types of structures.

The total estimated monetary damage to the structures in study area was ₹ 17.865 Crore or ₹ 178.65 million. Structures E (thatch with mud-plaster wall and tiled roof) and H (thatch without mud plaster and with thatch roof) comprised 35.3% and 27.4% of total damages. This is indicative of not only the vulnerability of structures but also the reflection of poverty in the study area.

It is concluded that methodology developed during the research has a tremendous potential to evolve as an effective application for estimating damage in a flood event at village or regional level.

6.2. Recommendations

Following are the recommendation for further work in the area

- Accuracy in estimation of depth is critical for flood damage studies. Ideally LiDAR data would be preferred, but since such data is rarely available in India, the next better option would be having a DEM generated using radar interferometry.
- The estimation of flood extent using radiometric thresholding was accurate only up to a limit. The fuzzy zone between T_{\min} and T_{\max} was left to making a rational judgement based on flood water continuity. Reduction of the fuzzy region needs to be further researched.
- When considering flood depth and duration to develop vulnerability, flood duration and depth maps are generated. Flood depth can be represented by a raster data where the pixels can be assigned a value equal to the duration of flood. While representing flood depth, such an assignment can be easily made by representing depth by a value of the pixel which represents average or maximum depth. However, in such an assignment the temporal variations of depth are not retained and are lost by simple averaging. If the temporal changes in depth are recorded, the accuracy of vulnerability indices would be improved.

REFERENCES

- Allen, B.P. (1975). Social distance and admiration reactions of “unprejudiced” whites. *Journal of Personality* 709–726.
- Andrews, H.C., and Hunt, B.R. (1977). *Digital Image Restoration* (Engle-Wood Cliffs: Prentice-Hall).
- Ayidiya, S.A., and McClendon, M.J. Response effects in mail surveys. *Public Opinion Quarterly* 229–247.
- Bartlett, J.E., Kotrlik, J.W., and Higgins, C.C. (2001). Organizational Research: Determining Appropriate Sample Size in Survey Research. *Information Technology, Learning, and Performance Journal* 19.
- Bhardwaj, A. (2013). Evaluation of DEM, and orthoimage generated from Cartosat-1 with its potential for feature extraction and visualization. *American Journal of Remote Sensing* 1(1): 1-6.
- Bhuvan, NRSC Bhuvan.
- Brakenridge, G.R., Tracy, B.T., and Knox, J.C. (1998). Orbital SAR remote sensing of a river flood wave. *Int. J. Remote Sens.* 19, 1439–1445.
- BSDMA, Bihar Disaster Management Department Statistics, Bihar.
- Canada Geodetic Survey CSRS-Precise Point Positioning.
- Cochran, W.G. (1977). *Sampling techniques* (New York: John Wiley & Sons).
- Cook, L. (1995). *A guide to good survey design* (New Zealand: Department of Statistics).
- Electoral Roll, Bihar View Final Roll - 18 Jan 2014.
- Eliason, E.M., and McEwen, A.S. (1990). Adaptive Box Filters for Removal of Random Noise from Digital Images. In *Photogrammetric Engineering & Remote Sensing*, pp. 453–458.
- Enc. Britannica Ganges River.
- Fellegi, I.P. (2003). *Survey Methods and Practices* (Ottawa, Canada: Statistics Canada).
- FMIS, Bihar Flood Management Information System, Bihar.
- Frost, V.S., Stiles, J.A., Shanmugan, K.S., and Holtzman, J.C. (1982). A Model for Radar Images and Its Application to Adaptive Digital Filtering of Multiplicative Noise. *IEEE Transactions on Pattern Analysis and Machine Intelligence PAMI-4*, 157–166.
- Gagnon, L., and Jauan, A. (1997). Speckle Filtering of SAR Images—a Comparative Study between Complex-Wavelet-Based and Standard Filters. In *Proceedings of SPIE Wavelet Applications in Signal And Image Processing V*, (San Diego, CA), pp. 80–91.
- Gove, W.R., and Geerken, M.R. (1977). Response bias in surveys of mental health: An empirical investigation. *American Journal of Sociology* 1289–1317.

- Hagg, W., and Sties, M. (1996). The Epos Speckle Filter: A Comparison with Some Well-Known Speckle Reduction Techniques. In XVIII ISPRS Congress, (Vienna, Austria), pp. 135–140.
- Henry, J.B. (2004). Spatial information system for floodplain inundation risk management. Ph.D. Dissertation, Strasbourg Univ. I.
- Holton, E.H., and Burnett, M.B. (1997). Qualitative Research Methods. In Human Resource Development Research Handbook: Linking Research and Practice, (San Francisco: Berrett-Koehler Publishers),.
- Horrit, M.S., Mason, D.C., and Luckman, A.J. (2001). Flood boundary delineation from synthetic aperture radar imagery using a statistical active contour model. *Int. J. Remote Sens.* 22, 2489–2507.
- Hostache, R., Matgen, P., Schumann, G., Puech, C., Hoffmann, L., and Pfister, L. (2009). Water Level Estimation and Reduction of Hydraulic Model Calibration Uncertainties Using Satellite SAR Images of Floods. *IEEE Transactions on Geoscience and Remote Sensing* 47.
- Jenson, J.R. (2000). *Remote Sensing of the Environment: An Earth Resource Perspective* (Upper Saddle River: NJ: Prentice Hall).
- Juster, F.T., and Smith, J.P. (1997). Improving the quality of economic data: Lessons from the HRS and AHEAD. *Journal of the American Statistical Association* 1268–1278.
- Kaplan, C.J., and Hegarty, D. (2006). *Understanding GPS: Principles and Applications*. Artech House, Boston, London pp 32.
- Kjorsvik, N.S., Ovstedal, O., Svendsen, J.G.G., and Blankenberg, L.E. (2005). A Multi-Base-Station Approach for Long Range Differential GNSS Positioning of Airborne Sensors. In *A Window on the Future of Geodesy*, F. Sansò, ed. (Springer Berlin Heidelberg), pp. 71–76.
- Krejcie, R.V., and Morgan, D.W. (1970). Determining sample size for research activities. In *Educational and Psychological Measurement*, pp. 607–610.
- Krosnick, J.A., and Presser, S. (2010). Question and Questionnaire Design. In *Handbook of Survey Research*, (Emerald Group Publishing Limited),.
- Lee, J.S. (1983). A Simple Speckle Smoothing Algorithm for Synthetic Aperture Radar Images. In *IEEE Transactions on Systems, Man, and Cybernetics*, pp. 85–89.
- Lee, J.-S. (1981). Speckle analysis and smoothing of synthetic aperture radar images. *Computer Graphics and Image Processing* 17, 24–32.
- Lee, J.S., Jurkevich, L., Dewaele, P., Wambacq, P., and Oosterlinck, A. (1994). Speckle filtering of synthetic aperture radar images: A review. *Remote Sensing Reviews* 8, 313–340.
- Lillesand, T.M., Kiefer, R.W., and Chipman, J.W. (2004). *Remote Sensing and Image Interpretation* (New York: John Wiley & Sons).
- Mansourpour, M., Rajabi, M.A., and Blais, J.A.R. (2006). Effects and performance of speckle noise reduction filters on active radar and SAR images.
- Morrison, M.L. (2008). Sample Survey Strategies. In *Wildlife Study Design*, (Springer Science + Business Media), pp. 136–197.

- Mukherjee, S., Joshi, P.K., Mukherjee, S., Ghosh, A., Garg, R.D., and Mukhopadhyay, A. (2013). Evaluation of vertical accuracy of open source Digital Elevation Model (DEM). *International Journal of Applied Earth Observation and Geoinformation* 205–217.
- NEA (1960). *Small Sample Techniques* (National Education Association).
- Oberstadler, R., Hönsch, H., and Huth, D. (1997). Assessment of the mapping capabilities of ERS-1 SAR data for flood mapping: A case study in Germany. *Hydrol. Process.* 11, 1415–1425.
- Qiu, F., Berglund, J., and Thakkar, P. (2004). Speckle Noise Reduction in SAR Imagery Using a Local Adaptive Median Filter. *GIScience and Remote Sensing* 41, 244–266.
- Quenouille, M.H. (1956). Note on bias in Estimation. *Biometrika* 43, 353–360.
- Raouf, A., and Lichtenegger, J. (1997). Integrated Use of SAR and Optical Data for Coastal Zone Management. In *ERS Satellite Radar Imagery*, (Florence, Italy), p. ESA SP-1204 (CD-ROM).
- Regmi, B. (2013). Long-Term Management of Kosi River Basin. In *Environmental Science and Engineering*.
- Rossiter, D.G. (2013). *Research Concepts & Skills : Concepts*.
- Schumann, G., Pappenberger, F., and Matgen, P. (2008). Estimating uncertainty associated with water stages from a single SAR image. *Adv. Water Resour.* 31, 1038–1047.
- Senthilnath, J., Shenoy, H.V., Rajendra, R., Omkar, S.N., Mani, V., and Diwakar, P.G. (2013). Integration of speckle de-noising and image segmentation using Synthetic Aperture Radar image for flood extent extraction. *Journal of Earth System Science* 122, 559–572.
- Shamsoddini, A., and Trinder, J.C. (2010). Image texture preservation in speckle noise suppression. (, Vienna, Austria),.
- Sheng, Y., and Xia, Z.-G. (1996). A comprehensive evaluation of filters for radar speckle suppression. In *Geoscience and Remote Sensing Symposium, 1996. IGARSS '96. "Remote Sensing for a Sustainable Future."*, International, pp. 1559–1561 vol.3.
- Singh, M., Singh, I.B., and Müller, G. (2007). Sediment characteristics and transportation dynamics of the Ganga River. *Geomorphology* 86, 144–175.
- Sinha, R., Bapalu, G.V., Singh, L.K., and Rath, B. (2008). Flood Risk Analysis in the Kosi River Basin, North Bihar using multi-parametric approach of Analytical Hierarchy Process (AHP). *Journal of the Indian Society of Remote Sensing* 36, 335–349.
- Smith, L.C. (1997). Satellite remote sensing of river inundation area, stage, and discharge: A review. *Hydrol. Process.* 11, 1427–1439.
- Starck, J.L., Murtagh, F., and Bijaoui, P. (1998). *Image Processing and Data Analysis - The multiscale approach* (Cambridge University Press).
- Sun, G., Ranson, K.J., Kharuk, V.I., and Kovacs, K. (2003). Validation of surface height from shuttle radar topography mission using shuttle laser altimeter. *Remote Sensing of Environment* 401–411.
- Thakur, P.K., Maiti, S., Kingma, N.C., Prasad, V.H., Aggarwal, S.P., and Bhardwaj, A. (2012). Estimation of structural vulnerability for flooding using geospatial tools in the rural area of Orissa, India. *Nat Hazards* 501–520.

UN Statistical Division UN Glossary of Classification Terms.

UNDP, Bihar UNDP, Bihar.

UNDRO (1991). Mitigation natural Disasters Phenomena, Effects and Options. A manual for planner.

UN-ISDR (2004). Living with Risk.

Wang, X., Ge, L., Xiaojing, and Li (2012). Evaluation of filters for ENVISAT ASAR speckle suppression in pasture area. In ISPRS Annals of the Photogrammetry, (Melbourne, Australia: Remote Sensing and Spatial Information Sciences),.

Van Westen, C. v., and Kingma, N.C. (2009). Guide book, Session 5: Vulnerability Assessment.

Wiki List of Rivers by Discharge.

Xiao, J., Li, J., and A., M. (2003). A Detail-Preserving and Flexible Adaptive Filter for Speckle Suppression in SAR Imagery. International Journal of Remote Sensing 2451–2465.

(2012). Per capita net state domestic product at current prices.

NRSC (2013). Flood Hazard Atlas for Bihar.

Planning Commission (2011). Report of Working Group on Flood Management and Region Specific Issues for XII Plan (New Delhi: Government of India).

Annexure 1

Rates of Compensation for Damage, Bihar

ID	Damage Particulars		Compensation	
1	Housing		<i>Pucca</i> (Brick based)	<i>Kutchha</i> (Thatch based)
	(a)	Fully damaged houses	35000	15000
	(b)	Severely damaged houses	6300	3200
	(c)	Partially damaged houses (atleast 15% damage)	1900	1900
	(d)	Damaged destroyed huts		2500
2	Agriculture (any crop)		6000 per hectare	

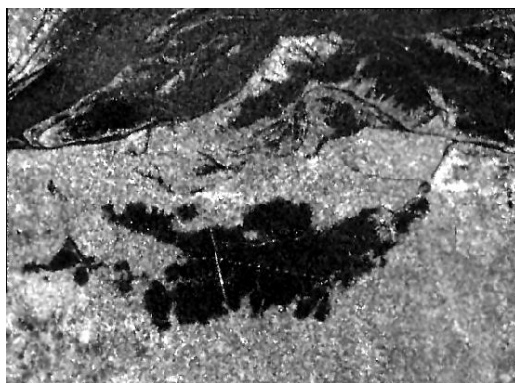
Annexure 2

Details of RISAT-I data used for Flood Intensity Analysis

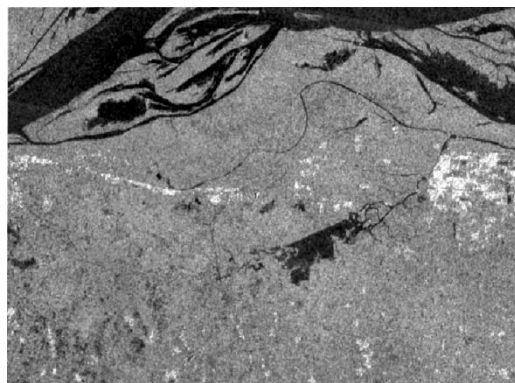
ID	Date	Scene	Sensor Mode	Polarisation	Raster Resolution (m)	Incidence Angle	Coeff.Of Variance
1	17 Jul 13	6742_1_14	MRS	HH	8.33	36.814	-0.370744
2	31 Jul 13	6961_1_1	CRS	RH	36	28.671	0.325578
3	04 Aug 13	7021_1_6	MRS	HH	8.33	39.595	-0.245367
4	11 Aug 13	7119_1_14	MRS	HH	8.33	36.819	-0.193777
5	30 Aug 13	7413_1_4	MRS	RH	8.33	50.195	-0.313916
6	05 Sep 13	7496_1_14	MRS	HH	8.33	36.41	-0.263265
7	07 Sep 13	7534_1_1	CRS	RH	36	26.203	0.362151
8	22 Sep 13	7760_1_1	MRS	RH	8.33	20.511	-0.53718
9	30 Sep 13	7873_1_14	MRS	HH	8.33	36.417	-0.522126
10	05 Oct 13	7956_1_3	CRS	RH	36	32.681	0.284115
11	25 Oct 13	8250_1_14	MRS	HH	8.33	36.416	-0.536072

Annexure 3

RISAT-I Data used for Research Objectives 2 and 3

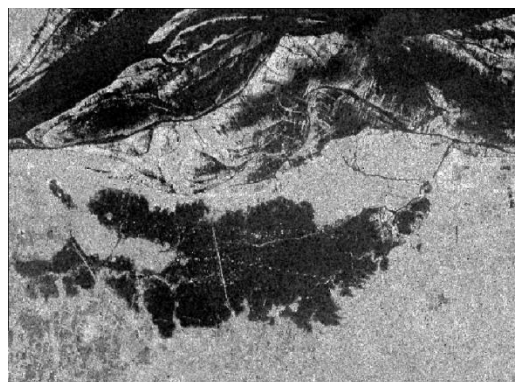


17 Jul 13

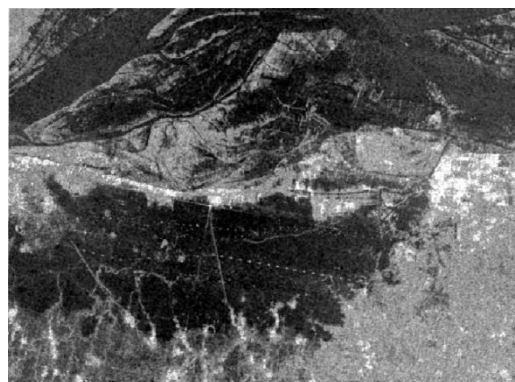


31 Jul 13

CRS



04 Aug 13



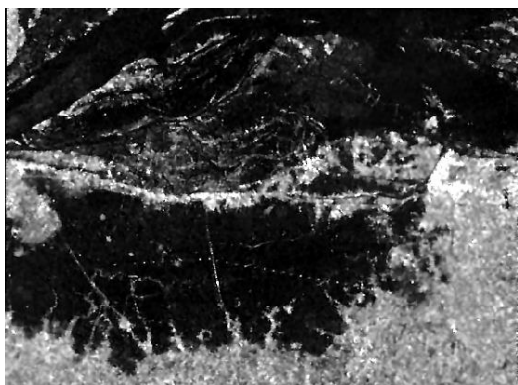
11 Aug 13



30 Aug 13



05 Sep 13

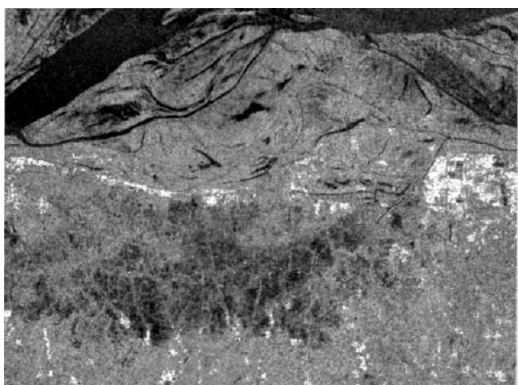


07 Sep 13

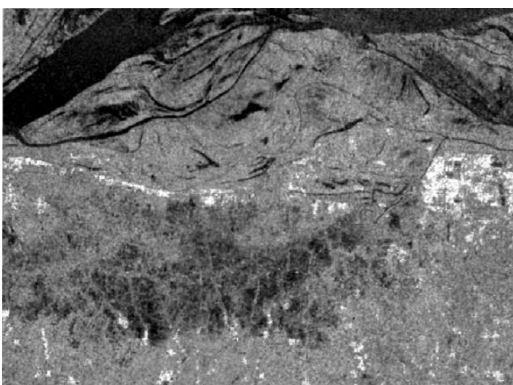
CRS



22 Sep 13

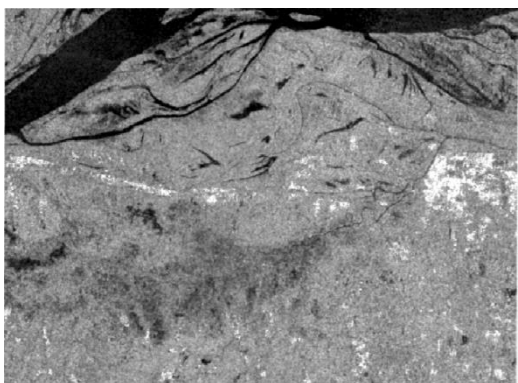


30 Sep 13



05 Oct 13

CRS



25 Oct 13

Annexure-4

Interview Schedule

1. Opening

- Brief introduction.
- Purpose of the interview.

Ask some of the following questions

- How long have you been living in this village?
- How has been this winter – very cold?
- If connected to grid, enquire about state of electric power supply in village?
- How do you keep yourself warm during winters?
- What do you for your living?
- Do your children go to school? How far do they have to go? How do they go to school?

2. Transition

- How do children go to school when it is flooded?
- Where did you stay when there was flood? What about your job?
- Was your house submerged? How deep? How did your children move out during flood? Did you use boats?

3. Core Survey

3.1. Flood Depth

- a) Are there any flood water marks on the walls in your house? *Measure height of flood from outside and inside the structure.*

OR

- b) How high did the flood reach outside your house during the last floods? *Obtain indication level based in relation to body height.*
- c) What was the flood level inside your house?

3.2. Flood Duration

- a) When did your house first start getting flood water outside and inside your house?
- b) When did your family leave the house and shift to shelter?
- c) How long had the flood already been there when you had taken away your family?

The duration of departure of family from flooded area and return may be established based on important festivals if date reference is not found practical.

- d) When did your family return back to the house?
- e) When your family returned was your house still flooded?
- f) How long did it last thereafter?

Based on interaction, estimate the number of days of flood duration and record it on the form.

3.3. Damage to structure

- a) What was the state of your house when you returned? Has it been repaired since then?

The flood damage should be recorded separately for floor, wall and roof in terms of area.

- b) Who carried out the repair work? How much did it cost?

The costing must be cross validated through alternative questioning.

- c) How much money do you spend every year on your house for repairs and maintenance?

3.4. Agriculture

- a) Do you own land? Where? How much? What do you cultivate?

- b) How much do you have to invest for seeds, fertilizers etc?

- c) How deep was the flood in your field?

- d) How long did the water remain stagnant?

- e) What is usually the yield if there is no flood?

- f) How much was the yield this year?

- g) At what rate are you able to sell your produce in the market?

4. Closing of Interview

- How do you make up for the educational loss your children suffer because of yearly floods?

Thank the individual with closing comments.

Annexure-5

SURVEY : DATA RECORDING FORM

1. Village.....2. Name.....
 3. GPS Coordinates (*Front Left*)

Flood Intensity2013

4. Flood Height Outside cm
 5. Flood Height Inside cm
 6. Flood Durationdays

Structure Details**7. Roof Type**

- ☐ Concrete ☐ Tiles ☐ Thatch

8. Wall Type

- ☐ Burnt Bricks joined by Cement ☐ Burnt Bricks joined with mud ☐ Thatch/Mud Plastering

9. Floor Type

- ☐ Cement ☐ Burnt bricks ☐ Mud

10. Plinth Protection (☒)..... 11. Building Height.....m
 12. Structure Length m 13. Structure Length m
 14. Age of building..... Years

Damage & Maintenance 2013

15. Roof Damage sq m 16. Wall Damagesq m
 17. Floor Damage.....sq m
 18. Soil Dumping.....trailer loads
 19. Miscellaneous maintenance cost..... Rs
 20. Maintenance frequency.....years
 21. Approximate amount spent on each maintenance..... Rs

Annexure – 6

Detailed Costing of Different Structures in the Study Area

Costing of Average Structure Size of 41.7 sqm								
Code	A	B	C	D	E	F	G	H
Roof	Concrete	Tiles	Tiles	Thatch	Tiles	Thatch	Tiles	Thatch
Wall	BBC	BBC	BBM	BBM	Mud Plastered	Mud Plastered	Thatch	Thatch
Floor	Mud	Mud	Mud	Mud	Mud	Mud	Mud	Mud
Item List								
COSTING OF ROOF								
Bricks								
Cement	18,250							
Sand	9,200							
Aggregate	14,400							
Fitments								
Iron Rods	32,500							
Tiles		9,200	9,200		9,200		9,200	
Bamboo		10,710	10,710	6,800	10,710	6,800	10,710	6,800
Thatch/Polythene		1,000	1,000	1,000	1,000	1,000	1,000	1,000
Labour cost	15,000	4,000	4,500	6,000	4,000	6,000	4,000	6,000
Total cost for new construction (a)	89,350	24,910	25,410	13,800	24,910	13,800	24,910	13,800
Cost of reusable items (b)		5,520	5,520		5,520		5,520	
Total for Reconstruction (a) - (b)	89,350	19,390	19,890	13,800	19,390	13,800	19,390	13,800
COSTING OF WALL								
Bricks	1,19,331	1,19,331	1,19,331	1,19,331				
Cement	10,800	10,800						
Sand	7,800	7,800						
Aggregate								
Fitments	13,541	13,541	13,541	13,541	6,770	6,770		
Iron Rods								
Tiles								
Bamboo					10,000	10,000	10,000	10,000
Thatch/Poly								
Labour	20,000	20,000	20,000	20,000	11,000	11,000	7,000	7,000

Costing of Average Structure Size of 41.7 sqm								
Code	A	B	C	D	E	F	G	H
Total cost for new construction (a)	1,71,472	1,71,472	1,52,872	1,52,872	27,770	27,770	17,000	17,000
Cost of reusable items (b)	78,369	78,369	1,26,102	1,26,102	3,385	3,385		
Total for Reconstruction (a) - (b)	93,103	93,103	26,771	26,771	24,385	24,385	17,000	17,000
COSTING OF FLOOR								
Mud Spreading & Tamping	1,000	1,000	1,000	1,000	1,000	1,000	1,000	1,000
Grand Total cost for new construction	2,61,822	1,97,382	1,79,282	1,67,672	53,680	42,570	42,910	31,800
Total Reusable after floods	79,369	84,889	1,32,622	1,27,102	9,905	4,385	6,520	1,000
Grand Total for Reconstruction	1,82,453	1,12,493	46,661	40,571	43,775	38,185	36,390	30,800

BBC : Burnt Brick joined with Concrete
BBM : Burnt Brick joined with Mud
MT : Mud Plastered Thatch

Scales of Reconstruction per m²

Code	Scales of Re-construction per m ²
A	4375.37
B	2697.67
C	1118.96
D	972.91
E	1049.76
F	915.71
G	872.66
H	738.61

Annexure-7

Scales of Re-construction for Structural Components

Structure Component/ Material	Cost (Rs) per m ² of floor area
ROOF	
Concrete	2143
Tiles	465
Thatch	331
Cost (Rs) per m ² of wall area	
WALL	
Burnt Bricks joining by Cement	1313
Burnt Bricks joining by Mud	424
Mud Plastered Thatch	493
Thatch	344
Cost (Rs) per m ² of floor area	
FLOOR	
Mud	24
MISCELLANEOUS	
Mud Shifting (Rupees per tractor trailer load)	400

Annexure - 8

Survey Database

ID	Village_Name	Roof	Wall	Floor	Length (m)	Width (m)	Flood Height (m)	Duration (Days)	Damage Roof (m ²)	Damage Wall (m ²)
1	Akbarnagar	Tiles	MT	Mud	6	4.3	1.1	30	12.0	20.0
2	Akbarnagar	Tiles	Thatch	Mud	8	6.9	1.2	70	53.1	55.8
3	Akbarnagar	Tiles	BBM	Mud	7	5.9	1.1	30	0.0	10.0
4	Akbarnagar	Thatch	BBM	Mud	7	5.9	1.3	60	41.9	63.4
5	Akbarnagar	Thatch	MT	Mud	7	5.9	1.3	70	43.7	50.8
6	Akbarnagar	Tiles	BBC	Mud	9	5.3	1.2	70	0.0	1.8
7	Akbarnagar	Tiles	MT	Mud	7	5	0.5	15	0.0	5.0
8	Akbarnagar	Thatch	Thatch	Mud	7	6.6	1.3	70	42.8	50.0
9	Akbarnagar	Tiles	BBM	Mud	7	6.2	1.3	30	0.0	4.0
10	Akbarnagar	Tiles	BBM	Mud	7	5.2	1.2	30	0.0	8.0
11	Akbarnagar	Tiles	Thatch	Mud	8	6	1.2	30	18.9	27.3
12	Akbarnagar	Tiles	MT	Mud	8	6.5	1.2	30	10.7	25.0
13	Akbarnagar	Tiles	BBM	Mud	7	6.4	1	30	0.0	4.8
14	Akbarnagar	Thatch	BBM	Mud	7	5.4	1.1	70	0.0	4.0
15	Akbarnagar	Tiles	BBM	Mud	6	4.6	1	30	1.0	9.0
16	Akbarnagar	Tiles	BBM	Mud	7	5.5	1.3	70	0.0	6.0
17	Akbarnagar	Tiles	MT	Mud	7	6.5	1.1	30	30.0	30.0
18	Balachauki	Tiles	MT	Mud	9	5.9	0.3	15	0.0	5.0
19	Balachauki	Tiles	BBM	Mud	7	5.9	0.5	15	0.0	0.0
20	Balachauki	Tiles	BBM	Mud	8	6.3	1.7	45	5.0	21.0
21	Balachauki	Thatch	MT	Mud	8	7	0.4	15	0.0	4.0
22	Balachauki	Tiles	BBC	Mud	8	5.2	0.5	15	0.0	0.5
23	Balachauki	Thatch	Thatch	Mud	7	5.5	0.5	30	2.0	11.0
24	Balachauki	Tiles	MT	Mud	7	6.5	0.6	30	2.3	12.0
25	Balachauki	Concrete	BBC	Mud	8	6.4	0.5	15	0.0	0.5
26	Balachauki	Tiles	BBM	Mud	6	5.3	0.5	15	0.0	0.0
27	Balachauki	Tiles	BBM	Mud	8	6.9	0.4	15	0.0	0.5
28	Balachauki	Tiles	BBM	Mud	7	6.4	1.6	30	1.0	8.0
29	Balachauki	Tiles	BBC	Mud	7	5.3	0.6	15	0.0	0.0
30	Balachauki	Tiles	BBM	Mud	8	7.3	0.3	15	0.0	0.0
31	Balachauki	Thatch	BBM	Mud	7	6	0.4	15	0.0	3.0
32	Baria Rattipur	Tiles	BBM	Mud	7	5.9	1.9	90	0.0	6.0

ID	Village_Name	Roof	Wall	Floor	Length (m)	Width (m)	Flood Height (m)	Duration (Days)	Damage Roof (m ²)	Damage Wall (m ²)
33	Baria Rattipur	Tiles	BBM	Mud	8	5.9	1.8	85	0.0	6.0
34	Baria Rattipur	Tiles	MT	Mud	8	4.3	2.1	85	33.0	45.5
35	Baria Rattipur	Tiles	Thatch	Mud	6	5	2.3	80	30.0	42.0
36	Baria Rattipur	Tiles	BBM	Mud	7	5.4	2.3	90	1.8	11.3
37	Baria Rattipur	Tiles	BBM	Mud	8	6.4	1.9	90	1.0	6.5
38	Baria Rattipur	Tiles	BBM	Mud	6	5.1	1.9	80	0.0	8.0
39	Baria Rattipur	Tiles	MT	Mud	9	5.7	2	85	49.0	54.6
40	Baria Rattipur	Tiles	Thatch	Mud	7	5.3	5	85	36.7	46.7
41	Baria Rattipur	Thatch	Thatch	Mud	6	5.2	3.7	90	33.3	44.3
42	Bethu	Thatch	Thatch	Mud	7	6.9	0.4	30	5.0	10.3
43	Bethu	Tiles	BBM	Mud	7	5.1	1.6	45	1.0	6.3
44	Bethu	Tiles	BBM	Mud	6	5.7	0.5	15	0.0	1.5
45	Bethu	Tiles	BBM	Mud	7	5	0.6	15	0.0	1.5
46	Bethu	Tiles	BBM	Mud	7	6.7	0.3	10	0.0	0.5
47	Bethu	Tiles	BBM	Mud	7	5.2	0.4	15	0.0	0.5
48	Bethu	Thatch	BBM	Mud	8	6	0.6	20	0.0	0.5
49	Bethu	Thatch	Thatch	Mud	7	6	0.6	30	12.6	21.0
50	Bethu	Thatch	MT	Mud	7	5	0.5	30	1.8	6.0
51	Bhatauria	Tiles	BBM	Mud	7	6.9	0.9	30	0.0	5.0
52	Bhatauria	Tiles	BBM	Mud	6	5.6	1	30	0.0	4.8
53	Bhatauria	Tiles	BBM	Mud	7	5.6	0.9	30	0.0	3.8
54	Bhatauria	Tiles	BBM	Mud	7	6.6	1	30	0.0	3.8
55	Bhatauria	Tiles	BBC	Mud	7	5.4	0.8	30	0.0	1.0
56	Bhatauria	Tiles	BBM	Mud	7	5.1	1	30	0.0	1.5
57	Bhatauria	Tiles	BBM	Mud	7	5	1	30	0.0	4.5
58	Bhatauria	Tiles	BBM	Mud	6	5.9	1	30	0.0	4.3
59	Bhatauria	Tiles	BBM	Mud	6	5.3	0.9	30	0.0	0.0
60	Bhatauria	Thatch	MT	Mud	7	5.5	1	70	36.3	46.2
61	Bhatauria	Tiles	MT	Mud	8	6.6	0.9	30	14.9	25.0
62	Bhatauria	Tiles	BBM	Mud	7	5.6	0.8	30	0.0	4.5
63	Gauripur	Thatch	MT	Mud	7	6	1.5	30	42.8	50.2
64	Gauripur	Thatch	MT	Mud	7	6.9	1.5	80	49.0	53.5
65	Gauripur	Tiles	BBC	Mud	6	5.7	1.3	70	0.0	1.5
66	Gauripur	Thatch	MT	Mud	7	5.6	1.3	70	37.5	47.0
67	Gauripur	Tiles	Thatch	Mud	7	5.4	1.4	90	39.4	48.5
68	Gauripur	Tiles	MT	Mud	7	6.6	1.3	30	4.5	15.0
69	Gauripur	Tiles	BBC	Mud	8	7	1.1	30	0.0	1.0

ID	Village_Name	Roof	Wall	Floor	Length (m)	Width (m)	Flood Height (m)	Duration (Days)	Damage Roof (m ²)	Damage Wall (m ²)
70	Gauripur	Tiles	MT	Mud	8	6.6	1.4	30	9.9	20.0
71	Gauripur	Tiles	BBM	Mud	7	5.9	0.9	15	0.0	1.0
72	Gauripur	Tiles	BBM	Mud	7	6	1.3	60	0.0	4.0
73	Golahu	Concrete	BBC	Mud	7	5.3	0.7	30	0.0	0.5
74	Golahu	Thatch	MT	Mud	8	6	0.7	20	5.0	15.0
75	Golahu	Tiles	BBC	Mud	9	7.3	0.7	15	0.0	0.8
76	Golahu	Tiles	BBM	Mud	8	6.3	0.8	15	0.0	3.0
77	Golahu	Tiles	BBM	Mud	6	5.6	0.8	15	0.0	3.0
78	Golahu	Tiles	MT	Mud	7	6.6	0.7	15	0.0	4.0
79	Golahu	Tiles	BBM	Mud	9	6.6	0.7	15	0.0	1.8
80	Golahu	Tiles	BBC	Mud	8	5.7	0.7	30	0.0	0.8
81	Golahu	Tiles	BBM	Mud	7	5.9	0.8	15	0.0	0.0
82	Golahu	Thatch	BBM	Mud	6	5	0.7	15	0.0	2.5
83	Golahu	Concrete	BBC	Mud	6	5.2	0.7	30	0.0	0.5
84	Golahu	Tiles	MT	Mud	7	5.8	0.7	30	8.2	14.0
85	Gosaindasapur	Tiles	BBM	Mud	8	5.9	0.6	15	0.0	1.0
86	Gosaindasapur	Thatch	Thatch	Mud	8	4.5	1.7	85	33.6	45.8
87	Gosaindasapur	Tiles	BBM	Mud	7	6.9	0.6	15	0.0	1.5
88	Gosaindasapur	Thatch	MT	Mud	7	7.2	1.7	85	53.3	55.8
89	Gosaindasapur	Tiles	BBM	Mud	8	6.1	1.5	80	0.0	7.0
90	Gosaindasapur	Tiles	BBM	Mud	7	6.1	0.6	15	0.0	0.8
91	Gosaindasapur	Tiles	BBM	Mud	8	5.3	1.2	80	0.0	6.0
92	Gosaindasapur	Thatch	MT	Mud	7	5.6	1.7	80	39.8	48.5
93	Gosaindasapur	Thatch	MT	Mud	6	6.9	1.7	90	43.2	50.3
94	Gosaindasapur	Tiles	BBM	Mud	7	5.1	1.4	80	0.0	2.5
95	Gosaindasapur	Tiles	BBC	Mud	8	6.4	1.7	30	0.0	1.5
96	Gosaindasapur	Tiles	BBM	Mud	7	6.2	1.7	80	0.5	6.0
97	Gosaindasapur	Concrete	BBC	Mud	8	6.5	1.7	80	0.0	1.5
98	Gosaindasapur	Tiles	BBC	Mud	7	5	1.7	30	0.0	2.8
99	Gosaindasapur	Tiles	MT	Mud	8	6.4	1.7	80	49.6	54.0
100	Haridasapur	Concrete	BBC	Mud	7	5.5	1.6	30	0.0	1.0
101	Haridasapur	Tiles	BBM	Mud	6	5.2	1.6	85	0.0	1.5
102	Haridasapur	Tiles	BBM	Mud	7	5.4	1.3	90	0.0	2.5
103	Haridasapur	Thatch	BBM	Mud	7	5.3	1.6	30	0.0	4.8
104	Haridasapur	Tiles	BBM	Mud	6	5.9	1.6	80	0.0	5.5
105	Haridasapur	Thatch	Thatch	Mud	6	5.1	1.6	85	31.6	43.2
106	Haridasapur	Concrete	BBC	Mud	7	6.2	1.7	80	0.0	0.5

ID	Village_Name	Roof	Wall	Floor	Length (m)	Width (m)	Flood Height (m)	Duration (Days)	Damage Roof (m ²)	Damage Wall (m ²)
107	Haridaspur	Tiles	MT	Mud	7	5.9	1.6	80	41.9	49.7
108	Haridaspur	Tiles	BBM	Mud	6	6.4	1.4	80	0.0	12.0
109	Haridaspur	Tiles	MT	Mud	7	6.6	1.6	85	47.4	52.6
110	Haridaspur	Thatch	BBM	Mud	7	5.3	0.8	15	0.0	2.5
111	Haridaspur	Thatch	Thatch	Mud	7	6.5	1.6	85	42.9	50.0
112	Harpur	Tiles	MT	Mud	8	5.6	0.6	15	0.0	4.0
113	Harpur	Concrete	BBC	Mud	6	5.6	0.2	15	0.0	0.0
114	Harpur	Thatch	MT	Mud	6	5.2	0.4	15	0.0	7.5
115	Harpur	Thatch	MT	Mud	7	6.7	0.3	15	1.6	7.5
116	Harpur	Tiles	MT	Mud	7	5.2	0.6	30	4.0	8.0
117	Harpur	Tiles	Thatch	Mud	7	5.3	0.6	15	0.0	5.3
118	Harpur	Thatch	MT	Mud	8	6.2	0.6	30	7.1	17.5
119	Harpur	Tiles	BBM	Mud	7	6	0.9	30	0.0	1.8
120	Harpur	Tiles	BBM	Mud	7	6.2	0.4	15	0.0	0.0
121	Harpur	Thatch	Thatch	Mud	6	4.5	0.6	15	0.0	3.8
122	Harpur	Thatch	BBM	Mud	6	6.3	0.5	15	0.0	0.5
123	Harpur	Thatch	Thatch	Mud	7	6.9	0.6	15	0.0	6.0
124	Jaitipur	Thatch	BBM	Mud	6	6.3	1.5	30	0.0	6.0
125	Jaitipur	Concrete	BBC	Mud	7	6.9	1.4	60	0.0	2.3
126	Jaitipur	Tiles	Thatch	Mud	7	7	1.3	30	15.0	25.8
127	Jaitipur	Tiles	MT	Mud	8	6.5	1.3	30	10.2	25.0
128	Jaitipur	Tiles	BBM	Mud	6	5.6	1.4	70	0.0	2.0
129	Jaitipur	Tiles	BBM	Mud	6	5.2	1.4	60	0.0	3.3
130	Jaitipur	Tiles	BBM	Mud	7	6.6	1.4	70	0.0	1.5
131	Jaitipur	Tiles	BBM	Mud	7	5.6	1.3	60	0.0	4.0
132	Jaitipur	Tiles	BBM	Mud	6	5.1	1.3	60	0.0	6.5
133	Jaitipur	Tiles	BBM	Mud	7	5	1.3	70	2.0	15.0
134	Jaitipur	Tiles	Thatch	Mud	6	6.7	1.4	30	12.3	25.3
135	Kasmabad	Thatch	MT	Mud	8	5.1	0.4	30	0.0	5.0
136	Kasmabad	Thatch	MT	Mud	7	5.6	0.6	15	1.0	7.0
137	Kasmabad	Tiles	BBM	Mud	7	5.9	0.6	15	0.0	1.5
138	Kasmabad	Thatch	MT	Mud	8	6.2	0.3	15	0.0	6.0
139	Kasmabad	Tiles	BBM	Mud	6	6.9	1.5	30	0.0	5.0
140	Kasmabad	Tiles	Thatch	Mud	7	5.1	0.5	30	6.7	17.0
141	Kasmabad	Tiles	MT	Mud	6	5.6	0.6	15	0.0	7.5
142	Kasmabad	Tiles	BBM	Mud	9	7.5	0.5	15	0.0	1.5
143	Khulli	Tiles	Thatch	Mud	7	5.7	0.7	15	0.0	5.3

ID	Village_Name	Roof	Wall	Floor	Length (m)	Width (m)	Flood Height (m)	Duration (Days)	Damage Roof (m ²)	Damage Wall (m ²)
144	Khulli	Thatch	Thatch	Mud	7	6.7	1.6	46	47.0	52.4
145	Khulli	Tiles	MT	Mud	7	5.2	0.7	20	7.6	16.3
146	Khulli	Tiles	Thatch	Mud	7	5.9	0.8	30	12.8	26.0
147	Khulli	Tiles	BBC	Mud	6	4.5	0.8	30	0.0	0.5
148	Khulli	Tiles	BBM	Mud	7	6.7	0.7	30	0.0	5.8
149	Khulli	Tiles	BBM	Mud	8	5.1	0.7	15	0.0	9.0
150	Khulli	Tiles	MT	Mud	8	6.8	0.7	30	0.0	10.0
151	Khulli	Tiles	BBM	Mud	7	5.5	0.7	30	0.0	2.0
152	Khulli	Tiles	BBC	Mud	7	6.7	0.8	30	0.0	0.5
153	Khulli	Tiles	BBM	Mud	7	5.6	0.8	15	0.0	1.8
154	Mirzapur	Tiles	MT	Mud	8	6.6	1.8	80	50.0	54.2
155	Mirzapur	Thatch	Thatch	Mud	8	5	1.7	30	38.0	48.1
156	Mirzapur	Tiles	BBM	Mud	6	5.8	1.4	80	0.0	4.5
157	Mirzapur	Tiles	Thatch	Mud	7	5.9	1.9	80	41.9	49.7
158	Mirzapur	Thatch	Thatch	Mud	9	5.6	1.8	80	48.2	54.2
159	Mirzapur	Thatch	MT	Mud	7	6.2	1.8	80	40.3	48.5
160	Mirzapur	Tiles	BBM	Mud	7	6.1	1.8	85	0.0	2.0
161	Mirzapur	Tiles	MT	Mud	8	6.6	1.8	80	49.7	54.0
162	Mirzapur	Tiles	BBM	Mud	7	5.2	1.8	85	0.0	7.0
163	Mirzapur	Tiles	BBM	Mud	6	5.3	1.7	30	0.0	8.0
164	Mirzapur	Concrete	BBC	Mud	7	5.4	1.8	90	0.0	2.0
165	Mohanpur	Thatch	MT	Mud	7	5.3	1.9	90	35.5	45.8
166	Mohanpur	Thatch	MT	Mud	6	5.9	2.3	80	36.0	45.8
167	Mohanpur	Tiles	BBC	Mud	7	5.3	2.1	85	0.0	2.5
168	Mohanpur	Tiles	MT	Mud	8	6.4	1.9	85	48.9	53.6
169	Mohanpur	Concrete	BBC	Mud	6	5.8	2.5	80	0.0	4.0
170	Mohanpur	Tiles	BBM	Mud	7	5.3	2.1	80	0.0	8.0
171	Mohanpur	Tiles	MT	Mud	6	5.2	1.9	80	32.2	43.5
172	Mohanpur	Concrete	BBC	Mud	9	6.3	2.1	85	0.0	2.8
173	Mohanpur	Tiles	BBM	Mud	8	6.9	1.9	90	0.0	8.5
174	Pachkathia	Tiles	BBM	Mud	7	5.7	0.9	30	0.0	4.5
175	Pachkathia	Tiles	BBC	Mud	8	6.6	0.8	30	0.0	1.5
176	Pachkathia	Tiles	BBC	Mud	7	6.2	0.9	30	0.0	1.8
177	Pachkathia	Tiles	BBC	Mud	7	6.2	0.9	30	0.0	1.0
178	Pachkathia	Tiles	BBM	Mud	9	6.7	0.9	30	5.0	18.0
179	Pachkathia	Tiles	BBM	Mud	8	5.7	0.9	30	0.0	1.5
180	Pachkathia	Tiles	MT	Mud	7	6.6	0.6	15	0.0	4.0

ID	Village_Name	Roof	Wall	Floor	Length (m)	Width (m)	Flood Height (m)	Duration (Days)	Damage Roof (m ²)	Damage Wall (m2)
181	Pachkathia	Concrete	BBC	Mud	8	6.4	0.9	30	0.0	0.8
182	Pachkathia	Tiles	BBM	Mud	6	5.4	0.9	30	0.0	2.5
183	Pachkathia	Thatch	MT	Mud	7	6.6	0.8	30	10.0	15.0
184	Tahawarnagar	Tiles	MT	Mud	7	4.6	1.6	90	34.2	45.9
185	Tahawarnagar	Tiles	MT	Mud	7	6.9	1.6	30	48.0	53.0
186	Tahawarnagar	Tiles	BBM	Mud	6	5.4	1.6	80	0.0	7.5
187	Tahawarnagar	Tiles	BBM	Mud	8	6.2	0.5	15	0.0	0.8
188	Tahawarnagar	Tiles	BBC	Mud	6	5	1.4	80	0.0	1.8
189	Tahawarnagar	Thatch	Thatch	Mud	6	5	1.6	30	30.5	42.4
190	Tahawarnagar	Tiles	BBM	Mud	7	6	0.4	15	0.0	0.0
191	Tahawarnagar	Tiles	MT	Mud	8	5.2	1.6	30	39.0	48.5
192	Tahawarnagar	Thatch	BBM	Mud	8	5.1	0.9	15	0.0	2.5
193	Tilakpur	Thatch	MT	Mud	7	6.6	1.1	70	48.8	53.5
194	Tilakpur	Thatch	MT	Mud	6	5.9	0.7	15	0.0	5.0
195	Tilakpur	Thatch	BBM	Mud	7	6.7	1.3	30	0.0	5.5
196	Tilakpur	Tiles	Thatch	Mud	6	5	1.1	30	10.0	19.5
197	Tilakpur	Tiles	BBM	Mud	6	5.3	1.1	70	0.0	6.5
198	Tilakpur	Tiles	MT	Mud	8	6.9	1.1	30	10.0	25.0
199	Tilakpur	Thatch	Thatch	Mud	7	6.7	1.1	30	29.0	32.5
200	Tilakpur	Tiles	BBM	Mud	7	6.7	1	30	0.0	4.8
201	Tilakpur	Tiles	MT	Mud	6	6.9	1.1	30	14.2	20.0
202	Tilakpur	Tiles	BBM	Mud	8	5	1.1	70	0.0	1.5
203	Tilakpur	Tiles	Thatch	Mud	8	5.1	1.1	30	12.0	18.0

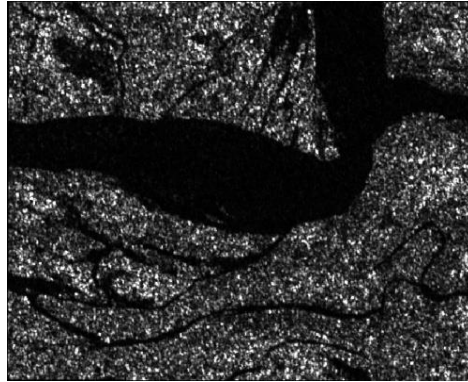
Annexure - 9

Measured Values for Different Filter and Window Sizes for Water Bodies

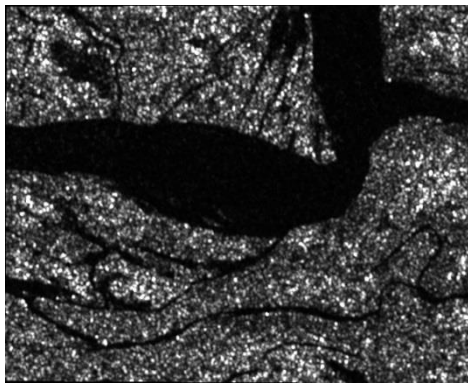
	MSE			Rank	Change in Ranking [Full Image - River Subset]	
	3 X 3	5 X 5	7 X 7			
Lee Sigma	0.000027	0.000046	0.000054	8	11	12
Lee	0.000009	0.000005	<u>0.000001</u>	5	3	1
Frost	0.000014	0.000008	0.000002	6	4	2
Local Region	0.000032	0.000078	0.000096	9	14	15
Gamma MAP	0.000056	0.000023	0.000033	13	7	10
	SNR			Rank	Change in Ranking [Full Image - River Subset]	
	3 X 3	5 X 5	7 X 7			
Lee Sigma	10.825	6.287	4.531	4	10	11
Lee	<u>15.726</u>	12.182	10.682	1	3	5
Frost	14.665	9.584	7.099	2	6	9
Local Region	7.462	3.130	1.596	8	13	15
Gamma MAP	8.696	4.429	2.699	7	12	14
	SSI			Rank	Change in Ranking [Full Image - River Subset]	
	3 X 3	5 X 5	7 X 7			
Lee Sigma	0.810	0.672	0.591	12	6	2
Lee	0.866	0.771	0.711	13	10	7
Frost	0.872	0.740	0.644	14	8	3
Local Region	0.915	0.769	0.645	15	9	4
Gamma MAP	0.779	0.651	<u>0.586</u>	11	5	1
	SMPI			Rank	Change in Ranking [Full Image - River Subset]	
	3 X 3	5 X 5	7 X 7			
Lee Sigma	0.771	0.616	0.533	12	5	2
Lee	0.852	0.764	0.710	14	11	9
Frost	0.850	0.729	0.641	13	10	6
Local Region	0.862	0.660	0.533	15	7	3
Gamma MAP	0.700	0.548	<u>0.473</u>	8	4	1

Annexure 10

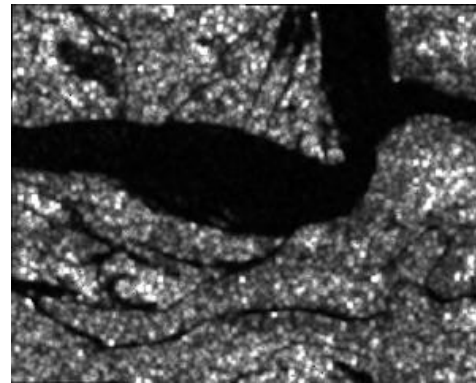
Preview of Unfiltered and Filtered Images of 3X3 and 7X7 window size



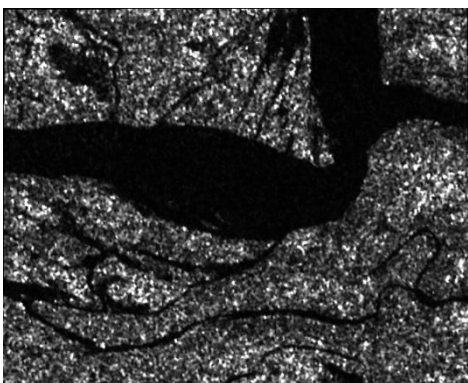
Unfiltered



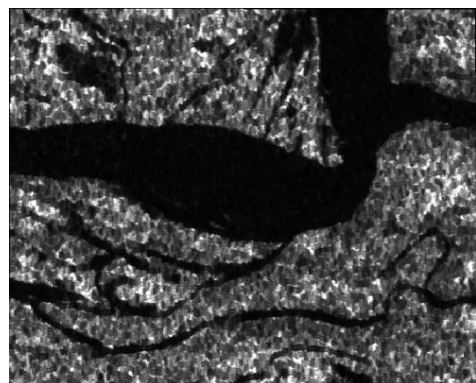
Gamma - MAP (3X3)



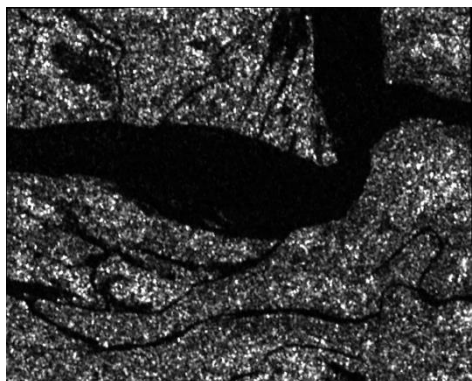
Gamma - MAP (7X7)



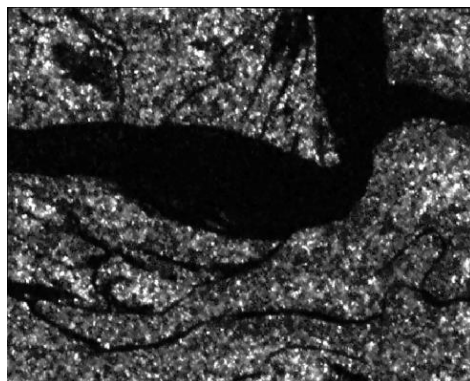
Lee Sigma (3X3)



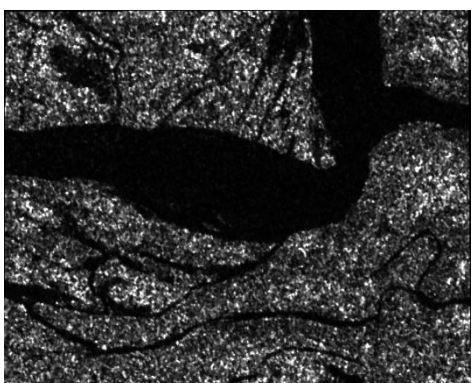
Lee Sigma (7X7)



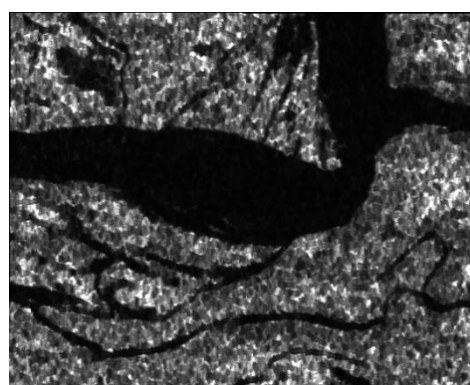
Lee (3X3)



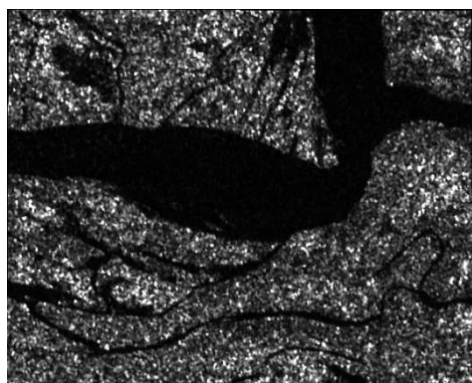
Lee (7X7)



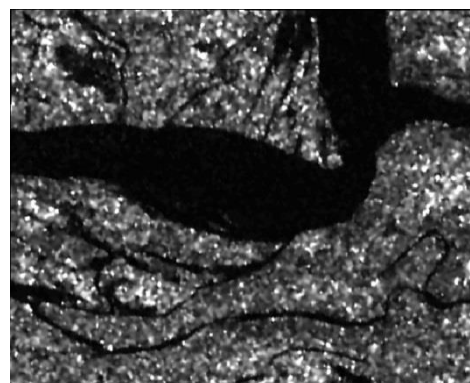
Local Region (3X3)



Local Region (7X7)



Frost (3X3)






Frost (7X7)


Annexure 11

Baseline Processing Report

Processing Summary

Observation	Solution Type	H. Prec. (Meter)	V. Prec. (Meter)	Geodetic Az.	Ellipsoid Dist. (Meter)	DHeight (Meter)
gps-0017 1735530	Fixed	0.029	0.041	241°43'52"	24604.683	-31.315
gcp-0020 1826069 	Float	0.131	0.089	222°53'19"	21752.122	-23.413
gcp-0011 1817380 	Float	0.086	0.068	268°32'36"	21556.281	-34.440
gcp-0014 1128294	Fixed	0.021	0.035	258°17'47"	21422.441	-36.569
gcp-0016 1520405	Fixed	0.023	0.030	245°51'01"	19891.749	-33.796
gcp-0015 1328030	Fixed	0.021	0.044	255°00'44"	19546.080	-35.447
gcp-0019 1505591	Fixed	0.021	0.029	178°14'19"	18371.793	-20.899
gcp-0007 1720147 	Float	0.081	0.065	275°24'43"	18208.557	-34.286
gcp-0018 1926350	Float	0.058	0.048	241°02'28"	17387.948	-32.662
gcp-0010 1627548	Float	0.057	0.060	266°34'56"	18022.408	-34.953
gcp-0009 1428220	Fixed	0.016	0.025	262°17'28"	15796.531	-34.768
gcp-0006 1446575	Fixed	0.014	0.024	275°21'06"	15976.571	-33.689
gcp-0005 1642162	Fixed	0.016	0.022	284°24'41"	14245.453	-34.426
gcp-0008 1233596	Fixed	0.011	0.022	261°30'28"	12365.629	-34.758
gcp-0004 1423132	Fixed	0.012	0.021	292°56'00"	11383.384	-34.346
gcp-0003 1230208	Fixed	0.010	0.019	285°25'01"	10093.128	-34.939
gcp-0002 1721206	Fixed	0.012	0.018	267°45'09"	11130.952	-34.313
gcp-0013 1733297	Fixed	0.010	0.015	233°08'11"	8645.259	-33.414
gcp-0012 1522311	Float	0.018	0.029	253°08'12"	8475.192	-35.404
gcp-0021 1348444	Fixed	0.005	0.009	63°45'14"	4406.513	-32.569
gcp-0001 1418491	Fixed	0.005	0.023	284°05'51"	6292.244	-35.806

Acceptance Summary

Processed	Passed	Flag 	Fail 
21	18	2	1

Annexure 12

Accuracy Assessment Report of GCPs

Check point residuals

Point ID	rX	rY	rZ
4	3.0909	-0.6962	-0.4615
6	-1.0321	-1.1137	4.7465
10	2.733	2.7298	2.347
15	2.5183	-3.5986	0.3796

meanX	meanY	meanZ
1.8275	-0.6697	1.7529

rmseX	rmseY	rmseZ
2.4713	2.352	2.6643

Control point residuals

Point_ID	rX	rY	rZ
1	0.4505	0.4786	-2.4141
2	-0.714	-0.4131	-2.5807
3	1.9063	0.0075	6.1208
5	-0.6297	2.2971	-2.29
7	1.0186	-1.2347	7.5421
8	-2.1555	-1.8584	-1.971
9	-0.5399	1.8549	-0.1581
11	-0.7434	-1.9216	2.3191
12	-0.3322	-2.0328	2.5596
13	1.2079	0.2376	-7.8932
14	0.8027	2.0899	-2.3846
17	-0.941	-0.0034	-3.6673
20	1.1561	0.4006	4.7655

meanX	meanY	meanZ
0.0374	-0.0075	-0.004

rmseX	rmseY	rmseZ
1.0992	1.4279	4.2251

Mean error of 8 image points: ax=-0.718, ay=-0.292

RMSE of 8 image points: mx=1.122, my=0.994

Mean error of 26 image points: ax=0.000, ay=-0.000

RMSE of 26 image points: mx=0.264, my=0.000

Check point image residuals

Image 1		Image 2		
Point_ID	Vx	Vy	Vx	Vy
10	-0.247	0.0	0.278	0.0
4	0.015	0.0	-0.017	0.0
6	-0.331	0.0	0.373	0.0
15	0.604	0.001	-0.680	-0.001
				</

Total number of all check image points = 8

Total meanx = -0.001, meany = 0.000

Total rmsex = 0.390, rmsey = 0.000

Control point image residuals

Image 1			Image 2	
Point_ID	Vx	Vy	Vx	Vy
1	-0.221	0.138	-0.293	0.74
3	-0.617	0.37	-0.318	-1.229
5	0.55	0.748	0.148	1.356
8	0.389	-0.957	0.906	-0.413
12	-0.039	-0.717	0.211	-1.368
13	-0.475	-0.079	-1.037	1.89
14	0.297	0.784	-0.817	1.379
2	0.194	-0.305	0.083	0.364
7	-0.473	-0.13	0.179	-2.072
9	0.524	0.659	0.203	0.723
11	0.262	-0.717	0.235	-1.296
17	0.193	-0.205	0.259	0.748
20	-0.625	0.411	0.288	-0.822
	meanX	meanY	meanX	meanY
	-0.003	0.0	0.004	0.0
	rmseX	rmseY	rmseX	rmseY
	0.414	0.557	0.489	1.218

Total number of all control image points = 26

Total meanx = 0.000 meany = -0.000

$$\text{Total rmsex} = 0.453 \text{ rmsey} = 0.947$$

Image RMSE based on Control and Check Points	0.663
Final RMSE after Tie Points	0.264

Annexure 13

Vertical Elevation - Measured and Computed

ID	Leica GPS 500 Height (m)	DEM Height (m)	Height Difference (m)
Control Points			
1	35.553	36.931	1.378
2	35.574	35.15	-0.424
3	34.947	35.985	1.038
5	33.872	31.826	-2.046
7	35.028	37.66	2.632
8	34.958	35.158	0.2
9	34.172	33.275	-0.897
11	35.797	39.173	3.376
12	36.845	36.821	-0.024
13	36.824	30.629	-6.195
14	47.747	39.952	-7.795
17	34.89	35.311	0.421
20	33.264	34.56	1.296
Check Points			
4	35.429	36.426	0.997
6	34.303	36.598	2.295
10	36.014	33.188	-2.826
15	38.198	39.828	1.63

Annexure -14

Flood Intensity Exposure to different types of Habitat Structures

	Depth Class	Duration Class		
		1	2	3
A	1	464	84	1
	2	46	67	7
	3	19	33	9
B	1	1095	198	4
	2	107	157	15
	3	46	77	20
C	1	7696	1390	27
	2	756	1104	109
	3	319	542	145
D	1	1139	206	4
	2	112	164	16
	3	47	80	21
E	1	2920	528	10
	2	287	419	41
	3	121	205	55
F	1	640	116	2
	2	63	92	9
	3	27	45	12
G	1	552	98	2
	2	54	79	8
	3	23	39	10
H	1	2259	408	8
	2	222	324	32
	3	94	159	42

Annexure-15

Average Depth and Number of Structures in Villages

ID	Village	Mean Depth (m)	Structures Exposed to Flood								Total
			A	B	C	D	E	F	G	H	
1	Abdulrasul	0.23	3	8	52	8	20	4	4	16	115
2	Ahmadpur Sahar	0.81		1	5	1	3			1	11
3	Ajmeripur	1.93	3	5	38	5	14	4	3	12	84
4	Akbarnagar	0.8	98	234	1640	240	621	138	118	482	3,571
5	Asrafpur	0.64	10	25	174	25	66	14	13	51	378
6	Baikatpur	1.86	1	3	21	3	8	1	3	7	47
7	Basant Chak	0.39		1	7	1	3			1	13
8	Bethu	0.78	16	37	261	38	98	22	18	76	566
9	Bharat Rasulpur	1.66	7	16	112	17	42	9	9	33	245
10	Bhatauria	0.65	14	33	228	34	87	20	17	68	501
11	Bhaunathpur	0.75	33	76	534	79	201	45	39	155	1,162
12	Bholapur	1.22	5	12	84	13	33	7	7	25	186
13	Chainnagar	0.5	7	16	114	18	43	9	8	34	249
14	Chandar Bhanpur	0.06	3	5	39	5	16	4	3	12	87
15	Chandpur	1.35	9	22	157	24	59	13	12	46	342
16	Chatarbhujpur	0.29			3		1			1	5
17	Damodarpur	0.6	12	26	188	28	72	16	13	55	410
18	Damodarpur Kalan	0.49	3	7	51	8	20	4	4	14	111
19	Fatehpur	0.29	16	37	262	38	100	22	18	77	570
20	Fatehpuri	0.96		1	7	1	3			1	13
21	Ganga Parsad	0.16	3	5	35	5	13	3	3	10	77
22	Gauriganj	0.99	7	14	98	14	37	8	7	29	214
23	Gauripur	0.64	5	13	93	13	35	8	7	28	202
24	Gobindpur	0.18	1	3	22	5	9	1	1	7	49
25	Golahu	0.75	17	39	277	41	105	24	20	81	604
26	Goriasi	0.97	7	17	115	18	43	9	8	34	251
27	Gosaindasapur	0.86	67	157	1105	161	419	93	79	324	2,405
28	Haridasapur	1.44	14	35	249	35	94	21	18	73	539
29	Hariharapur	0.17	1	3	16	3	7			5	35
30	Hario	0.64	10	24	168	25	64	13	12	50	366
31	Harpur	0.47	16	35	252	37	94	21	18	73	546
32	Hasan Chak	0.34	1	3	14	3	5			4	30
33	Jagan Chak	1.82	3	5	37	5	14	3	3	10	80
34	Jagdish Chak	8.35			3		3			1	7
35	Jairampur	0.55	7	16	114	18	43	9	8	34	249
36	Jaitipur	1.33	18	43	303	45	114	25	21	89	658
37	Jaitipur Arazi	0.21	3	8	51	8	20	4	4	16	114
38	Kaleanpur	1.46	3	5	39	7	16	4	3	12	89
39	Kanjhia	0.59			3		1			1	5
40	Karanpur Arazi	1.45							4	5	9
41	Khaira Kishunpur	0.77		1	8	1	3	1		4	18
42	Khotia	0.19	12	29	206	30	77	17	14	60	445
43	Khulli	0.42	12	29	202	30	76	17	14	59	439

ID	Village	Mean Depth (m)	Structures Exposed to Flood								Total
			A	B	C	D	E	F	G	H	
44	Khutaha	1.35	9	22	152	22	58	13	10	45	331
45	Khutahari	1.08	1	4	30	4	12	3	3	8	65
46	Kishunpur	0.21	1	3	17	3	7	1	1	4	37
47	Madhopur	0.39	20	47	337	50	127	28	24	98	731
48	Maheshi	0.37	21	49	341	50	129	29	25	100	744
49	Makanpur	0.3	9	20	140	21	54	12	10	42	308
50	Makanpur Chhit	0.13	1	4	25	4	9	3	1	8	55
51	Makenpur	0.17	1	4	26	4	9	3	1	8	56
52	Makunpur	1.17	1	5	33	5	12	3	3	9	71
53	Manullah Hawaldar	0.23			3		1			1	5
54	Mathurapur	2.15	3	8	54	9	20	4	4	16	118
55	Mirhati	0.42	1	4	31	5	12	3	3	9	68
56	Mirzapur	0.59	52	122	861	126	325	72	62	252	1,872
57	Mohanpur	2.49	5	12	87	13	33	8	7	25	190
58	Mohiuddinpur	1.92	5	12	85	13	33	8	7	25	188
59	Muhammadpur	0.1	1	3	20	3	8	1	1	5	42
60	Murarpur	0.62	1	3	20	3	8	1	1	5	42
61	Neamatkhan Hawaldar	0.23			1		3				4
62	Pachkathia	0.23	10	24	168	25	63	14	12	49	365
63	Paranpur	0.27		1	10	3	4	1	1	3	23
64	Parmanandpur	0.78		1	9	1	4	1		3	19
65	Patauni	0.23	4	8	54	8	21	5	4	16	120
66	Purani Sarai	1.37	1	3	16	3	7			5	35
67	Rabiachak	0.12	4	9	68	10	26	5	5	20	147
68	Rabichak	0.23			3		1				4
69	Raghopur	1.75	8	17	123	18	47	10	9	37	269
70	Rasidpur	0.36		1	10	3	4	1	1	3	23
71	Rassidpur	2.66			1		3				4
72	Rattipur	1.71	12	28	193	29	73	16	13	56	420
73	Sarha	0.49	5	13	92	13	35	8	7	28	201
74	Sarokh	0.22	3	5	37	7	14	3	3	10	82
75	Serampur	0.97	22	52	365	54	138	30	26	108	795
76	Shahpur	0.45	1	3	17	3	7	1	1	5	38
77	Shahzadpur	1.19	3	7	42	7	16	4	3	13	95
78	Shankar Chak	0.68		1	5	1	1			1	9
79	Sirampur	1.64		1	7	1	3			1	13
80	Sujapur	0.33	4	8	56	8	21	5	4	17	123
81	Tahawarnagar	1.7	9	20	143	21	54	12	10	42	311
82	Tilakpur	0.91	46	106	750	110	285	63	54	220	1,634
83	Yadgar	0.82	16	38	266	39	101	22	18	77	577
TOTAL			727	1,717	12,085	1,789	4,590	1,006	867	3,550	26,331

Annexure-16

Damage to Different Types of Structures in each Village

ID	Village	A	B	C	D	E	F	G	H	Total
1	Abdulrasul	0.01			0.04					0.05
2	Ahmadpur Sahar		0.02	0.14	0.02	0.44			0.15	0.78
3	Ajmeripur	0.11	0.21	1.74	0.17	5.71	1.65	0.94	4.14	14.67
4	Akbarnagar	2.25	5.06	44.05	5.36	89.36	27.84	15.13	73.07	262.11
5	Asrafpur	0.19	0.42	3.84	0.48	5.09	2.08	1.05	5.23	18.38
6	Baikatpur	0.04	0.12	0.95	0.10	3.17	0.40	0.92	2.36	8.06
7	Basant Chak		0.01	0.08	0.01					0.10
8	Bethu	0.36	0.78	6.87	0.83	13.36	4.31	2.21	11.10	39.82
9	Bharat Rasulpur	0.24	0.60	4.77	0.55	15.23	3.38	2.54	10.30	37.62
10	Bhatauria	0.27	0.56	5.10	0.66	7.11	3.05	1.43	7.21	25.39
11	Bhaunathpur	0.72	1.53	13.60	1.69	25.04	8.39	4.47	21.30	76.74
12	Bholapur	0.15	0.37	3.02	0.37	8.92	2.12	1.52	6.11	22.57
13	Chainnagar	0.11	0.18	1.90	0.28	0.13	0.81	0.23	1.64	5.29
14	Chandar Bhanpur									
15	Chandpur	0.28	0.73	5.99	0.71	17.74	4.24	2.86	12.26	44.82
16	Chatarbhujpur			0.01						0.01
17	Damodarpur	0.22	0.40	3.88	0.51	4.16	2.13	0.88	4.86	17.04
18	Damodarpur Kalan	0.05	0.08	0.83	0.12		0.34	0.10	0.61	2.13
19	Fatehpur	0.11		1.29	0.31					1.71
20	Fatehpuri		0.03	0.22	0.02	0.60			0.19	1.05
21	Ganga Parsad									
22	Gauriganj	0.18	0.37	3.08	0.35	7.69	2.02	1.21	5.75	20.66
23	Gauripur	0.10	0.22	2.05	0.25	2.70	1.19	0.57	2.87	9.94
24	Gobindpur				0.01					0.01
25	Golahu	0.37	0.79	7.05	0.88	13.08	4.47	2.29	11.13	40.07
26	Goriasi	0.18	0.44	3.57	0.45	8.67	2.23	1.35	6.59	23.48
27	Gosaindasapur	1.61	3.64	31.41	3.76	69.37	20.36	11.34	54.27	195.75
28	Haridasapur	0.45	1.21	9.85	1.07	30.08	7.17	4.54	20.50	74.87
29	Hariharpur				0.00					0.00
30	Hario	0.19	0.40	3.70	0.48	4.93	1.93	0.97	5.13	17.74
31	Harpur	0.23	0.34	3.87	0.55		1.58	0.29	2.53	9.40
32	Hasan Chak	0.01	0.01	0.12	0.03					0.17
33	Jagan Chak	0.11	0.20	1.65	0.17	5.46	1.19	0.91	3.32	13.01
34	Jagdish Chak			0.23		2.54			0.67	3.44
35	Jairampur	0.12	0.21	2.14	0.31	1.36	1.01	0.39	2.35	7.90
36	Jaitipur	0.56	1.41	11.47	1.32	33.76	8.07	4.95	23.43	84.97
37	Jaitipur Arazi	0.01			0.03					0.03

ID	Village	A	B	C	D	E	F	G	H	Total
38	Kaleanpur	0.10	0.17	1.55	0.22	5.19	1.38	0.77	3.41	12.78
39	Kanjhia			0.06		0.05			0.08	0.20
40	Karanpur Arazi							1.02	1.41	2.43
41	Khaira Kishunpur		0.02	0.21	0.02	0.40	0.19		0.57	1.41
42	Khotia	0.00			0.07					0.07
43	Khulli	0.15	0.21	2.61	0.40		0.82		0.59	4.79
44	Khutaha	0.28	0.73	5.80	0.65	17.44	4.24	2.39	12.00	43.53
45	Khutahari	0.03	0.11	1.00	0.11	2.81	0.82	0.57	1.74	7.19
46	Kishunpur	0.00			0.01					0.01
47	Madhopur	0.23	0.27	3.82	0.61		0.86			5.80
48	Maheshi	0.22	0.22	3.48	0.58		0.53			5.03
49	Makanpur	0.07		0.79	0.18					1.04
50	Makanpur Chhit									
51	Makenpur				0.00					0.00
52	Makunpur	0.03	0.15	1.16	0.14	3.09	0.88	0.63	2.12	8.19
53	Manullah Hawaldar									
54	Mathurapur	0.12	0.35	2.60	0.33	8.80	1.75	1.35	5.90	21.19
55	Mirhati	0.01	0.03	0.40	0.07		0.15		0.09	0.75
56	Mirzapur	0.94	1.81	17.46	2.28	17.12	9.31	3.97	21.34	74.23
57	Mohanpur	0.20	0.56	4.47	0.50	15.97	3.78	2.58	10.03	38.08
58	Mohiuddinpur	0.18	0.49	3.89	0.45	13.40	3.28	2.19	8.60	32.49
59	Muhammadpur									
60	Murarpur	0.02	0.05	0.43	0.06	0.54	0.14	0.07	0.48	1.78
61	Neamatkhan Hawaldar									
62	Pachkathia	0.03			0.12					0.15
63	Paranpur			0.03	0.02					0.06
64	Parmanandpur		0.02	0.24	0.02	0.55	0.20		0.44	1.46
65	Patauni	0.01			0.04					0.05
66	Purani Sarai	0.03	0.10	0.62	0.09	2.14			1.35	4.32
67	Rabiachak									
68	Rabichak									
69	Raghopur	0.28	0.66	5.38	0.60	17.78	3.88	2.64	11.97	43.21
70	Rasidpur		0.00	0.10	0.03		0.01			0.15

ID	Village	A	B	C	D	E	F	G	H	Total
71	Rassidpur			0.05		1.51				1.56
72	Rattipur	0.42	1.08	8.35	0.95	27.12	6.12	3.75	17.84	65.63
73	Sarha	0.08	0.14	1.50	0.20		0.68	0.17	1.23	4.00
74	Sarokh	0.01			0.03					0.04
75	Serampur	0.57	1.35	11.32	1.35	27.82	7.43	4.39	20.95	75.18
76	Shahpur	0.01	0.03	0.25	0.04		0.06	0.01	0.13	0.53
77	Shahzadpur	0.09	0.21	1.49	0.20	4.21	1.18	0.64	3.11	11.12
78	Shankar Chak		0.02	0.12	0.02	0.10			0.12	0.37
79	Sirampur		0.04	0.30	0.03	1.08			0.31	1.75
80	Sujapur	0.04	0.02	0.43	0.08					0.56
81	Tahawarnagar	0.31	0.77	6.17	0.69	19.96	4.57	2.87	13.32	48.67
82	Tilakpur	1.15	2.59	22.23	2.65	52.01	14.64	8.39	39.58	143.25
83	Yadgar	0.37	0.84	7.29	0.88	15.28	4.57	2.40	12.09	43.73
	Total	15.22	33.36	294.10	36.64	630.01	183.44	103.91	489.86	1786.54